

# Bayesian non-conjugate regression via variational belief updating

Cristian Castiglione  
cristian.castiglione@phd.unipd.it

Mauro Bernardi  
mauro.bernardi@unipd.it

*Department of Statistical Sciences, University of Padova.  
Via Cesare Battisti 241, 35121 Padova, Italy.*

## Abstract

We present an efficient semiparametric variational method to approximate the Gibbs posterior distribution of Bayesian regression models, which predict the data through a linear combination of the available covariates. Remarkable cases are generalized linear mixed models, support vector machines, quantile and expectile regression. The variational optimization algorithm we propose only involves the calculation of univariate numerical integrals, when no analytic solutions are available. Neither differentiability, nor conjugacy, nor elaborate data-augmentation strategies are required. Several generalizations of the proposed approach are discussed in order to account for additive models, shrinkage priors, dynamic and spatial models, providing a unifying framework for statistical learning that cover a wide range of applications. The properties of our semiparametric variational approximation are then assessed through a theoretical analysis and an extensive simulation study, in which we compare our proposal with Markov chain Monte Carlo, conjugate mean field variational Bayes and Laplace approximation in terms of signal reconstruction, posterior approximation accuracy and execution time. A real data example is then presented through a probabilistic load forecasting application on the US power load consumption data.

**Keywords:** General Bayesian inference; Mixed regression models; Non-conjugate models; Semiparametric variational Bayes.

## 1 Introduction

The increasing prevalence of big volume and velocity data, eventually coming from different data sources, entails a great opportunity but also a major challenge of modern data analysis and, in particular, of Bayesian statistics. The computational burden required by Markov chain Monte Carlo simulation, that is the state-of-the-art approach to Bayesian inference, is often not compatible with time constraints and memory limits. Therefore, in the last two decades many efforts have been spent to develop alternative estimation methods not involving posterior simulation. In this context, optimization-based algorithms play an important role because of their ability to provide a reasonably good approximation of the

posterior, while keeping a high level of efficiency. Within this family, two remarkable examples are the Laplace approximation, along with its integrated nested generalization (Rue et al., 2009), and the variational inference approach, which includes, among others, local variational approximation (Jaakkola and Jordan, 2000), mean field variational Bayes (Ormerod and Wand, 2010; Blei et al., 2017), expectation propagation (Minka, 2013; Bishop, 2006, Chapter 10) and stochastic variational inference (Hoffman et al., 2013; Kucukelbir et al., 2017; Ong et al., 2018). All of these are mainly concerned with the estimation of hierarchical Bayesian models underling a regular likelihood function, often belonging to the exponential family. For instance, both Laplace approximation and stochastic variational inference require for the log-likelihood function to be differentiable with continuity from one to three times, depending on the implementation. On the other hand, mean field variational Bayes and expectation propagation are employed when the hierarchical model can be described through a Bayesian factor graph with locally conjugate nodes, like for the Gibbs sampling algorithm.

The joint lack of smoothness and conjugacy constitutes one of the main issues when it comes to approximating a posterior density. In such cases, well-designed data-augmentation strategies might help in representing an *elaborate* distribution (Wand et al., 2011) as the marginal law of an enlarged joint model by introducing a set of latent working variables. This tool, firstly introduced for motivating the expectation-maximization algorithm (Dempster et al., 1977), usually permits to restore the regularity in the augmented parameter space, drastically simplifying the calculations. Though, a convenient stochastic representation is not always available and sometimes can lead to important computational drawbacks, mainly concerned with a slowdown of the convergence speed and a worsening of the approximation quality in the original parameter space. See for instance Neville et al. (2014) and Johndrow et al. (2019). Further, the lack of general recipes for extending model-specific augmentation techniques strongly narrows the range of applications of the approach for solving general inferential problems.

Many of these issues are amplified when the parameters of interest do not index a known family of probability distributions but are defined according to a minimum risk criterion and, hence, are linked to the data through a loss function. In these cases, the minimal regularity conditions for an estimation problem to be well-defined may not be satisfied, as it happens for support vector machines (Vapnik, 1998), quantile and expectile regression (Koenker, 2005).

The present work aims to introduce a unified variational methodology for approximating the general posterior distribution of a Bayesian regression model which combines our subjective prior beliefs with the information coming from an empirical risk function. Doing this, we take the subjective perspective introduced by Bissiri et al. (2016), which proved the theoretical coherence of updating a prior to the posterior using the negative loss as it was the kernel of a proper log-likelihood. In this context, we also mention the work of Alquier et al. (2016) and Alquier and Ridgway (2020), which investigated both the finite- and large-sample properties of variational approximations to Gibbs posteriors, while Wang and Blei (2019) established the frequentist consistency and asymptotic normality of variational Bayes under model misspecification.

The range of applications of the present method virtually permits dealing with all the standard regression and classification models predicting the response variable through a linear predictor, including generalized linear models. Here, particular attention is dedicated to loss functions characterized by a non-regular behaviour and for which standard Bayesian approximation techniques can not be directly employed. Our approach combines the efficiency and modularity of mean field variational Bayes with Gaussian variational approximations to deal with parameters not having a conjugate distribution. Previously a similar strategy, known as semiparametric variational Bayes (Knowles and Minka, 2011; Wand, 2014; Rohde and Wand, 2016), has been used for the estimation of Bayesian generalized linear models and heteroscedastic regression models by, e.g., Ormerod and Wand (2012), Tan and Nott (2013),

Wand (2014), Luts and Wand (2015) and Menictas and Wand (2015).

The article is organized as follows. Section 2 introduces the notation. Section 3 reviews some fundamental concepts of mean field variational inference and semiparametric variational Bayes. Section 4 describes our method and characterizes its properties. Section 5 provides some examples for particular model specifications. Section 6 provide a theoretical connection between our approach and data-augmentation-based mean field variational Bayes. Section 7 discusses some possible extensions for different model specifications. The quality of the approximation is then assessed via an extensive simulation study in Section 8. A real data problem concerned with the probabilistic load forecasting of the electric power consumption in US is described in Section 9. Section 10 is devoted to a closing discussion.

## 2 Notation

This Section introduces the basic notation and results for manipulating the variational approximation method outlined henceforth.

### 2.1 Vector and matrix notation

The  $d$ -dimensional identity matrix is  $\mathbf{I}_d$ , the  $d \times p$  zero matrix is  $\mathbf{O}_{d,p}$ , while  $\mathbf{1}_d$  and  $\mathbf{0}_d$  are  $d$ -dimensional vectors filled by ones and zeros, respectively.

We denote with  $\|\cdot\|$  and  $\|\cdot\|_\infty$  the Euclidean and the supremum norm of a vector. As concern matrices, the trace and the determinant of a matrix are denoted by  $\text{trace}(\cdot)$  and  $\det(\cdot)$ . The operator mapping a vector into a diagonal matrix is  $\text{diag}(\cdot)$  and, in the same way, block-diagonal matrices are defined through the operator  $\text{blockdiag}(\cdot)$ , that is

$$\text{diag}(a_1, \dots, a_n) = \begin{bmatrix} a_1 & & \\ & \ddots & \\ & & a_n \end{bmatrix}, \quad \text{blockdiag}(\mathbf{A}_1, \dots, \mathbf{A}_n) = \begin{bmatrix} \mathbf{A}_1 & & \\ & \ddots & \\ & & \mathbf{A}_n \end{bmatrix}.$$

Moreover, we adopt the convention that any scalar valued function  $f : \mathbb{R} \rightarrow \mathbb{R}$  applied to a  $d$ -dimensional vector  $\mathbf{x} \in \mathbb{R}^d$  has to be interpreted as the element-wise application of  $f$  to each component of  $\mathbf{x}$ , namely  $f(\mathbf{x}) = (f(x_1), \dots, f(x_d))^\top$ . The notations  $\nabla_{\mathbf{x}} = \partial/\partial\mathbf{x}$  and  $\nabla_{\mathbf{x}}^2 = \partial^2/\partial\mathbf{x}\partial\mathbf{x}^\top$  stay for the gradient and Hessian operators calculated with respect to  $\mathbf{x}$ . We use  $f_r(x)$  to indicate the  $r$ -th order weak derivative of the scalar valued function  $f(x)$ ,  $x \in \mathbb{R}$ .

### 2.2 Probability distributions

The probability density function of the random variable  $x$  is denoted by  $p(x)$  as well as the joint and conditional densities of  $(x, y)$  are denoted by  $p(x, y)$  and  $p(x|y)$ . The mean and variance of  $x$  are  $\mathbb{E}(x)$  and  $\mathbb{V}\text{ar}(x)$ , respectively.

We denote the variational approximation of  $p(x)$  with  $q(x)$  (see Section 3) and, moreover, we introduce the notation  $\mathbb{E}_q(x)$  for indicating the variational expectation of  $x$  calculated with respect to the density function  $q$ .

Let  $\mathbf{x} \sim \mathcal{N}_d(\boldsymbol{\mu}, \boldsymbol{\Sigma})$  be a  $d$ -dimensional Gaussian random vector with mean vector  $\boldsymbol{\mu} \in \mathbb{R}^d$  and positive definite variance matrix  $\boldsymbol{\Sigma} \in \mathbb{R}^{d \times d}$  having probability density function

$$\phi_d(\mathbf{x}; \boldsymbol{\mu}, \boldsymbol{\Sigma}) = (2\pi)^{-d/2} \det(\boldsymbol{\Sigma})^{-1/2} \exp \left\{ -\frac{1}{2} (\mathbf{x} - \boldsymbol{\mu})^\top \boldsymbol{\Sigma}^{-1} (\mathbf{x} - \boldsymbol{\mu}) \right\}, \quad \mathbf{x} \in \mathbb{R}^d,$$

and cumulative density function  $\Phi_d(\mathbf{x}; \boldsymbol{\mu}, \boldsymbol{\Sigma})$ . Similarly,  $x \sim \mathcal{N}(\mu, \sigma^2)$  is a univariate Gaussian random variable with density function  $\phi(x; \mu, \sigma^2)$  and cumulative density  $\Phi(x; \mu, \sigma^2)$ . For standard Gaussian variables with  $\mu = 0$  and  $\sigma^2 = 1$ , we omit the parameters, i.e.  $\phi(x) = \phi(x; 0, 1)$  and  $\Phi(x) = \Phi(x; 0, 1)$ .

Further, we define the Inverse-Gamma distribution  $x \sim \text{IG}(A, B)$  with shape  $A > 0$ , rate  $B > 0$  and density  $p(x; A, B) = B^A x^{-(A+1)} \exp(-B/x) / \Gamma(A)$ ,  $x > 0$ ,  $\Gamma(x)$  denotes the Euler's Gamma function.

The indicator function over the interval  $(a, b]$  is given by  $\mathbb{I}_{(a,b]}(\cdot)$  and, similarly, the indicator function over the unbounded interval  $(-\infty, b]$  is given by  $\mathbb{I}_{\leq b}(\cdot)$ .

### 3 Semiparametric variational Bayes

Variational Bayes is a family of deterministic approximation methods that turns the Bayesian inference challenge into an optimization problem. The true posterior  $p(\boldsymbol{\theta}|\mathbf{y})$  is replaced with a convenient distribution  $q(\boldsymbol{\theta})$  belonging to a simplified functional space  $\mathcal{Q}$ . The optimal approximating distribution  $q^*(\boldsymbol{\theta})$  is then selected by minimizing the Kullback-Leibler divergence between  $q(\boldsymbol{\theta})$  and  $p(\boldsymbol{\theta}|\mathbf{y})$ , i.e.

$$\text{KL}\{q(\boldsymbol{\theta}) \parallel p(\boldsymbol{\theta}|\mathbf{y})\} = - \int_{\Theta} q(\boldsymbol{\theta}) \log \left\{ \frac{p(\boldsymbol{\theta}|\mathbf{y})}{q(\boldsymbol{\theta})} \right\} d\boldsymbol{\theta}. \quad (1)$$

Equivalently,  $q^*(\boldsymbol{\theta})$  represents the maximizer of the so-called lower bound on the marginal log-likelihood, or evidence lower bound, defined as

$$\log \underline{p}\{\mathbf{y}; q(\boldsymbol{\theta})\} = \int_{\Theta} q(\boldsymbol{\theta}) \log \left\{ \frac{p(\mathbf{y}, \boldsymbol{\theta})}{q(\boldsymbol{\theta})} \right\} d\boldsymbol{\theta}. \quad (2)$$

The Kullback-Leibler divergence (1) and the lower bound (2) are thus linked with the marginal log-likelihood of the model, say  $\log p(\mathbf{y}) = \log \int_{\Theta} p(\mathbf{y}, \boldsymbol{\theta}) d\boldsymbol{\theta}$ , through the equation  $\log p(\mathbf{y}) = \log \underline{p}\{\mathbf{y}; q(\boldsymbol{\theta})\} + \text{KL}\{q(\boldsymbol{\theta}) \parallel p(\boldsymbol{\theta}|\mathbf{y})\}$ .

The assumptions made upon the functional space  $\mathcal{Q}$  may strongly affect the shape and the quality of the approximation and, further, they give rise to different variational algorithms. We here consider a semiparametric variational Bayes (Rohde and Wand, 2016) approach which generalizes mean field variational Bayes (Ormerod and Wand, 2010) allowing for possibly non-conjugate relations between prior and likelihood.

Semiparametric variational Bayes involves two types of restrictions on the searching space  $\mathcal{Q}$ : a mean field constraint and a parametric assumption. First, consider the partition  $\boldsymbol{\theta} = (\boldsymbol{\psi}, \boldsymbol{\phi}) = (\boldsymbol{\psi}, \phi_1, \dots, \phi_m)$ , then the mean field condition, also called factorization restriction, requires that the joint approximating distribution factorizes according to the product

$$p(\boldsymbol{\theta}|\mathbf{y}) \approx q(\boldsymbol{\theta}) = q(\boldsymbol{\psi}) q(\phi_1) \cdots q(\phi_m).$$

Second, we assume that  $q(\boldsymbol{\psi}) \equiv q(\boldsymbol{\psi}; \boldsymbol{\xi})$  belongs to a parametric family indexed by the variational parameter  $\boldsymbol{\xi} \in \Xi$ . As a consequence of these two constraints, the maximization of the semiparametric lower bound, that is  $\log \underline{p}\{\mathbf{y}; q, \boldsymbol{\xi}\} = \log \underline{p}\{\mathbf{y}; q(\boldsymbol{\theta}; \boldsymbol{\xi})\}$ , can be carried out in a coordinatewise fashion, taking advantages of closed form solutions for the  $\boldsymbol{\phi}$ -component and a feasible parametric approximation for  $\boldsymbol{\psi}$ .

The resulting algorithm cycles over the following updates until convergence:

$$q^*(\boldsymbol{\psi}) \leftarrow q(\boldsymbol{\psi}; \hat{\boldsymbol{\xi}}) \quad \text{with} \quad \hat{\boldsymbol{\xi}} \leftarrow \underset{\boldsymbol{\xi} \in \Xi}{\text{argmax}} \{ \log \underline{p}\{\mathbf{y}; q, \boldsymbol{\xi}\} \}, \quad (3)$$

$$q^*(\phi_j) \leftarrow \exp [\mathbb{E}_{-\phi_j} \{ \log p(\phi_j | \text{rest}) \}] / Z_j, \quad j = 1, \dots, m, \quad (4)$$

where  $\leftarrow$  denotes the assignment operator,  $p(\phi_j|\text{rest})$  is the full-conditional distribution of  $\phi_j$ ,  $\mathbb{E}_{-\phi_j}(\cdot)$  is the variational expectation calculated with respect to all the parameters excluding  $\phi_j$ , and  $Z_j$  is a normalization constant. We use the hat-notation  $\hat{\xi}$  to denote the optimal value of  $\xi$  maximizing the lower bound on the marginal log-likelihood.

Typically, the mean field restriction is chosen in order to break the dependence between parameters having conjugate and non-conjugate distributions, respectively,  $\phi$  and  $\psi$ . Indeed, for conjugate models, the expectation  $\mathbb{E}_{-\phi_j}(\cdot)$  is available in analytic form, as well as the associated optimal approximating distribution. For more details on the mean field variational Bayes update (4) and a complete review of the existing literature refer to Bishop (2006), Ormerod and Wand (2010), and Blei et al. (2017).

As pointed out by Wand (2014), in a coordinate ascent scheme that recursively alternates (3) and (4) is not necessary to perform a complete maximization over  $\xi$  at each iteration. It is sufficient, and typically more efficient, to just move the current estimate  $\hat{\xi}$  along an increasing direction. This may be found, for instance, using gradient-free methods or quasi-Newton algorithms Nocedal and Wright (2006), depending on the characteristics of the lower bound  $\log \underline{p}(\mathbf{y}; q, \xi)$ . As shown by Knowles and Minka (2011), Wand (2014) and Rohde and Wand (2016), this strategy is particularly effective when  $q(\psi; \xi)$  is a member of the exponential family having canonical parameter  $\xi$ . In the remarkable case of Gaussian approximations, where  $q(\psi; \xi) \equiv q(\psi; \mu, \Sigma) = \phi(\psi; \mu, \Sigma)$ , the authors derived the so-called Knowles-Minka-Wand formula for updating the mean vector  $\mu$  and the variance-covariance matrix  $\Sigma$ , which corresponds to the Newton-like iteration

$$\mu_{\text{new}} \leftarrow \mu_{\text{old}} - \mathbf{H}_{\text{old}}^{-1} \mathbf{g}_{\text{old}}, \quad \Sigma_{\text{new}} \leftarrow -\mathbf{H}_{\text{old}}^{-1}. \quad (5)$$

Here,  $\mathbf{g}(\mu, \Sigma) = \nabla_{\mu} \ell(\mu, \Sigma)$  and  $\mathbf{H}(\mu, \Sigma) = \nabla_{\mu}^2 \ell(\mu, \Sigma)$  are the gradient and Hessian of  $\ell(\mu, \Sigma) \equiv \mathbb{E}_q\{\log p(\mathbf{y}, \theta)\}$ , which is the expected unnormalized log-posterior of  $\theta$ . Then, the evidence lower bound can be written as  $\log \underline{p}(\mathbf{y}; q, \mu, \Sigma) = \ell(\mu, \Sigma) - \mathbb{E}_q\{\log q(\theta)\}$ . Under standard differentiability conditions on  $\log p(\mathbf{y}, \theta)$ , we can write  $\mathbf{g}(\mu, \Sigma) = \mathbb{E}_q\{\nabla_{\psi} \log p(\mathbf{y}, \theta)\}$  and  $\mathbf{H}(\mu, \Sigma) = \mathbb{E}_q\{\nabla_{\psi}^2 \log p(\mathbf{y}, \theta)\}$  (see Ormerod, 2011), thereby (5) can be interpreted as a variational implementation of the iterated re-weighted least squares algorithm (McCullagh and Nelder, 1989) for the lower bound maximization.

Differently from conjugate mean field variational Bayes, the Newton-like step (5) does not guarantee for the semiparametric variational Bayes optimization scheme to converge monotonically to the maximum. For this reason, we take a slightly different approach, employing a modified update for  $\mu$ , that scales the searching direction  $\mathbf{d}_{\text{new}} = -\mathbf{H}_{\text{old}}^{-1} \mathbf{g}_{\text{old}}$  with a step-size parameter  $\rho \in (0, 1]$ , that is  $\mu_{\text{new}} \leftarrow \mu_{\text{old}} + \rho \mathbf{d}_{\text{new}}$ . The step-length  $\rho$  can then be determined using an efficient line-search algorithm that enforces the Wolf conditions to be satisfied (Nocedal and Wright, 2006). This improvement has two main advantages: first, it stabilizes the iterative optimization, preventing the risk of jumping too far from the optimum; second, it helps in scaling up the convergence speed, adaptively calibrating the step-size to the shape of the lower bound surface.

## 4 Approximate belief updating

We now suppose to be interested in the unknown parameter  $\theta \in \Theta$ , which describes some latent features of the random variable  $y \in \mathcal{Y} \subseteq \mathbb{R}$ . Let  $y \sim \mathbb{P}$  be distributed according to the probability law  $\mathbb{P}$  defined over  $\mathcal{Y}$ . Then, we define  $\theta$  as the minimizer of the risk

$$R(\theta) = \mathbb{E}\{L(y, \theta)\} = \int_{\mathcal{Y}} L(y, \theta) \mathbb{P}(dy), \quad (6)$$

with  $L : \mathcal{Y} \times \Theta \rightarrow \mathbb{R}_+$  denoting a loss function measuring the misfit between  $y$  and  $\theta$ . For example, the mean of  $y$  can be obtained by specifying  $L(y, \theta) = (y - \theta)^2$ , while, for the median, we need  $L(y, \theta) = |y - \theta|$ . Whenever  $\theta$  allows to be described as a parameter indexing a known family of probability density functions, i.e.  $\mathbb{P}(dy) = p(y|\theta) dy$ , the natural choice for  $L(y, \theta)$  is the negative log-likelihood function, being  $L(y, \theta) = -\log p(y|\theta)$ , so as to recover the standard likelihood-based theory.

In a Bayesian vein, we represent our subjective beliefs about  $\theta$  through the prior distribution  $p(\theta)$ . Then, when a random sample  $\mathbf{y} = (y_1, \dots, y_n)^\top \in \mathcal{Y}^n$  generated by  $\mathbb{P}$  is observed, the prior  $p(\theta)$  can be coherently updated to the posterior  $p(\theta|\mathbf{y})$  by means of the generalized Bayes formula (Bissiri et al., 2016):

$$p(\theta|\mathbf{y}) \propto p(\theta) p(\mathbf{y}|\theta) = p(\theta) \exp\{-nR_n(\theta)/\phi\}, \quad (7)$$

where  $R_n(\theta) = \sum_{i=1}^n L(y_i, \theta)/n$  is the empirical risk function approximating the expectation in Equation (6), while  $p(\mathbf{y}|\theta) = \exp\{-nR_n(\theta)/\phi\}$  is the pseudo-likelihood function induced by the empirical risk. The parameter  $1/\phi > 0$  controls the weight of the risk function relative to the prior and is often called *temperature* in the Gibbs posterior and PAC Bayes literature.

Whenever a proper log-likelihood is considered for the specification of the loss  $L(y, \theta)$ , the most natural candidate for the temperature parameter is  $\phi = 1$ . In all the other cases, the elicitation of  $\phi$  is more delicate and, to some extent, arbitrary. Alternatively, the choice of  $\phi$  can be driven by inferential considerations, for example, calibrating  $\phi$  to guarantee some frequentist coverage level of the posterior confidence intervals. This selection problem has been faced, among others, by Germain et al. (2016) and Bissiri et al. (2016). Despite the practical and theoretical importance of choosing an appropriate value for  $\phi$ , this is not the main concern of this work. For this reason, hereafter, we will consider  $\phi$  as it was selected in advance either by an arbitrary decision of the researcher, or by using some objective selection criteria.

The generalized Bayes update (7) is particularly important when it comes to estimating robust regression models for an arbitrary loss function  $L(y, \theta)$ , not being necessary associated with the kernel of a probability density function. In what follows we leverage this representation for dealing with a wide range of mixed prediction models in a unified way.

## 4.1 Model specification

Supervised mixed regression and classification models aim to predict the response variable  $y_i \in \mathcal{Y}$  through a deterministic transformation of the covariate vectors  $\mathbf{x}_i \in \mathbb{R}^p$  and  $\mathbf{z}_i \in \mathbb{R}^d$ , for  $i = 1, \dots, n$ . To this end, we define the linear predictor  $\eta_i = \mathbf{x}_i^\top \boldsymbol{\beta} + \mathbf{z}_i^\top \mathbf{u}$ , with  $\boldsymbol{\beta} \in \mathbb{R}^p$  and  $\mathbf{u} \in \mathbb{R}^d$  being the fixed- and random-effect regression parameters, respectively. We assume for  $\boldsymbol{\beta}$  and  $\mathbf{u}$  to be the maximizers of the negative empirical risk function, i.e. the pseudo log-likelihood,

$$\log p(\mathbf{y}|\theta) = -\frac{n}{\phi} R_n(\theta) = -\frac{1}{\phi} \sum_{i=1}^n L(y_i, \theta) = -\frac{n}{\phi} \log \sigma_\varepsilon^2 - \frac{1}{\phi} \sum_{i=1}^n \psi(y_i, \eta_i)/\sigma_\varepsilon^2, \quad (8)$$

where  $\psi : \mathcal{Y} \times \mathbb{R} \rightarrow \mathbb{R}_+$  is a continuous, typically convex, function measuring the misfit between the  $i$ -th data point  $y_i$  and the corresponding linear predictor  $\eta_i$ ;  $\sigma_\varepsilon^2$  is a dispersion parameter measuring the variability of the marginal prediction error calculated in the loss scale;  $\phi$  is a fixed temperature parameter calibrating the relative weight of the risk function.

In the same vein of generalized linear models, which are based upon the specification of an exponential family, a linear predictor and a link function, the risk formulation in (8) encapsulates a large number of regression models defined by a loss function and a linear predictor. Moreover, for an appropriate

specification of  $\psi$ , generalized linear models can be included in our model specification and  $\sigma_\varepsilon^2$  can be interpreted as the dispersion parameter of an exponential dispersion family. More details are outlined in Section 5.

We complete the model specification by introducing a prior distribution which reflect our subjective beliefs about the parameter vector  $\boldsymbol{\theta} = (\boldsymbol{\beta}, \mathbf{u}, \sigma_u^2, \sigma_\varepsilon^2)$ :

$$\begin{aligned} \boldsymbol{\beta} &\sim \text{N}_p(\mathbf{0}_p, \sigma_\beta^2 \mathbf{I}_p), & \sigma_\varepsilon^2 &\sim \text{IG}(A_\varepsilon, B_\varepsilon), \\ \mathbf{u} | \sigma_u^2 &\sim \text{N}_d(\mathbf{0}_d, \sigma_u^2 \mathbf{R}^{-1}), & \sigma_u^2 &\sim \text{IG}(A_u, B_u), \end{aligned} \quad (9)$$

where  $\sigma_\beta^2, A_\varepsilon, B_\varepsilon, A_u, B_u > 0$  are fixed user-specified prior parameters;  $\sigma_u^2 > 0$  is an unknown scale parameter controlling the marginal variability of the random effect vector  $\mathbf{u}$ ; while  $\mathbf{R} \in \mathbb{R}^{d \times d}$  is a non-stochastic positive semi-definite matrix determining the prior conditional correlation structure among the elements of  $\mathbf{u}$ .

For models where  $\sigma_\varepsilon^2$  is not required, its prior distribution can be set as a Dirac delta function centred in 1, i.e.  $p(\sigma_\varepsilon^2) = \delta_1(\sigma_\varepsilon^2)$ . In this way, we obtain a formulation coherent with the limiting case  $\mathbb{E}(\sigma_\varepsilon^2) \rightarrow 1$ ,  $\text{Var}(\sigma_\varepsilon^2) \rightarrow 0$ , which corresponds to an Inverse-Gamma distribution with parameters  $A_\varepsilon \rightarrow \infty$ ,  $B_\varepsilon \rightarrow \infty$ .

As proved by Bissiri et al. (2016), the most rational way to update our prior knowledge about  $\boldsymbol{\theta}$  using the information coming from the empirical risk (6) is to combine prior and pseudo-likelihood through the Bayes theorem, as in Equation (7). The resulting generalized posterior density is then given by

$$p(\boldsymbol{\beta}, \mathbf{u}, \sigma_u^2, \sigma_\varepsilon^2 | \mathbf{y}) \propto p(\mathbf{y} | \boldsymbol{\beta}, \mathbf{u}, \sigma_\varepsilon^2) p(\boldsymbol{\beta}) p(\mathbf{u} | \sigma_u^2) p(\sigma_u^2) p(\sigma_\varepsilon^2). \quad (10)$$

Typically, such a posterior can not be normalized analytically, even when the pseudo-likelihood is conditionally conjugate with the prior distributions. For this reason, an efficient and general approximation algorithm is needed to perform posterior inference on (10) without changing the approximation scheme every time that a new  $\psi$ -function is considered.

## 4.2 Variational approximation

For approximating the conditional density function (10) with a semiparametric variational approach, we impose the minimal product restriction

$$p(\boldsymbol{\beta}, \mathbf{u}, \sigma_u^2, \sigma_\varepsilon^2 | \mathbf{y}) \approx q(\boldsymbol{\beta}, \mathbf{u}, \sigma_u^2, \sigma_\varepsilon^2) = q(\boldsymbol{\beta}, \mathbf{u}) q(\sigma_u^2, \sigma_\varepsilon^2).$$

which leads to the induced factorization  $q(\sigma_u^2, \sigma_\varepsilon^2) = q(\sigma_u^2) q(\sigma_\varepsilon^2)$ , because of the separability properties of the Bayesian factor graph describing the conditional dependence structure of (10). Further, we restrict the density  $q(\boldsymbol{\beta}, \mathbf{u}) \sim \text{N}_K(\boldsymbol{\mu}, \boldsymbol{\Sigma})$  to be multivariate Gaussian with mean vector and covariance matrix

$$\boldsymbol{\mu} = \begin{bmatrix} \boldsymbol{\mu}_\beta \\ \boldsymbol{\mu}_u \end{bmatrix}, \quad \boldsymbol{\Sigma} = \begin{bmatrix} \boldsymbol{\Sigma}_{\beta\beta} & \boldsymbol{\Sigma}_{\beta u} \\ \boldsymbol{\Sigma}_{u\beta} & \boldsymbol{\Sigma}_{uu} \end{bmatrix},$$

where the subscripts refer to the  $p$ - and  $d$ -dimensional sub-blocks corresponding to  $\boldsymbol{\beta}$  and  $\mathbf{u}$ , so that  $\boldsymbol{\mu}_\beta \in \mathbb{R}^p$ ,  $\boldsymbol{\Sigma}_{\beta\beta} \in \mathbb{R}^{p \times p}$  and  $\boldsymbol{\Sigma}_{\beta u} \in \mathbb{R}^{p \times d}$ . We denote with  $K = p + d$  the total number of regression parameters in the model. Such a parametric assumption leads to a Gaussian variational distribution for the linear predictor, that is  $q(\boldsymbol{\eta}) \sim \text{N}_n(\mathbf{m}, \mathbf{V})$  with mean and variance

$$\mathbb{E}_q(\boldsymbol{\eta}) = \mathbf{m} = \mathbf{C}\boldsymbol{\mu}, \quad \text{Var}_q(\boldsymbol{\eta}) = \mathbf{V} = \mathbf{C}\boldsymbol{\Sigma}\mathbf{C}^\top.$$



Here,  $\mathbf{C} = [\mathbf{X}, \mathbf{Z}]$  is the  $n \times K$  completed design matrix having  $i$ -th row equal to  $\mathbf{c}_i^\top = (\mathbf{x}_i^\top, \mathbf{z}_i^\top)$ , so that  $\mathbb{E}_q(\eta_i) = m_i = \mathbf{c}_i^\top \boldsymbol{\mu}$  and  $\text{Var}_q(\eta_i) = \nu_i^2 = \mathbf{c}_i^\top \boldsymbol{\Sigma} \mathbf{c}_i$ .

As shown in Appendix B, a direct application of the variational updates (4) and (5) gives rise to the optimal variational updates summarized in the following optimal distributions:

- $q^*(\sigma_\varepsilon^2) \sim \text{IG}(\hat{\alpha}_\varepsilon, \hat{\beta}_\varepsilon)$  where  $\hat{\alpha}_\varepsilon \leftarrow A_\varepsilon + n/\phi$  and  $\hat{\beta}_\varepsilon \leftarrow B_\varepsilon + \mathbf{1}_n^\top \boldsymbol{\Psi}_0/\phi$ ;
- $q^*(\sigma_u^2) \sim \text{IG}(\hat{\alpha}_u, \hat{\beta}_u)$  where  $\hat{\alpha}_u \leftarrow A_u + d/2$  and  $\hat{\beta}_u \leftarrow B_u + \frac{1}{2} \hat{\boldsymbol{\mu}}_u^\top \mathbf{R} \hat{\boldsymbol{\mu}}_u + \frac{1}{2} \text{trace}(\mathbf{R} \hat{\boldsymbol{\Sigma}}_{uu})$ .
- $q^*(\boldsymbol{\beta}, \mathbf{u}) \sim \text{N}_K(\hat{\boldsymbol{\mu}}, \hat{\boldsymbol{\Sigma}})$  with  $(\hat{\boldsymbol{\mu}}, \hat{\boldsymbol{\Sigma}})$  being the fixed-point of the Knowles-Minka-Wand recursion (5). Thanks to Proposition 6 in Appendix A, the gradient vector  $\mathbf{g}$  and the Hessian matrix  $\mathbf{H}$  for our model specification take the form

$$\begin{aligned} \mathbf{g}(\boldsymbol{\mu}, \boldsymbol{\Sigma}) &= - \begin{bmatrix} \sigma_\beta^{-2} \boldsymbol{\mu}_\beta \\ \hat{\gamma}_u \mathbf{R} \boldsymbol{\mu}_u \end{bmatrix} - \hat{\gamma}_\varepsilon \mathbf{C}^\top \boldsymbol{\Psi}_1 / \phi, \\ \mathbf{H}(\boldsymbol{\mu}, \boldsymbol{\Sigma}) &= - \begin{bmatrix} \sigma_\beta^{-2} \mathbf{I}_p & \mathbf{O}_{p,d} \\ \mathbf{O}_{d,p} & \hat{\gamma}_u \mathbf{R} \end{bmatrix} - \hat{\gamma}_\varepsilon \mathbf{C}^\top \text{diag}[\boldsymbol{\Psi}_2] \mathbf{C} / \phi, \end{aligned} \quad (11)$$

where  $\mathbb{E}_q(1/\sigma_u^2) = \hat{\gamma}_u = \hat{\alpha}_u/\hat{\beta}_u$  and  $\mathbb{E}_q(1/\sigma_\varepsilon^2) = \hat{\gamma}_\varepsilon = \hat{\alpha}_\varepsilon/\hat{\beta}_\varepsilon$ .

Here, the  $i$ -th element of the  $n$ -dimensional vector  $\boldsymbol{\Psi}_r = (\Psi_{r,1}, \dots, \Psi_{r,n})^\top$  is defined as

$$\Psi_{r,i} = \Psi_r(y_i, m_i, \nu_i) = \mathbb{E}_q\{\psi_r(y_i, \eta_i)\}, \quad r = 0, 1, 2, \quad i = 1, \dots, n, \quad (12)$$

where  $\psi_r(y, \eta)$  is the  $r$ -th order weak derivative of  $\psi(y, \eta)$  with respect to  $\eta$ . The existence and regularity of  $\Psi_r$  is guaranteed by the following proposition.

**Theorem 1.** *Let  $\psi(y, \eta)$  be a function such that, for any  $y \in \mathcal{Y}$  and  $r = 1, \dots, R$ , the  $r$ -th order weak derivative  $\psi_r(y, \eta)$  is well-defined. Then, the following statements hold:*

- (1)  $\Psi_r(y, \eta, \nu)$  has infinitely many continuous derivatives with respect to  $\eta$  and  $\nu$ ;
- (2) if  $\psi_r$  is continuous in  $\eta$ , then  $\Psi_r(y, \eta, \nu) \rightarrow \psi_r(y, \eta)$  as  $\nu \rightarrow 0$ ;
- (3) if  $\psi$  is convex in  $\eta$ , then  $\Psi_0$  is jointly convex with respect to  $\eta$  and  $\nu$ ;
- (4) if  $\psi$  is convex in  $\eta$ , then  $\psi(y, \eta) \leq \Psi_0(y, \eta, \nu)$  for any  $\nu \geq 0$ .

*Proof.* Theorem 1 follows from Proposition 5 in Appendix A.  $\square$

**Remark 1.** *Theorem 1 does not require for the loss function  $\psi$  to satisfy classical regularity assumptions, like differentiability, since the weak derivative  $\psi_r$  may exist even though  $\psi$  is not  $r$ -times differentiable all over its domain. This fact permits to employ our variational approximation even for models with non-regular (misspecified) log-likelihood.*

It is worth noting that, for any dimension of  $p$  and  $d$ , only univariate numerical integrations are required in the calculation of (11), since  $\Psi_r(y, m, \nu) = \int_{-\infty}^{+\infty} \psi_r(y, \eta) \phi(\eta; m, \nu^2) d\eta$ . This fact leads to a scalable optimization routine not depending on cumbersome high-dimensional integration problems. Clearly, efficiency and stability in the calculation of (11) highly depend on the algorithm used for evaluating the  $n$  expectations in (12). In our experience, whenever no analytic solutions are available, adaptive Gauss-Hermite quadrature (Liu and Pierce, 1994) leads to fast calculations and robust results.



Further, it is worth emphasizing the generality of Equations (11), that, together with (5), goes far beyond the few examples presented in the following section, for which we found simple analytic solutions. It indeed includes, as special cases, the algorithms proposed by e.g. Tan and Nott (2013), Wand (2014) and Luts and Ormerod (2014) for logistic, Poisson and Negative-Binomial regression models. Moreover, it is strongly connected with the Gaussian variational approximation proposed by Ormerod and Wand (2012) for estimating frequentist generalized mixed models.

The last ingredient of our variational method is the objective function, say the evidence lower bound on the marginal log-likelihood, which takes the closed form expression

$$\begin{aligned} \log p(\mathbf{y}; q) = & -\hat{\gamma}_\varepsilon \mathbf{1}_n^\top \boldsymbol{\Psi}_0 / \phi + \frac{1}{2} \log \det(\hat{\boldsymbol{\Sigma}}) - \frac{1}{2} \hat{\boldsymbol{\mu}}^\top \mathbf{Q} \hat{\boldsymbol{\mu}} - \frac{1}{2} \text{trace}(\mathbf{Q} \hat{\boldsymbol{\Sigma}}) \\ & - \log \left\{ \Gamma(A_u) / \Gamma(\hat{\alpha}_u) \right\} + A_u \log(B_u / \hat{\beta}_u) - (d/2) \log \hat{\beta}_u - (B_u - \hat{\beta}_u) \hat{\gamma}_u \\ & - \log \left\{ \Gamma(A_\varepsilon) / \Gamma(\hat{\alpha}_\varepsilon) \right\} + A_\varepsilon \log(B_\varepsilon / \hat{\beta}_\varepsilon) - (n/\phi) \log \hat{\beta}_\varepsilon - (B_\varepsilon - \hat{\beta}_\varepsilon) \hat{\gamma}_\varepsilon \\ & + \text{const}, \end{aligned} \quad (13)$$

for  $\mathbf{Q} = \text{blockdiag}[\sigma_\beta^{-2} \mathbf{I}_p, \hat{\gamma}_u \mathbf{R}]$ . Here, “const” denotes a constant additive term not depending on the variational parameters, namely  $\{\alpha_\varepsilon, \beta_\varepsilon, \alpha_u, \beta_u, \boldsymbol{\mu}, \boldsymbol{\Sigma}\}$ . The derivation of formula (13) is outlined in Appendix B.

**Remark 2.** Let us assume that all the variational parameters in (13) but  $\boldsymbol{\mu}$  and  $\boldsymbol{\Sigma}$  are fixed. Then, Theorem 1 guarantees the joint differentiability and concavity of  $\log p(\mathbf{y}; q)$  as a function of  $\boldsymbol{\mu}$  and  $\boldsymbol{\Sigma}$ . Therefore, under the assumptions of Theorem 1 the updating iteration (5) converges to a global maximum of the evidence lower bound (13). See, e.g., Lange (2010), Chapter 12.

### 4.3 Algorithm

The recursive refinement of the optimal distributions gives rise to the coordinate ascent variational inference routine summarized in Algorithm 1. We assess the algorithm convergence by looking at the relative change of the variational parameters and the lower bound (13). A well-behaved variational Bayes algorithm is expected to produce a non-decreasing sequence of lower bound values, thereby, providing a practical role for monitoring the convergence and detecting pathological behaviours of the algorithm. At the end of the estimation process, the evidence lower bound can also be used for model selection purposes, being a variational approximation of the true marginal log-likelihood.

In Algorithm 1, the notation  $\text{LineSearch}(\mathbf{g}, \mathbf{H})$  is used to denote a function taking as arguments the actual objective function  $\ell$ , the gradient vector  $\mathbf{g}$  and Hessian matrix  $\mathbf{H}$  and returning the selected step-size parameter  $\rho \in (0, 1]$  as an output. Such a routine can be easily implemented using an iterative backtracking method (Nocedal and Wright, 2006) until the step-length satisfies some minimal requirements, such as the Armijo-Wolfe conditions.

Assuming for  $\mathbf{X}$ ,  $\mathbf{Z}$  and  $\mathbf{R}$  to be dense matrices, the number of flops required by one iteration of the algorithm is of order  $\mathcal{O}(nK^2 + K^3)$ , which is equivalent to expectation-maximization, Gibbs sampling and mean field variational Bayes when applied to models of the form (8). However, if some sparsity patterns are observed, efficient sparse linear algebra routines may help in calculating  $\mathbf{H}^{-1}$  and  $\mathbf{H}^{-1}\mathbf{g}$ , turning down the complexity of the algorithm to a lower order. In such cases, the computational gain depends on the specific sparsity patterns and implementation details. Notice that we are here assuming that the calculation of  $\boldsymbol{\Psi}_r$  is dominated by the evaluation of  $m_i = \mathbf{c}_i^\top \boldsymbol{\mu}$  and  $\nu_i^2 = \mathbf{c}_i^\top \boldsymbol{\Sigma} \mathbf{c}_i$ ,  $i = 1, \dots, n$ , that is of order  $\mathcal{O}(nK^2)$ . In our experience, this assumption is satisfied for all the statistical models we tried, even when no analytic solutions are available and numerical quadrature is required.

---

**Algorithm 1:** Semiparametric variational Bayes algorithm for approximate Bayesian inference in model (8) with prior (9).

---

**Data:**  $\mathbf{y}, \mathbf{X}, \mathbf{Z}, \mathbf{R}$

**Input:**  $\sigma_\beta^2, A_u, B_u, A_\varepsilon, B_\varepsilon$

**Output:**  $\hat{\boldsymbol{\mu}}, \hat{\boldsymbol{\Sigma}}, \hat{\alpha}_u, \hat{\beta}_u, \hat{\alpha}_\varepsilon, \hat{\beta}_\varepsilon$

**while** *convergence is not reached* **do**

    Evaluate  $\boldsymbol{\Psi}_0, \boldsymbol{\Psi}_1, \boldsymbol{\Psi}_2$ ;  $\mathcal{O}(nK^2)$

$\hat{\alpha}_\varepsilon \leftarrow A_\varepsilon + n/\phi$ ;     $\hat{\beta}_\varepsilon \leftarrow B_\varepsilon + \mathbf{1}_n^\top \boldsymbol{\Psi}_0/\phi$ ;  $\mathcal{O}(n)$

$\hat{\alpha}_u \leftarrow A_u + d/2$ ;     $\hat{\beta}_u \leftarrow B_u + \{\hat{\boldsymbol{\mu}}_u^\top \mathbf{R} \hat{\boldsymbol{\mu}}_u + \text{trace}[\mathbf{R} \hat{\boldsymbol{\Sigma}}_{uu}]\}/2$ ;  $\mathcal{O}(d^2)$

$\hat{\gamma}_u \leftarrow \hat{\alpha}_u/\hat{\beta}_u$ ;     $\hat{\gamma}_\varepsilon \leftarrow \hat{\alpha}_\varepsilon/\hat{\beta}_\varepsilon$ ;     $\mathbf{Q} \leftarrow \text{blockdiag}[\sigma_\beta^{-2} \mathbf{I}_p, \hat{\gamma}_u \mathbf{R}]$ ;  $\mathcal{O}(1)$

$\mathbf{g} \leftarrow -\mathbf{Q} \hat{\boldsymbol{\mu}} - \hat{\gamma}_\varepsilon \mathbf{C}^\top \boldsymbol{\Psi}_1/\phi$ ;     $\mathbf{H} \leftarrow -\mathbf{Q} - \hat{\gamma}_\varepsilon \mathbf{C}^\top \text{diag}[\boldsymbol{\Psi}_2] \mathbf{C}/\phi$ ;  $\mathcal{O}(nK^2)$

$\rho \leftarrow \text{LineSearch}(\mathbf{g}, \mathbf{H})$ ;     $\hat{\boldsymbol{\Sigma}} \leftarrow -\mathbf{H}^{-1}$ ;     $\hat{\boldsymbol{\mu}} \leftarrow \hat{\boldsymbol{\mu}} - \rho \mathbf{H}^{-1} \mathbf{g}$ ;  $\mathcal{O}(K^3)$

---

An important feature of the computational framework described above is that it is shared across all the linear models defined through minimum-risk criteria. What distinguishes different models is the specification of the  $\boldsymbol{\Psi}$ -vectors, which bring the individual information about the local behaviour of the expected loss function, similarly as the gradient and Hessian of the log-likelihood do in the classical penalized re-weighted iterated least squares algorithm. However, differently from standard gradient-based methods, we do not require the loss function to be differentiable, since the weak derivatives of  $\psi$  may exist even though the proper derivatives of  $\psi$  are not well-defined. Moreover, from Proposition 1 it follows that  $\boldsymbol{\Psi}_0, \boldsymbol{\Psi}_1, \boldsymbol{\Psi}_2$  are smooth functions of  $\boldsymbol{\mu}$  and  $\boldsymbol{\Sigma}$ , since the convolution of any function with a Gaussian kernel produces a smooth transformation. More details and proofs can be found in Appendix A.

For a stable numerical implementation, we suggest truncating the values of  $\boldsymbol{\Psi}_2$  from below to a small positive constant, say  $10^{-6}$ , to prevent some elements of the vector to approach 0. In our numerical experiments, however this correction never had a significant impact on the final solution, but often helped the convergence in the very early epochs of the iterative optimization routine.

## 5 Models

As pointed out in Section 4, Algorithm 1 provides a general recipe for performing variational inference on a wide range of Bayesian models. In this section, we present some remarkable examples coming from both machine learning and statistical literature. Specifically, we show how to specify the  $\boldsymbol{\Psi}$ -vectors for different settings spacing from support vector machines (Section 5.1 and 5.2) to quantile and expectile regression (Sections 5.3 and 5.4). Finally, we move to the exponential family case (Section 5.5) for discussing the estimation of generalized linear models. In doing this, we make an extensive use of Propositions 7 and 8, which constitute the key results for calculating the necessary  $\boldsymbol{\Psi}$ -functions in closed form.

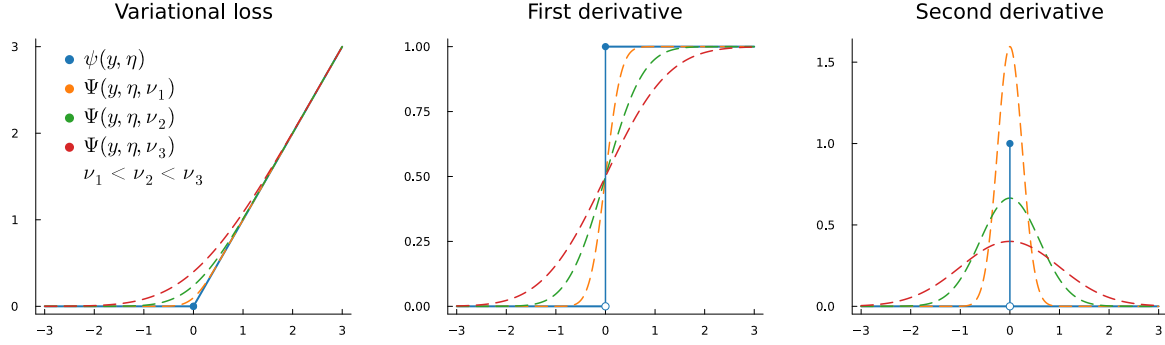


Figure 1: Support vector classification:  $\psi_r$  and  $\Psi_r$  functions for different values of  $\eta$  and  $\nu$ . From left to right:  $r = 0, 1, 2$ .

## 5.1 Support vector classification

Support vector machines have been originally designed to solve classification tasks in such a way to predict  $y_i \in \mathcal{Y} \equiv \{-1, +1\}$  using the decision function  $\text{sign}(\eta_i)$  with  $\eta_i = \mathbf{x}_i^\top \boldsymbol{\beta} + \mathbf{z}_i^\top \mathbf{u}$ . The parameters are then estimated so that to maximize the margin between data with opposite labeling (Vapnik, 1998; Hastie et al., 2009). The loss function characterizing the support vector classification (SVC) problem is the so-called Hinge loss:

$$\psi^{\text{SVC}}(y, \eta) = 2 \max(0, 1 - y\eta). \quad (14)$$

Classical non-linear support vector machines are included in our model specification by representing the random effect covariate vector  $\mathbf{z}_i$  as a sequence of basis functions. In this way, we can jointly learn the posterior distribution of the basis coefficients and the smoothing parameter, namely  $1/\sigma_u^2$ , controlling the amount of regularization needed to prevent overfitting phenomena.

A complete Bayesian treatment of the support vector estimation problem has been discussed by Polson and Scott (2011), which introduced a popular data augmentation technique to represent the Hinge pseudo-likelihood as a location-scale mixture of Gaussian distributions. The authors then proposed a Gibbs sampler and an expectation-maximization algorithm to estimate the model parameters. Luts and Ormerod (2014) considered a similar approach and leveraged the conditional conjugacy of the augmented model to approximate the posterior distribution with a mean field variational Bayes approach.

Unlike existing methods, the major advantage of the proposed approach consists of avoiding to transform the pseudo-likelihood or to introduce additional auxiliary variables in the model specification. Instead, we use a semiparametric variational Bayes scheme to approximate the posterior distribution without modifying the loss function (14). Then, all the parameters in the model can be estimated using Algorithm 1 and specifying the  $\Psi$ -vectors according to the following proposition.

**Proposition 1.** *The  $\Psi$ -functions for the support vector classification model are*

$$\begin{aligned} \Psi_0^{\text{SVC}}(y, m, \nu) &= 2\{(1 - ym) \Phi(1; ym, \nu^2) + \nu^2 \phi(1; ym, \nu^2)\}, \\ \Psi_1^{\text{SVC}}(y, m, \nu) &= -2y \Phi(1; ym, \nu^2), \\ \Psi_2^{\text{SVC}}(y, m, \nu) &= 2 \phi(1; ym, \nu^2). \end{aligned}$$

*Proof.* The proof is deferred to Appendix B. □

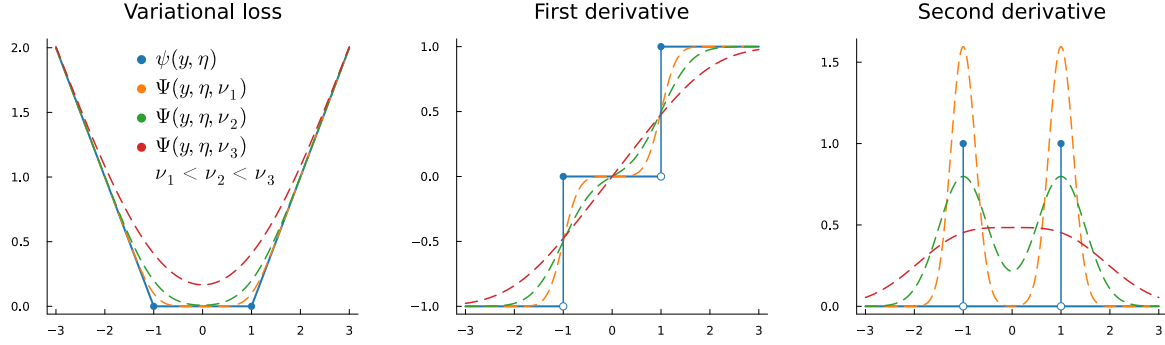


Figure 2: Support vector regression ( $\epsilon = 1$ ):  $\psi_r$  and  $\Psi_r$  functions for different values of  $\eta$  and  $\nu$ . From left to right:  $r = 0, 1, 2$ .

Figure 1 shows the behavior of both  $\psi^{\text{SVC}}(\cdot)$  and  $\Psi^{\text{SVC}}(\cdot)$  along with their first and second weak derivatives for different values of the variational parameters. As we might expect from Propositions 5 and 6,  $\Psi^{\text{SVC}}(\cdot)$  looks like a smoothed approximation of  $\psi^{\text{SVC}}(\cdot)$ . The mean parameter  $\boldsymbol{\mu}$  corrects for the location of the estimates, while the variance parameter  $\boldsymbol{\Sigma}$  selects adaptively the scale of the approximation, which is in turn connected with the degree of smoothing around the corner of the Hinge loss.

## 5.2 Support vector regression

Support vector regression (SVR, Vapnik, 1998) is a robust prediction model designed to extend the support vector geometric approach to solve regression tasks. This finds the best linear predictor  $\eta_i = \mathbf{x}_i^\top \boldsymbol{\beta} + \mathbf{z}_i^\top \mathbf{u}$  able to fit the data  $y_i$  estimating the parameters  $\boldsymbol{\beta}$  and  $\mathbf{u}$  in such a way to minimize a penalized empirical risk function associated to the  $\epsilon$ -insensitive loss

$$\psi^{\text{SVR}}(y, \eta) = 2 \max(0, |y - \eta| - \epsilon). \quad (15)$$

The support vector loss in (15) is insensitive to all the regression errors lower than the tolerance parameter  $\epsilon \geq 0$ , namely that every residual  $\varepsilon_i = y_i - \eta_i$  such that  $|y_i - \eta_i| \leq \epsilon$  will produce  $\psi^{\text{SVR}}(y_i, \eta_i) = 0$ . Outside the insensitivity band,  $\psi^{\text{SVR}}(\cdot)$  has a linear behaviour, so that to trade off goodness of fit and robustness to outlier contamination.

Either frequentist and Bayesian estimation procedures have been developed to fit support vector regression models. Among others, Zhu et al. (2012) and Zhu et al. (2014) adopted a double data augmentation strategy useful to build an expectation-maximization algorithm for penalized pseudo-likelihood maximization, Gibbs sampling for posterior simulation and mean field variational Bayes for deterministic posterior approximation. In this context, our proposal is to directly approximate the marginal posterior distribution (10) using Algorithm 1 and defining the  $\Psi$ -functions (Figure 2) according to Proposition 2.

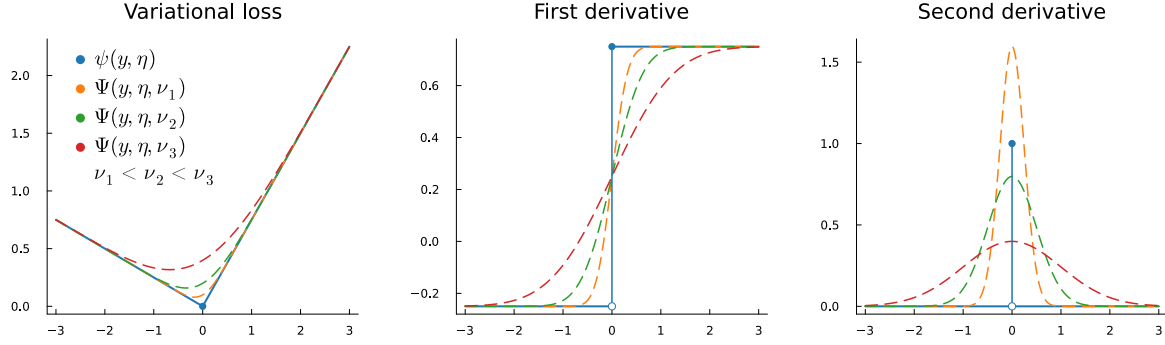


Figure 3: Quantile regression ( $\tau = 0.75$ ):  $\psi_r$  and  $\Psi_r$  functions for different values of  $\eta$  and  $\nu$ . From left to right:  $r = 0, 1, 2$ .

**Proposition 2.** *The  $\Psi$ -functions for the support vector regression model are*

$$\begin{aligned}\Psi_0^{\text{SVR}}(y, m, \nu) &= 2\{(y_\epsilon^- - m) \Phi(y_\epsilon^+; m, \nu^2) + \nu^2 \phi(y_\nu^+; m, \nu^2) \\ &\quad + (y_\epsilon^+ - m) \Phi(y_\epsilon^-; m, \nu^2) + \nu^2 \phi(y_\epsilon^-; m, \nu^2)\}, \\ \Psi_1^{\text{SVR}}(y, m, \nu) &= 2\{1 - \Phi(y_\epsilon^+; m, \nu^2) - \Phi(y_\epsilon^-; m, \nu^2)\}, \\ \Psi_2^{\text{SVR}}(y, m, \nu) &= 2\{\phi(y_\epsilon^+; m, \nu^2) + \phi(y_\epsilon^-; m, \nu^2)\},\end{aligned}$$

where  $y_\epsilon^+ = y + \epsilon$  and  $y_\epsilon^- = y - \epsilon$ , for  $\epsilon \geq 0$ .

*Proof.* The proof is deferred to Appendix B.  $\square$

The  $\epsilon$ -insensitive loss in (15) can be viewed as a symmetrized version of the Hinge loss introduced in (14). Therefore, Figures 1 and 2 have a similar interpretation in terms of variational loss averaging and smoothing of the original loss.

### 5.3 Quantile regression

The quantile regression (QR) model, firstly introduced by Koenker and Bassett (1978), aims to estimate the  $\tau$ -th conditional quantile of  $y_i$  given  $\mathbf{x}_i$  and  $\mathbf{z}_i$  assuming the linear model specification  $\eta_i = \mathbf{x}_i^\top \boldsymbol{\beta} + \mathbf{z}_i^\top \mathbf{u}$  and minimizing the empirical risk associated to the so-called check function

$$\psi^{\text{QR}}(y, \eta) = |y - \eta| \cdot |\tau - \mathbb{I}_{\leq 0}(y - \eta)|. \quad (16)$$

By definition of Equation (16), the quantile risk function is nothing but a sum of asymmetrically weighted absolute errors corresponding to the pseudo-likelihood of a misspecified asymmetric-Laplace model. This fact has been pointed out by, e.g., by Yu and Moyeed (2001). Such an equivalence helped the development of many computational tools for estimating the posterior distribution of a quantile regression model. For instance, Kozumi and Kobayashi (2011) proposed a Gibbs sampling method to perform Markov chain Monte Carlo inference, while Wand et al. (2011) and McLean and Wand (2019) derived two implementations of mean field variational Bayes for approximate inference on asymmetric-Laplace likelihood models. Here, we take a semiparametric variational Bayes approach and we use Algorithm 1 with a proper definition of the  $\Psi$ -functions (Figure 3), that is provided in the following proposition.

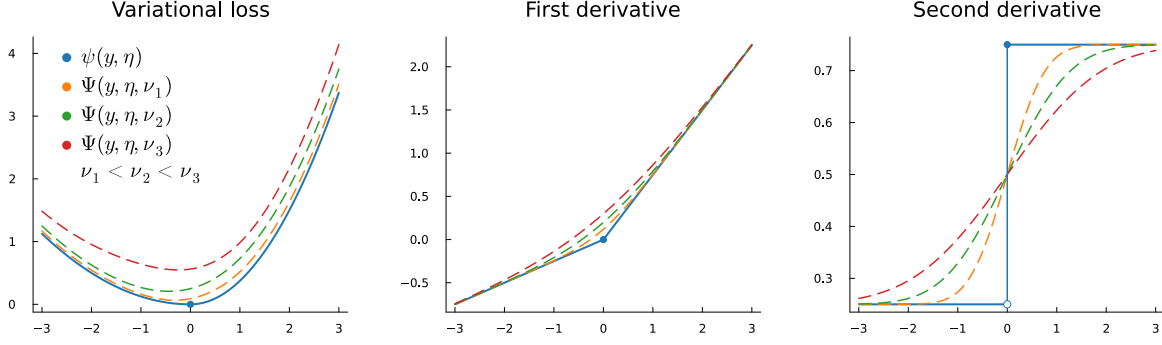


Figure 4: Expectile regression ( $\tau = 0.75$ ):  $\psi_r$  and  $\Psi_r$  functions for different values of  $\eta$  and  $\nu$ . From left to right:  $r = 0, 1, 2$ .

**Proposition 3.** *The  $\Psi$ -functions for the quantile regression model are*

$$\begin{aligned}\Psi_0^{\text{QR}}(y, m, \nu) &= (y - m) \{ \Phi(y; m, \nu^2) + \tau - 1 \} + \nu^2 \phi(y; m, \nu^2), \\ \Psi_1^{\text{QR}}(y, m, \nu) &= 1 - \tau - \Phi(y; m, \nu^2), \\ \Psi_2^{\text{QR}}(y, m, \nu) &= \phi(y; m, \nu^2).\end{aligned}$$

*Proof.* The proof is deferred to Appendix B. □

As shown in Figure 3, the check function (16) is a piecewise linear loss weighting the positive and negative errors differently. This characteristic is maintained by the variational loss introduced in Proposition 3, which has an asymptotic linear behaviour on the tails, but an almost quadratic smooth trajectory in a neighborhood of the minimum.

## 5.4 Expectile regression

Expectile regression (ER, Koenker, 2005) is a statistical model alternative to quantile regression that was proposed, among others, by Newey and Powell (1987) and Efron (1991). The original idea behind expectile regression was to replace the minimization of an asymmetrically weighted sum of absolute errors (quantile regression) with the minimization of an asymmetrically weighted sum of squared errors. Then, the expectile loss is

$$\psi^{\text{ER}}(y, \eta) = (y - \eta)^2 |\tau - \mathbb{I}_{\leq 0}(y - \eta)|. \quad (17)$$

The linear predictor  $\eta_i = \mathbf{x}_i^\top \boldsymbol{\beta} + \mathbf{z}_i^\top \mathbf{u}$  minimizing the expectile risk is called conditional  $\tau$ -expectile of  $y_i$  given  $\mathbf{x}_i$  and  $\mathbf{z}_i$ . Notice that for  $\tau = 0.5$  we recover the squared error loss  $\psi^{\text{ER}}(y_i, \eta_i) = (y_i - \eta_i)^2$ , hence the central expectile is equal to the mean, in the same way as the central quantile corresponds to the median.

Expectiles arise to be particularly important in financial applications when it comes to measuring risks. Indeed, differently from the quantile counterpart, the expectile loss function induces a coherent subadditive elicitable risk measure, as proved by Bellini and Bignozzi (2015) and Ziegel (2016).

Classical Bayesian inference on expectile regression models is performed via Metropolis-Hastings simulation from the posterior distribution using as working likelihood an Asymmetric-Gaussian model.

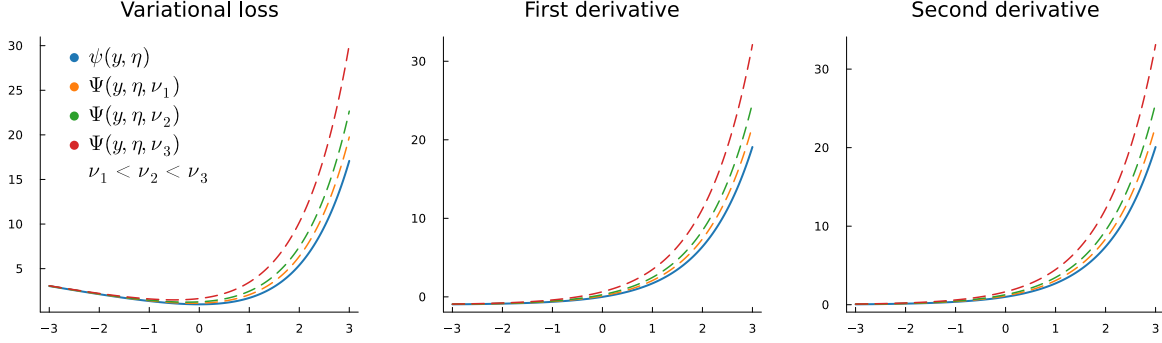


Figure 5: Poisson regression:  $\psi_r$  and  $\Psi_r$  functions for different values of  $\eta$  and  $\nu$ . From left to right:  $r = 0, 1, 2$ .

See, for example, the works of [Sobotka and Kneib \(2012\)](#), [Xing and Qian \(2017\)](#) and [Waldmann et al. \(2017\)](#). To the best of our knowledge, no conditionally conjugate stochastic representation of the Asymmetric-Gaussian model have been proposed in literature. Therefore, expectation-maximization, Gibbs sampling, or mean field variational Bayes algorithms are not available as an alternative to Metropolis-Hastings.

Like for the models presented so far, we can adopt Algorithm 1 in order to estimate the approximate posterior distribution of the conditional  $\tau$ -expectile of  $y_i$ . To do so we use the specification of the  $\Psi$ -functions (Figure 4) outlined in Proposition 4.

**Proposition 4.** *The  $\Psi$ -functions for the expectile regression model are*

$$\begin{aligned}\Psi_0^{\text{ER}}(y, m, \nu) &= \frac{1}{2} \{ (y - m)^2 + \nu^2 \} \{ (1 - \tau) - (1 - 2\tau) \Phi(y; m, \nu^2) \} - \frac{1}{2} (1 - 2\tau) (y - m) \nu^2 \phi(y; m, \nu^2), \\ \Psi_1^{\text{ER}}(y, m, \nu) &= -(y - m) \{ (1 - \tau) - (1 - 2\tau) \Phi(y; m, \nu^2) \} + (1 - 2\tau) \nu^2 \phi(y; m, \nu^2), \\ \Psi_2^{\text{ER}}(y, m, \nu) &= (1 - \tau) - (1 - 2\tau) \Phi(y; m, \nu^2).\end{aligned}$$

*Proof.* The proof is deferred to Appendix B. □

As shown in Figure 4, the variational loss averaging mapping  $\psi^{\text{ER}}(\cdot)$  to  $\Psi^{\text{ER}}(\cdot)$  helps to regularize the derivatives of the original loss (17), producing a new objective function having continuous derivatives up to the second order.

## 5.5 Exponential family

The exponential family (EF) is a wide class of distributions that includes, among others, the Gaussian, Gamma, Binomial and Poisson probability laws. It constitutes the theoretical foundation of generalized linear models ([McCullagh and Nelder, 1989](#)) and is characterized by a probability density function of the form

$$p(y_i | \xi_i) = \exp \{ y_i \xi_i - b(\xi_i) + c(y_i) \}, \quad i = 1, \dots, n,$$

where  $\xi_i$  is the so-called canonical parameter, while  $a(\cdot)$ ,  $b(\cdot)$ ,  $c(\cdot)$  are functions specific to the members of the family. The canonical parameter  $\xi_i$  is then linked with the linear predictor through the equation



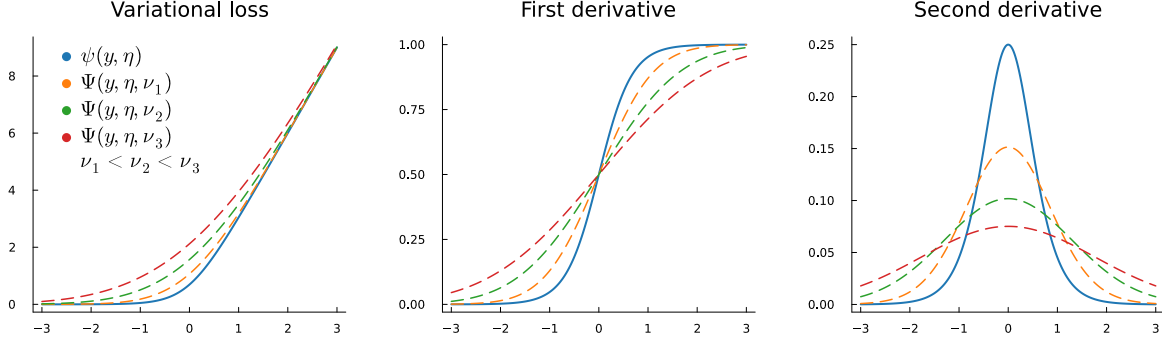


Figure 6: Logistic regression:  $\psi_r$  and  $\Psi_r$  functions for different values of  $\eta$  and  $\nu$ . From left to right:  $r = 0, 1, 2$ .

$\eta_i = (g \circ b')(\xi_i)$ , where  $g(\cdot)$  is a bijective link function and  $b'(\cdot)$  is the derivative of the convex, two times differentiable map  $b(\cdot)$ .

Assuming for simplicity that a canonical link function is considered, i.e.  $g^{-1}(\cdot) = b'(\cdot)$  and  $\xi_i = \eta_i$ , the  $\psi$ -loss associated to the exponential family log-likelihood takes the form

$$\psi^{\text{EF}}(y, \eta) = -y\eta + b(\eta). \quad (18)$$

The variational expectations  $\Psi_r^{\text{EF}}$ ,  $r = 0, 1, 2$ , are thus given by

$$\begin{aligned} \Psi_0^{\text{EF}}(y, m, \nu) &= -ym + \mathbb{E}_q\{b(\eta)\}, \\ \Psi_1^{\text{EF}}(y, m, \nu) &= -y + \mathbb{E}_q\{b'(\eta)\}, \\ \Psi_2^{\text{EF}}(y, m, \nu) &= \mathbb{E}_q\{b''(\eta)\}. \end{aligned}$$

Depending on the shape of  $b(\cdot)$ , the integrals  $\mathbb{E}_q(d^r b/dx^r)$ ,  $r = 0, 1, 2$ , may be computed analytically or approximated via univariate quadrature. For instance, in the Poisson regression model, where  $b(\eta) = \exp(\eta)$ , the explicit solution  $\mathbb{E}_q\{b(\eta)\} = \mathbb{E}_q\{b'(\eta)\} = \mathbb{E}_q\{b''(\eta)\} = \exp(m + \nu^2/2)$  is available. Differently, in the Binomial regression framework, where  $b(\eta) = \log(1 + e^\eta)$ , we may employ an adaptive Gauss-Hermite quadrature for an efficient and stable calculation, as discussed in the supplement material of [Ormerod and Wand \(2012\)](#).

A large number of papers have been published on both frequentist and Bayesian generalized linear mixed models. From a variational perspective, the most relevant contributions related to our work are: [Ormerod and Wand \(2012\)](#) (frequentist variational approximations for Poisson and Bernoulli mixed models), [Tan and Nott \(2013\)](#) (variational message passing for generalized linear mixed models), [Wand \(2014\)](#) (simplified multivariate normal updated for non-conjugate variational message passing), [Luts and Wand \(2015\)](#) (semiparametric variational Bayes for count response data). Further, we suggest the books of [Ruppert et al. \(2003\)](#), [Gelman and Hill \(2006\)](#), [Wood \(2017\)](#) for a comprehensive treatment of the theory of generalized linear mixed models and their semiparametric additive extensions.

## 6 Connection with data-augmented variational inference

Let us assume that the pseudo-likelihood function  $p(\mathbf{y}|\boldsymbol{\theta}) \propto \exp\{-nR_n(\boldsymbol{\theta})/\phi\}$  can be expressed as the convolution of an augmented pseudo-likelihood  $p(\mathbf{y}|\boldsymbol{\omega}, \boldsymbol{\theta})$  with a mixing density  $p(\boldsymbol{\omega}|\boldsymbol{\theta})$ , namely

$$p(\mathbf{y}|\boldsymbol{\theta}) = \int_{\Omega} p(\mathbf{y}|\boldsymbol{\omega}, \boldsymbol{\theta}) p(\boldsymbol{\omega}|\boldsymbol{\theta}) d\boldsymbol{\omega}, \quad (19)$$

where  $\boldsymbol{\omega} \in \Omega$  is a non-observed latent vector.

Let us suppose that the interest of the analysis is to estimate the marginal posterior distribution for the parameters  $\boldsymbol{\theta} \in \Theta$ , while  $\boldsymbol{\omega} \in \Omega$  can be considered as a vector of nuisance latent variables. The augmented representation (19) often may help in simplifying the calculations, permitting the design of iterative estimation algorithms with closed-form updating formulas. This is the case, for example, of algorithms based on local conjugate structures, like expectation-maximization, Gibbs sampling, or mean field variational Bayes.

If both the marginal and the completed models are available and a variational approximation can be produced with a similar computational effort in both cases, it is worth to understand if and how there is a convenience working with the larger model. To this end, one could compare the approximation accuracy obtained under the two approximation methods with some meaningful metric, like the Kullback-Leibler divergence. This section is devoted to explore this connection from a theoretical point of view.

We define the marginal and the augmented approximations, respectively,  $q_{\mathbf{M}}(\boldsymbol{\theta}) \in \mathcal{Q}_{\mathbf{M}}$  and  $q_{\mathbf{A}}(\boldsymbol{\omega}, \boldsymbol{\theta}) \in \mathcal{Q}_{\mathbf{A}}$ . Further, we define  $q_{\mathbf{A}}(\boldsymbol{\theta}) = \int_{\Omega} q_{\mathbf{A}}(\boldsymbol{\omega}, \boldsymbol{\theta}) d\boldsymbol{\omega}$  as the marginal density obtained by integrating out  $\boldsymbol{\omega}$  from the augmented approximation  $q_{\mathbf{A}}(\boldsymbol{\omega}, \boldsymbol{\theta})$ . Then, the optimal densities  $q_{\mathbf{M}}^*(\boldsymbol{\theta})$  and  $q_{\mathbf{A}}^*(\boldsymbol{\omega}, \boldsymbol{\theta})$  are obtained by minimizing the following Kullback-Leibler divergences

$$q_{\mathbf{M}}^*(\boldsymbol{\theta}) = \underset{q \in \mathcal{Q}_{\mathbf{M}}}{\operatorname{argmin}} \operatorname{KL}\{q(\boldsymbol{\theta}) \parallel p(\boldsymbol{\theta}|\mathbf{y})\}, \quad q_{\mathbf{A}}^*(\boldsymbol{\omega}, \boldsymbol{\theta}) = \underset{q \in \mathcal{Q}_{\mathbf{A}}}{\operatorname{argmin}} \operatorname{KL}\{q(\boldsymbol{\omega}, \boldsymbol{\theta}) \parallel p(\boldsymbol{\omega}, \boldsymbol{\theta}|\mathbf{y})\}. \quad (20)$$

Here, we assume for  $q_{\mathbf{M}}^*(\boldsymbol{\theta})$  and  $q_{\mathbf{A}}^*(\boldsymbol{\omega}, \boldsymbol{\theta})$  to be the global minimizers of the respective optimization problems. Henceforth, we do not consider possible local minima.

In order to establish some connection between these two approximations, along with the respective divergences, some *compatibility* assumption has to be imposed over  $\mathcal{Q}_{\mathbf{M}}$  and  $\mathcal{Q}_{\mathbf{A}}$ .

**Definition 1** (Compatibility). *We say that  $\mathcal{Q}_{\mathbf{A}}$  is a density space compatible with  $\mathcal{Q}_{\mathbf{M}}$  if any marginal distribution  $q_{\mathbf{A}}(\boldsymbol{\theta})$  induced by the marginalization of  $\boldsymbol{\omega} \in \Omega$  from  $q_{\mathbf{A}}(\boldsymbol{\omega}, \boldsymbol{\theta})$  belongs to  $\mathcal{Q}_{\mathbf{M}}$ . That is*

$$\mathcal{Q}_{\mathbf{A}} = \left\{ q_{\mathbf{A}}(\boldsymbol{\omega}, \boldsymbol{\theta}) : q_{\mathbf{A}}(\boldsymbol{\theta}) = \int_{\Omega} q_{\mathbf{A}}(\boldsymbol{\omega}, \boldsymbol{\theta}) d\boldsymbol{\omega} \in \mathcal{Q}_{\mathbf{M}} \right\}.$$

For instance, if we assume for  $q_{\mathbf{M}}(\boldsymbol{\theta})$  to be a Gaussian density, also  $q_{\mathbf{A}}(\boldsymbol{\theta})$  should be a Gaussian density in order to keep the compatibility condition satisfied. Similarly, if we do not specify any parametric assumption, but instead we assume a mean field factorization  $q_{\mathbf{M}}(\boldsymbol{\theta}) = \prod_k q_{\mathbf{M}}(\boldsymbol{\theta}_k)$  over a given partition of  $\boldsymbol{\theta}$ , because of the compatibility, also  $q_{\mathbf{A}}(\boldsymbol{\theta}) = \prod_k q_{\mathbf{A}}(\boldsymbol{\theta}_k)$  will factorize according to the same partition.

Under this hypothesis, we can characterize the behaviour of the Kullback-Leibler divergence under the two approximation schemes using the following results.

**Theorem 2.** *Let  $\mathcal{Q}_{\mathbf{M}}$  and  $\mathcal{Q}_{\mathbf{A}}$  be compatible spaces as defined in Definition 1. Let  $q_{\mathbf{M}}^*(\boldsymbol{\theta}) \in \mathcal{Q}_{\mathbf{M}}$  and  $q_{\mathbf{A}}^*(\boldsymbol{\omega}, \boldsymbol{\theta}) \in \mathcal{Q}_{\mathbf{A}}$  be the optimal approximating distributions defined as in (20). Then, we have*

$$\operatorname{KL}\{q_{\mathbf{M}}^*(\boldsymbol{\theta}) \parallel p(\boldsymbol{\theta}|\mathbf{y})\} \leq \operatorname{KL}\{q_{\mathbf{A}}^*(\boldsymbol{\theta}) \parallel p(\boldsymbol{\theta}|\mathbf{y})\} \leq \operatorname{KL}\{q_{\mathbf{A}}^*(\boldsymbol{\omega}, \boldsymbol{\theta}) \parallel p(\boldsymbol{\omega}, \boldsymbol{\theta}|\mathbf{y})\}.$$

*Proof.* The proof is deferred to Appendix C.  $\square$

Starting from the right inequality, Theorem 2 states that the divergence in the augmented space is always higher than the divergence in the marginal space. The difference between the two can then be interpreted as the loose of information required for approximating a larger model keeping fixed the available set of data.

On the other hand, the left hand side inequality in Theorem 2 establishes that a loose of information in the augmented parameter space, i.e.  $\Omega \times \Theta$ , also reflects on a worsening of the approximation even in the marginal space of interest, i.e.  $\Theta$ . So that, under the assumption in Definition 1, marginal approximations always dominate data-augmentation based approximations in the Kullback-Leibler metric.

This fact motivates the usage of our semiparametric variational Bayes approach for posterior approximation as an alternative to data-augmented mean field variational Bayes algorithms (see, e.g., Wand et al., 2011 and McLean and Wand, 2019), especially once the posterior approximation in the two cases take the same form. This is the case, for instance, of all the models presented in Section 5.

In Section 8 an extensive simulation experiment validates the result in Theorem 2, empirically showing that the dominance in the Kullback-Leibler metric reflects also on an higher posterior accuracy calculated with different metrics.

## 7 Possible extensions

The semiparametric variational Bayes methodology discussed so far can be easily extended to accommodate more structured model specifications, including, e.g., additive models, inducing shrinkage priors, dynamic linear models and spatial random fields. In this Section we present a brief discussion about each one of these generalizations, showing how to modify and use Algorithm 1 for the estimation of a wide class of flexible models.

The present exposition is inspired by Hodges (2014), which we refer to for an exhaustive treatment of the models introduced in the following.

### 7.1 Additive models

Additive models (Wood, 2017) are a straightforward generalization of model (8) which permits to deal with multiple heterogeneous random effects  $\mathbf{u}_1, \dots, \mathbf{u}_H$  within the same linear predictor. This way, for each observation we have

$$\eta_i = \mathbf{x}_i^\top \boldsymbol{\beta} + \sum_{h=1}^H \mathbf{z}_{i,h}^\top \mathbf{u}_h, \quad \mathbf{u}_h | \sigma_h^2 \sim \mathcal{N}_{d_h}(\mathbf{0}_{d_h}, \sigma_h^2 \mathbf{R}_h^{-1}), \quad \sigma_h^2 \sim \text{IG}(A_h, B_h), \quad (21)$$

with  $\mathbf{z}_{i,h} \in \mathbb{R}^{d_h}$ ,  $\mathbf{u}_h \in \mathbb{R}^{d_h}$ ,  $h = 1, \dots, H$ ,  $i = 1, \dots, n$ . The total number of random effects is  $d = d_1 + \dots + d_H$ .

The model specified in (21) can be represented in a more compact way as  $\eta_i = \mathbf{x}_i^\top \boldsymbol{\beta} + \mathbf{z}_i^\top \mathbf{u}$  where  $\mathbf{z}_i = (\mathbf{z}_{i,1}^\top, \dots, \mathbf{z}_{i,H}^\top)^\top \in \mathbb{R}^d$  and  $\mathbf{u} = (\mathbf{u}_1^\top, \dots, \mathbf{u}_H^\top)^\top \in \mathbb{R}^d$ . Then, we may use Algorithm 1 for performing parameter estimation. The only difference we have to account for is concerned with the presence of multiple variance parameters  $\sigma_1^2, \dots, \sigma_H^2$ . However, under the mean field factorization

$$q(\boldsymbol{\beta}, \mathbf{u}, \sigma_1^2, \dots, \sigma_H^2, \sigma_\varepsilon^2) = q(\boldsymbol{\beta}, \mathbf{u}) q(\sigma_1^2) \times \dots \times q(\sigma_H^2) q(\sigma_\varepsilon^2),$$

we are able to explicitly calculate the optimal variational approximation  $q^*(\sigma_h^2) \sim \text{IG}(\hat{\alpha}_h, \hat{\beta}_h)$ ,  $h = 1, \dots, H$ , that is an Inverse-Gamma density with variational parameters

$$\hat{\alpha}_h \leftarrow A_h + d_h/2, \quad \hat{\beta}_h \leftarrow B_h + \frac{1}{2} \hat{\boldsymbol{\mu}}_h^\top \mathbf{R}_h \hat{\boldsymbol{\mu}}_h + \frac{1}{2} \text{trace}(\mathbf{R}_h \hat{\boldsymbol{\Sigma}}_{hh}).$$

Such a modified algorithm still maintains the same computational complexity of Algorithm 1 and all the updates are available in closed form.

## 7.2 Inducing shrinkage priors

The automatic identification of non-relevant covariates is an omnipresent issue in statistics. From a Bayesian point of view, this challenge has been faced with a number of different approaches, which are all concerned with the specification of a convenient prior distribution. In principle, we wish to define a prior law able to operate an aggressive shrinkage toward zero for the non-relevant effects, while not introducing much *bias* on the estimates of the relevant coefficients.

According to the recent literature on continuous shrinkage prior, we propose to extend model (9) according with the following Gaussian scale-mixture specification:

$$\mathbf{u} | \boldsymbol{\lambda}^2, \delta^2 \sim \text{N}_d(\mathbf{0}_d, \delta^2 \boldsymbol{\Lambda}^2), \quad \boldsymbol{\Lambda}^2 = \text{diag}(\boldsymbol{\lambda}^2), \quad \boldsymbol{\lambda} \sim p(\boldsymbol{\lambda}), \quad \delta \sim p(\delta),$$

where  $\boldsymbol{\lambda}$  is a vector of local scale parameters and  $\delta$  is a global scale parameter. Depending on the particular specification of  $p(\boldsymbol{\lambda})$  and  $p(\delta)$  different models are obtained and, as a consequence, also different variational approximations arise. See, among others, the Bayesian Lasso (Park and Casella, 2008), the Horseshoe (Carvalho et al., 2010), the Normal-Exponential-Gamma (Griffin and Brown, 2011), the generalized double-Pareto (Armagan et al., 2013), the adaptive Bayesian Lasso (Leng et al., 2014), the Dirichlet-Laplace (Bhattacharya et al., 2015) models.

Assuming for the approximate posterior distribution the mean field factorization

$$q(\boldsymbol{\beta}, \mathbf{u}, \boldsymbol{\lambda}^2, \delta^2, \sigma_\varepsilon^2) = q(\boldsymbol{\beta}, \mathbf{u}) q(\lambda_1^2) \times \dots \times q(\lambda_d^2) q(\delta^2) q(\sigma_\varepsilon^2),$$

the optimal densities  $q^*(\boldsymbol{\beta}, \mathbf{u})$  and  $q^*(\sigma_\varepsilon^2)$  maintain the same structure described in Section 4, except that we need to replace  $\gamma_u \mathbf{R}$  in Equation (11) with  $\text{diag}[\mathbb{E}_q(1/\delta^2) \mathbb{E}_q(1/\boldsymbol{\lambda}^2)]$ .

Further, if we consider a set of conjugate distributions for  $p(\mathbf{u} | \boldsymbol{\lambda}, \tau)$ ,  $p(\boldsymbol{\lambda})$  and  $p(\delta)$ , also the approximating densities  $q^*(\lambda_j^2)$  and  $q^*(\delta^2)$  will enjoy analytic solutions, as well as the evidence lower bound. This is the case of all the popular prior laws cited so far. See, e.g., Neville et al. (2014).

## 7.3 Dynamic linear models

Dynamic linear models (Triantafyllopoulos, 2021) generalize the static specification (8) by introducing a latent transition equation which determines the evolution of the random effects over time, that is

$$\eta_i = \mathbf{x}_i^\top \boldsymbol{\beta} + \mathbf{z}_i^\top \mathbf{u}_i, \quad \mathbf{u}_{i+1} = \mathbf{T} \mathbf{u}_i + \mathbf{w}_i, \quad \mathbf{w}_i | \sigma_u^2 \sim \text{N}_d(\mathbf{0}_d, \sigma_u^2 \mathbf{R}^{-1}),$$

with  $i = 1, \dots, n$  denoting the time index. We complete the model by specifying the initial distribution  $\mathbf{u}_0 \sim \text{N}_d(\boldsymbol{\mu}_0, \boldsymbol{\Sigma}_0)$ . Here,  $\mathbf{T}$  is a  $d \times d$  transition matrix,  $\mathbf{R}$  is a  $d \times d$  precision matrix, while  $\boldsymbol{\nu}_t$  is a  $d \times 1$  vector of latent innovations.

Stacking all the random effects by column, i.e.  $\mathbf{u} = (\mathbf{u}_1^\top, \dots, \mathbf{u}_t^\top, \dots, \mathbf{u}_n^\top)^\top \in \mathbb{R}^{nd}$ , we obtain a prior law for  $\mathbf{u}$  that is a rank-deficient Gaussian distribution with block-tridiagonal precision matrix. Moreover, we

can express the linear predictor as  $\eta_i = \mathbf{x}_i^\top \boldsymbol{\beta} + (\mathbf{e}_i \otimes \mathbf{z}_i)^\top \mathbf{u}$ , where  $\mathbf{e}_i$  is the  $i$ -th column of a  $n$ -dimensional identity matrix and  $\otimes$  denotes the Kronecker product. This joint representation (Chan and Jeliazkov, 2009) allows us to approximate the posterior distribution by employing Algorithm 1. Kalman filter and smoother routines (Durbin and Koopman, 2012) can then be used for an efficient numerical evaluation of  $\hat{\boldsymbol{\mu}}$  and  $\hat{\boldsymbol{\Sigma}}$ .

Since in the dynamic specification the dimension of the latent states grows together with the number of observed data, also the asymptotic computational complexity of the algorithm increases. Assuming for simplicity that no fixed covariates are included, i.e.  $K = d$ , the complexity of the algorithm is dominated by the Kalman filter and smoother, which require  $\mathcal{O}(nK^3)$  flops each.

## 7.4 Spatial random fields

Latent Gaussian random fields (Rue et al., 2009) are the standard tool in Bayesian hierarchical modelling for dealing with spatially correlated data. Let us assume that the observations have been gathered on a set of  $n$  spatial locations  $\mathbf{p}_1, \dots, \mathbf{p}_n$ , which lie in the spatial domain  $\Gamma$ . Then, we can account for spatial dependence in the data by specifying the following mixed model for the linear predictor:

$$\eta_i = \mathbf{x}_i^\top \boldsymbol{\beta} + u(\mathbf{p}_i), \quad u(\cdot) \sim \text{Gaussian random field over } \Gamma.$$

Depending on the shape of the domain  $\Gamma$  and on the assumptions made upon  $u(\cdot)$ , different models arise.

For instance, if  $\Gamma$  is a finite discrete spatial domain, like an areal map or a finite network, common specifications for  $\mathbf{u} = (u(\mathbf{p}_1), \dots, u(\mathbf{p}_n))$  are simultaneous and conditional autoregressive models (Cressie, 2015), or Gaussian Markov random fields (Rue and Held, 2005). All of these lead to a multivariate Gaussian prior distribution  $\mathbf{u} | \sigma_u^2 \sim N_n(\mathbf{0}_n, \sigma_u^2 \mathbf{R}^{-1})$ , where the form and the sparsity pattern of the precision matrix  $\mathbf{R}$  are determined by the selected model.

Gaussian random fields over continuous domains can be dealt as well by approximating  $u(\cdot)$  with a penalized basis expansion:  $u(\cdot) \approx \mathbf{u}^\top \mathbf{z}(\cdot)$ . Here,  $\mathbf{z}(\cdot) = (z_1(\cdot), \dots, z_d(\cdot))^\top$  is a vector of locally supported basis functions defined over  $\Gamma$ , while  $\mathbf{u} | \sigma_u^2 \sim N_d(\mathbf{0}_d, \sigma_u^2 \mathbf{R}^{-1})$  is a Gaussian Markov random field with sparse precision  $\mathbf{R}$ . In literature this representation is used, e.g., for discretizing a wide class of Wittle-Matérn fields implicitly defined as the solution to a fractional stochastic partial differential equation (Lindgren et al., 2011, 2022).

Both the discrete and the continuous cases fit in formulation (9) and, hence, they can be efficiently estimated using Algorithm 1. Doing this, a careful management of sparse linear algebra routines is necessary for avoiding the explicit inversion of high-dimensional sparse matrices.

## 8 Simulation studies

In the following numerical examples we only consider synthetic datasets in order to reliably assess the empirical qualities of the semiparametric variational Bayes (SVB) approach discussed in Sections 4 when the truth is known. The models we consider for this analysis are: quantile regression (QR), expectile regression (ER), support vector regression (SVR), support vector classification (SVC) and logistic regression (Logit).

The performances of our method are then compared with alternative approaches developed in the literature; for all the models, we approximate the posterior via Markov chain Monte Carlo (MCMC), conjugate mean field variational Bayes (MFVB), or Laplace approximation when MFVB is not available.

Here, MCMC is used as a proxy of the *true* posterior distribution.

Table 1: References for the estimation algorithms used in the estimation of the models considered along all the simulation studies in Section 8.

Model	Method	Reference
Expectile regression	MCMC	<a href="#">Waldmann et al. (2017)</a>
	Laplace	Standard BFGS optimization
Quantile regression	MCMC	<a href="#">Kozumi and Kobayashi (2011)</a>
	MFVB	<a href="#">Wand et al. (2011)</a>
Support vector regression	MCMC	Extension of <a href="#">Polson and Scott (2011)</a>
	MFVB	Extension of <a href="#">Luts and Ormerod (2014)</a>
Support vector classification	MCMC	<a href="#">Polson and Scott (2011)</a>
	MFVB	<a href="#">Luts and Ormerod (2014)</a>
Logistic regression	MCMC	<a href="#">Polson et al. (2013)</a>
	MFVB	<a href="#">Durante and Rigon (2019)</a>

Except for expectile regression, all the other models considered here enjoy a conditional Gaussian representation, thereby MCMC and MFVB algorithms are based upon a conditional Gaussian data-augmentation strategy useful to restore the conjugacy between the likelihood function and the prior distributions. For the Laplace approximation, the optimal densities are obtained in a transformed space such that all the parameters in the model belong in an unconstrained support. See Table 2.1 for the detailed references for all the models and estimation methods considered.

The numerical routines used for the estimation have been implemented in **Julia** (Version 1.7.1). The simulations have been performed on the first author’s **Dell XPS 15** laptop with 4.7 gigahertz processor and 32 gigabytes of random access memory.

## 8.1 Performance measures

The simulations we propose rely on regression tasks, where an underlying regression function  $f(x)$  is estimated using a semiparametric model. To evaluate the ability of our method in reconstructing the original signal, we calculate the integrated absolute error (IAE) between the estimated and the true curve, that is defined as

$$\text{IAE}(f) = \int_0^1 |\hat{f}(x) - f(x)| dx. \quad (22)$$

For the quantile/expectile model, the predictions have been compared with the true underlying quantile/expectile. For support vector regression, instead we compare the prediction with the true mean function. For the support vector classification, we compare the true decision function with the estimated one. While for logistic regression, we compare the true and estimated probability of success.

The posterior approximation accuracy is quantified by means of four accuracy measures: the relative absolute error (RAE) on the posterior mean vector, the relative absolute error on the posterior variance-covariance matrix, the average marginal accuracy score (Acc) and the evidence lower bound (ELBO) obtained at the end of the optimization. The absolute relative errors are calculated as

$$\text{RAE}(\boldsymbol{\mu}) = \|\hat{\boldsymbol{\mu}} - \boldsymbol{\mu}\|_{\infty} / \|\boldsymbol{\mu}\|_{\infty}, \quad \text{RAE}(\boldsymbol{\Sigma}) = \|\hat{\boldsymbol{\Sigma}} - \boldsymbol{\Sigma}\|_{\infty} / \|\boldsymbol{\Sigma}\|_{\infty}, \quad (23)$$

where  $\boldsymbol{\mu}$  and  $\boldsymbol{\Sigma}$  denote the *true* mean vector and variance matrix, evaluated via Monte Carlo

Table 2: Non-linear functions characterizing the three simulation settings described in the text.

Setting	Non-linear functions
A	$f_\mu(x) = 1.6 \sin(3\pi x^2)$ $f_\sigma(x) = -0.6 + 0.5 \cos(4\pi x)$ $f_\pi(x) = 1.74 \sin(3\pi x^2) - 1.076$
B	$f_\mu(x) = -1.02x + 0.018x^2 + 0.4\phi(x; 0.38, 0.08) + 0.08\phi(x; 0.75, 0.03)$ $f_\sigma(x) = -0.25 + 0.15x^2 - 0.5\phi(x; 0.2, 0.1)$ $f_\pi(x) = -1.357x + 0.024x^2 + 0.532\phi(x; 0.38, 0.08) + 0.106\phi(x; 0.75, 0.03) - 0.003$
C	$f_\mu(x) = \sin(3\pi x^3) + 1.02x + 0.01x^2 + 0.4\phi(x; 0.38, 0.08)$ $f_\sigma(x) = -0.4 + 0.3x^2 + \cos(3\pi x) - 0.5\phi(x; 0.2, 0.1)$ $f_\pi(x) = 0.91 \sin(3\pi x^3) + 0.929x + 0.009x^2 + 0.364\phi(x; 0.38, 0.08) - 1.076$

approximation. Then, the average accuracy score is given by

$$\text{Acc}(q) = \frac{1}{K} \sum_{k=1}^K \text{Acc}_k(q_k), \quad \text{Acc}_k(q_k) = 1 - \frac{1}{2} \int_{-\infty}^{+\infty} |q_k(\vartheta_k) - p(\vartheta_k|\mathbf{y})| d\vartheta_k, \quad (24)$$

where  $K$  is the total number of regression parameters in the model and  $\vartheta_k$  is the  $k$ -th element of the parameter vector  $\boldsymbol{\vartheta}$ . All these metrics are normalized and can be interpreted as proportions lying in  $[0, 1]$ .

In addition to the accuracy measures described so far, we also gathered the execution time in seconds and the number of iterations needed for all the algorithms to reach the convergence.

## 8.2 First simulation setup: semiparametric regression

The synthetic data have been generated according to the non-linear model

$$y_i | x_i \sim \begin{cases} \text{N}(\mu_i, \sigma_i^2) & \text{for quantile and expectile regression,} \\ \text{t}(\mu_i, \sigma, v) & \text{for support vector regression,} \\ \text{Be}(\pi_i) & \text{for logistic and support vector classification,} \end{cases} \quad (25)$$

where

$$\mu_i = f_\mu(x_i), \quad \log(\sigma_i) = f_\sigma(x_i), \quad \text{logit}(\pi_i) = f_\pi(x_i), \quad x_i \sim \text{U}(0, 1),$$

are deterministic non-linear functions,  $\text{t}(\mu, \sigma, v)$  is the t distribution with location  $\mu \in \mathbb{R}$ , scale  $\sigma > 0$  and degrees of freedom  $v > 0$ ,  $\text{Be}(\pi)$  is the Bernoulli distribution with probability parameter  $\pi \in (0, 1)$ ,  $\text{U}(0, 1)$  is the Uniform distribution on the interval  $[0, 1]$  and  $\text{logit}(x) = \log\{x/(1-x)\}$  is the logistic transformation. Three specifications are considered for the non-linear functions in (25), named A, B, C. These are shown in Table 2. For each setting we generated 100 independent data-sets having the same number of observations, namely  $n = 500$ .

For all the considered scenarios, we model the linear predictor  $\eta_i = \mathbf{x}_i^\top \boldsymbol{\beta} + \mathbf{z}_i^\top \mathbf{u}$  using a mixed model based penalized spline. The covariate vectors  $\mathbf{x}_i = (1, x_i)^\top$  and  $\mathbf{z}_i = (z_1(x_i), \dots, z_d(x_i))^\top$  represent an orthogonalized O'Sullivan spline basis expansion (Wand and Ormerod, 2008), with corresponding fixed and random effect coefficients  $\boldsymbol{\beta} = (\beta_0, \beta_1)^\top$  and  $\mathbf{u} = (u_1, \dots, u_d)^\top$ . The dimension of the basis expansion is  $d = 40$ . The prior distributions of  $\boldsymbol{\beta}$ ,  $\mathbf{u}$ ,  $\sigma_\varepsilon^2$ ,  $\sigma_u^2$  are specified as in Equation (9), where  $\sigma_\beta^2 = 10^6$ ,



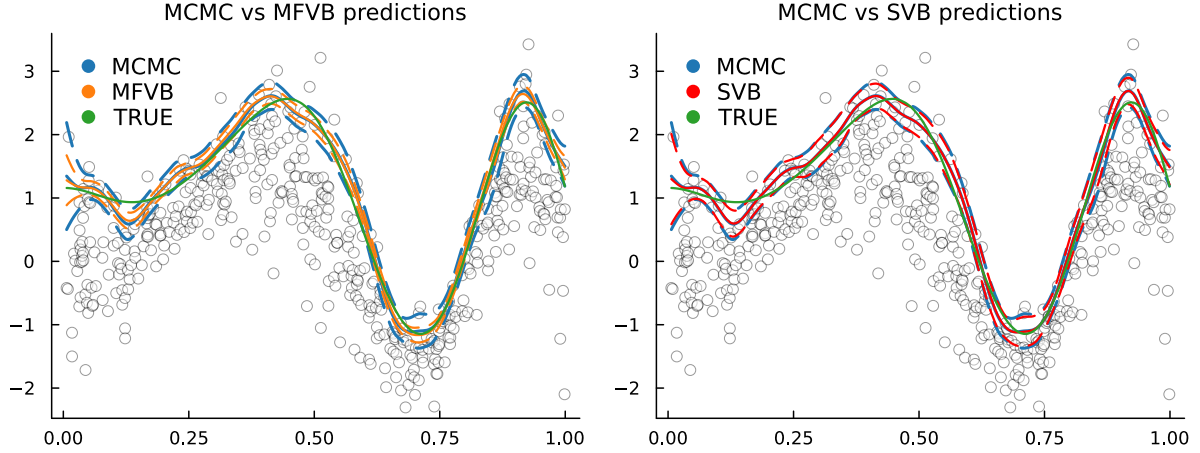


Figure 7: Posterior pointwise predictions (solid lines) and credibility bands (dashed lines) for the 90% quantile regression model described in the text. The estimates are obtained using one dataset from simulation setting A. Left: MFVB against MCMC. Right: SVB against MCMC.

$A_\varepsilon = A_u = 2.0001$  and  $B_\varepsilon = B_u = 1.0001$ . These correspond to Inverse-Gamma distributions having mean  $\mathbb{E}(\sigma_\varepsilon^2) = \mathbb{E}(\sigma_u^2) = 1$  and variance  $\text{Var}(\sigma_\varepsilon^2) = \text{Var}(\sigma_u^2) = 10^3$ . In each setting, for heteroschedastic data we estimate expectile and quantile regression models with  $\tau = 0.9$ ; for the homoschedastic t-distributed data we estimate support vector regression model with  $\epsilon = 0.01$ ; for the Bernoulli data we estimate logistic and support vector classification models. In all these cases, Algorithm 1 is stopped when the relative change of both the lower bound and the variational parameters fall below  $10^{-4}$ .

Table 3 reports the accuracy measures described in Section 8.1 for each model, algorithm and setting. Only one dataset is considered for such an analysis. In terms of prediction accuracy and signal reconstruction (fifth column), semiparametric variational Bayes, mean field variational Bayes and Laplace approximation perform quite similarly. However, in terms of posterior approximation accuracy the situation is pretty different. The evidence lower bound (fourth column) of semiparametric variational Bayes is always higher than mean field variational Bayes, indicating a better approximation of the joint posterior density. This also reflects on the average accuracy score (last column), indeed semiparametric variational Bayes outperforms mean field variational Bayes in almost all the simulations and for all the considered models, while being slightly less precise than Laplace approximation for expectile regression.

The improvement of semiparametric variational Bayes over the mean field approximation is mainly due to a more precise quantification of the posterior variance of the regression coefficients, as can be seen by looking at the relative absolute errors in Table 3 (sixth and seventh columns). This fact is also highlighted by Figures 7 and 8, which show the predictive distribution and the marginal posterior density functions for some parameters in the model. Both figures refer to a quantile regression model estimated over one dataset from simulation setting A. Mean field variational Bayes systematically overshrinks the posterior variability producing narrow credibility bands for the estimated curve, see Figure 7. On the other side, semiparametric variational Bayes tends to mimic in a more accurate way the Markov chain Monte Carlo posterior (Figure 8), producing reliable credibility intervals and prediction bands (Figure 7).

As we mentioned so far, the evidence lower bound for the semiparametric variational approach is always higher than the evidence lower bound obtained with the data augmented mean field approximation

Table 3: Performance measure comparisons between SVB, MFVB and Laplace based on the 3 simulation setting outlined in the text and in Table 2.

Setting	Model	Method	ELBO	IAE( $f$ )	RAE( $\mu$ )	RAE( $\Sigma$ )	Acc( $q$ )
A	ER	Laplace		0.4757	0.0651	0.2114	0.9743
		SVB	249.3842	0.4450	0.1282	0.2466	0.9687
	QR	MFVB	-626.4552	0.7423	0.2833	0.5066	0.7809
		SVB	-621.0120	0.7402	0.0498	0.2412	0.8760
	SVR	MFVB	-547.6501	0.1265	0.1543	0.3785	0.8903
		SVB	-544.8723	0.1280	0.0267	0.1346	0.9324
	SVC	MFVB	-666.3824	0.0340	0.2958	0.7426	0.7537
		SVB	-664.1825	0.0300	0.1372	0.5491	0.8565
	Logit	MFVB	-334.9531	0.0619	0.0430	0.2558	0.9568
		SVB	-334.8914	0.0608	0.0315	0.1993	0.9570
B	ER	Laplace		0.5350	0.0347	0.1762	0.9678
		SVB	217.1924	0.5126	0.0479	0.1839	0.9669
	QR	MFVB	-656.9304	0.8259	0.1201	0.4614	0.8488
		SVB	-652.4221	0.8261	0.0360	0.1990	0.9136
	SVR	MFVB	-552.2767	0.1399	0.1625	0.4148	0.8724
		SVB	-549.2169	0.1398	0.0258	0.1490	0.9139
	SVC	MFVB	-573.2292	0.1080	0.1767	0.4468	0.8731
		SVB	-571.7809	0.1080	0.1051	0.3035	0.8915
	Logit	MFVB	-307.3833	0.0438	0.1293	0.3642	0.9318
		SVB	-307.1958	0.0424	0.1021	0.2995	0.9444
C	ER	Laplace		0.7467	0.1233	0.4780	0.9456
		SVB	89.9416	0.7107	0.1983	0.5413	0.9277
	QR	MFVB	-776.0003	1.0132	0.1453	0.5421	0.8220
		SVB	-771.6341	1.0200	0.0619	0.2812	0.8668
	SVR	MFVB	-638.7977	0.1105	0.0558	0.3575	0.8964
		SVB	-636.0827	0.1139	0.0218	0.1610	0.9372
	SVC	MFVB	-578.2343	0.0260	0.1806	0.4983	0.8328
		SVB	-575.9832	0.0260	0.0918	0.3328	0.8785
	Logit	MFVB	-291.6064	0.0347	0.0407	0.2926	0.9520
		SVB	-291.3853	0.0342	0.3261	0.1977	0.9567

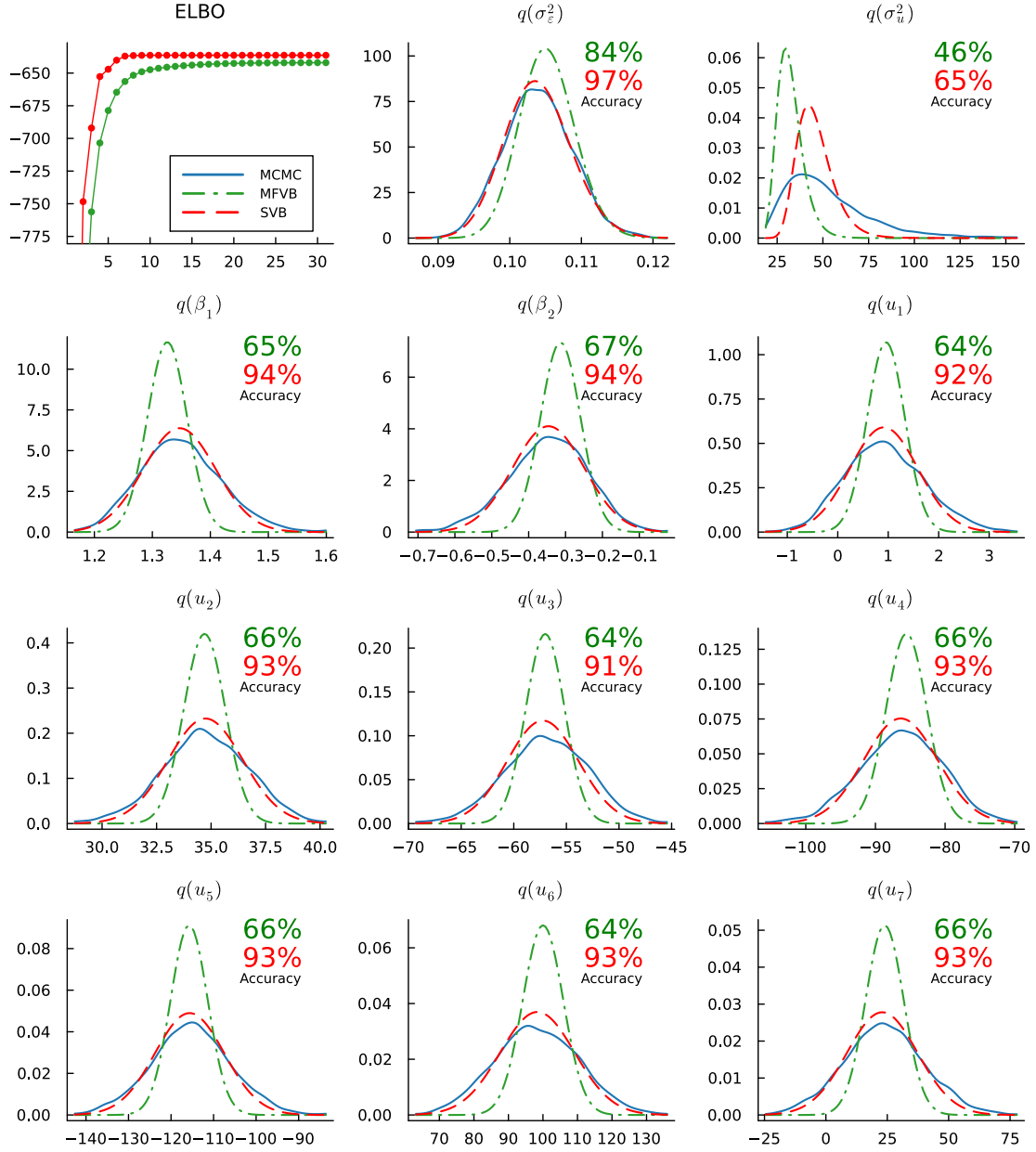


Figure 8: Top left: evidence lower bound evolution over the algorithm iterations. Others: optimal posterior density functions of the parameters in the 90% quantile regression model described in the text. The estimates are obtained using one dataset from simulation setting A. The solid blue line is for MCMC, the dashed red one for SVB and the dash-dotted green one for MFVB. The percentages denote the correspondent marginal accuracy scores defined in (24).

(Table 3 and Figure 8). This fact constitutes an empirical evidence in favour of Theorem 2, since Assumption 1 is satisfied and the inequality  $\log p\{\mathbf{y}; q_{\text{SVB}}^*(\boldsymbol{\theta})\} \geq \log p\{\mathbf{y}; q_{\text{MFVB}}^*(\boldsymbol{\theta})\}$  implies

$$\text{KL}\{q_{\text{SVB}}^*(\boldsymbol{\theta}) \parallel p(\boldsymbol{\theta}|\mathbf{y})\} \leq \text{KL}\{q_{\text{MFVB}}^*(\boldsymbol{\theta}) \parallel p(\boldsymbol{\theta}|\mathbf{y})\}.$$

To verify that Assumption 1 is accommodated, we just observe that both the approximations  $q_{\text{SVB}}^*(\boldsymbol{\theta})$  and  $q_{\text{MFVB}}^*(\boldsymbol{\theta})$  factorize according to the same partition, i.e.  $q(\boldsymbol{\theta}) = q(\boldsymbol{\beta}, \mathbf{u})q(\sigma_u^2)q(\sigma_\varepsilon^2)$ , and they take the same functional form, i.e.  $q(\boldsymbol{\beta}, \mathbf{u})$  is Gaussian, while  $q(\sigma_u^2)$  and  $q(\sigma_\varepsilon^2)$  are Inverse-Gamma.

Figure 9 summarizes the results obtained by replicating the analysis described so far over a set of 100 datasets for each simulation setting. Coherently with the previous findings, semiparametric variational Bayes uniformly outperforms conjugate mean field variational Bayes in terms of marginal posterior approximation (first row). On the other hand, semiparametric variational inference has a slightly worse accuracy score than Laplace approximation for the expectile regression model. Still, this loss in the marginal accuracy for the expectile model does not have a significant impact on the relative errors for the posterior mean and variance, that are statistically equivalent for the two approximations (third and fourth rows). The performance in terms of signal reconstruction is almost equivalent among different approximation methods (second row).

For what concerns the computational complexity, both the number of iterations and the execution times obtained with the proposed approach are competitive with the alternatives methods in literature (fifth and sixth rows, Figure 9). This evidence is consistent with the theoretical computational complexity derived for Algorithm 1, i.e.  $\mathcal{O}(nK^2 + K^3)$ , that is the same of Laplace approximation and data-augmented mean field variational Bayes for the models considered here.

### 8.3 Second simulation setup: random intercept models

In this second simulation study, we assess the relative quality of the proposed variational approximation for a random intercept model when the sample size and the number of parameters change. We consider two simulation setups: in the first one, setting A, the number of parameters is fixed and the sample dimension grows; in the second one, setting B, the sample size is kept fixed and the number of parameters increases.

In both the scenarios, the considered data generating mechanism is analogous to the one presented in (25): we have a heteroscedastic Gaussian model for quantile and expectile regression, a homoscedastic t-distributed model for support vector regression, and a Bernoulli model for support vector classification and logistic regression. In formulas,

$$y_{ij}|x_{ij} \sim \begin{cases} \text{N}(\mu_{ij}, \sigma_{ij}^2) & \text{for quantile and expectile regression,} \\ \text{t}(\mu_{ij}, \sigma, \nu) & \text{for support vector regression,} \\ \text{Be}(\pi_{ij}) & \text{for logistic and support vector classification.} \end{cases}$$

A random intercept specification is considered for  $\mu_{ij}$ ,  $\sigma_{ij}$  and  $\pi_{ij}$ , that is

$$\mu_{ij} = \beta_0 + \beta_1 x_{ij} + u_j, \quad \log(\sigma_{ij}) = \gamma_0 + \gamma_1 x_{ij} + v_j, \quad \text{logit}(\pi_{ij}) = \mu_{ij},$$

where the indices  $i = 1, \dots, n$  and  $j = 1, \dots, d$  identify, respectively, the  $i$ -th subject and the  $j$ -th group under study. The fixed effect parameters  $\beta_0, \beta_1$  and  $\gamma_0, \gamma_1$  are generated according to a  $\text{N}(0, 1/2)$  distribution, the random intercepts  $u_1, \dots, u_d$  and  $v_1, \dots, v_d$  are generated according to a  $\text{N}(0, 1/4)$  distribution, while  $\sigma = 1/10$  and  $\nu = 4$ .

In simulation setting A, the considered sample sizes are  $n = 250, 500, 1000, 2000, 4000$ , and the fixed number of groups is  $d = 20$ . In simulation setting B, the fixed sample size is  $n = 500$  and the random

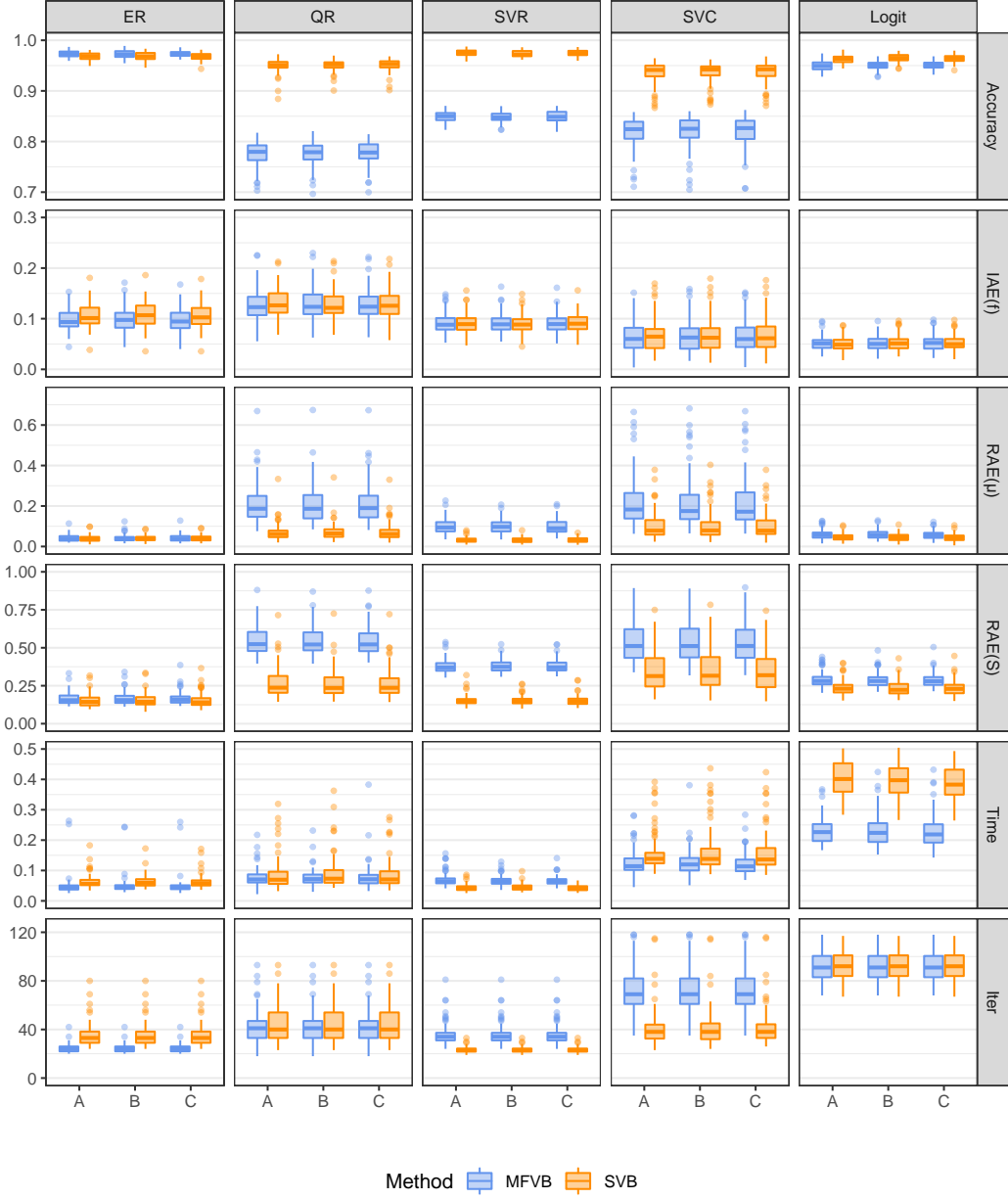


Figure 9: Boxplots of the summary statistics for the simulation study described in the text (Sections 8.1 and 8.2). Each column corresponds to a model. Each row corresponds to a performance index. Within each panel, we find three groups of paired boxplot which correspond to the three simulation settings, i.e., A, B, C (see Equation 25 and Table 2). Each boxplot is calculated over 100 replications, i.e. 100 simulated datasets.

intercept groups are  $d = 5, 10, 25, 50, 100$ . For each simulation setting, sample dimension and number of groups, we generate 100 datasets using the sampling design described so far.

For the estimation, we specify the linear predictor as  $\eta_{ij} = \mathbf{x}_{ij}^\top \boldsymbol{\beta} + \mathbf{z}_{ij}^\top \mathbf{u}$ , where  $\mathbf{x}_{ij}^\top = (1, x_{ij})$  is a covariate vector and  $\mathbf{z}_{ij}^\top$  is a  $1 \times d$  selection vector associated to the  $j$ -th group, whose  $j$ -th entry is equal to 1 and all the others are 0.

The prior distributions of  $\boldsymbol{\beta}, \mathbf{u}, \sigma_\varepsilon^2, \sigma_u^2$  are specified as in Equation (9), where  $\sigma_\beta^2 = 10^4$ ,  $A_\varepsilon = A_u = 2.0001$  and  $B_\varepsilon = B_u = 1.0001$ . For the heteroscedastic data, we estimate quantile and expectile regression models with  $\tau = 0.9$ ; for the homoscedastic t-distributed data, we estimate a support vector regression model with  $\epsilon = 0.01$ ; for the Bernoulli data, we estimate a support vector classification model and a logistic regression.

In Figure 10, we show the boxplots of the average accuracy scores (24) calculated over a bunch of 100 datasets per each scenario, both under simulation setting A (left) and B (right). As we might expect, at the increase of the sample dimension (setting A), the accuracy scores improve both for semiparametric and mean field variational approximations. The opposite happens when the sample size is kept fixed and the number of groups, i.e., the number of parameters, grows (setting B). Furthermore, we observe a clear dominance of semiparametric variational Bayes over conjugate mean field variational Bayes in all the considered simulation setups, except for expectile regression, which is compared with Laplace approximation. Such a behavior confirms our findings in Section 8.2.

For what concerns the computation efficiency, Figure 11 provides the boxplots of the  $\log_{10}$ -transformed execution times measured for each model considered in simulation settings A and B. In both the scenarios, the execution time increase with the dimension of the problem, or in terms of sample size, or in terms of number of random effect parameters. For all the models and scenarios, our semiparametric variational routine reaches a computational time relative to or lower than the mean field competitor. The only exception is logistic regression, for which our algorithm systematically takes more time than mean field coordinate ascent, while maintaining the same computational complexity. This is due to the fact that we do not have closed form integration results for the  $\Psi$  functions in the logistic regression case (see Section 5.5), and we need to rely on numerical quadrature techniques. Therefore, each iteration of the algorithm requires a higher, but fixed, number of operations than conjugate mean field variational Bayes.

## 9 Real data application

In this section, we present a real data problem concerning the forecast of the global electricity load consumption. In such a context, the data are usually highly dominated by non-stationary trends, multiple seasonal cycles of different lengths, like daily, weekly and monthly patterns, heteroscedasticity and by the presence of extreme values. Therefore, for the management of the power supply, it is of critical importance to understand and predict the behaviour of the distribution of the load consumption, especially during exceptional events. To this end, a non-parametric density forecasting approach can be taken by pooling the information coming from several quantile estimates. Each conditional quantile can then be express as a non-linear function of the available meteorological, economic and social information, for example, using an additive model specification.

Here we consider the data used in the load forecasting track of the Global Energy Competition 2014 (Hong et al., 2016), which have already been analysed by, e.g., Gaillard et al. (2016) and Fasiolo et al. (2021). The dataset collects the half-hourly load consumption and temperatures over the period going from January 2005 to December 2011. Our aim is then to estimate in a semiparametric way 19 equally spaced conditional quantiles between  $\tau = 0.05$  and  $\tau = 0.95$ . This way, we provide an approximation

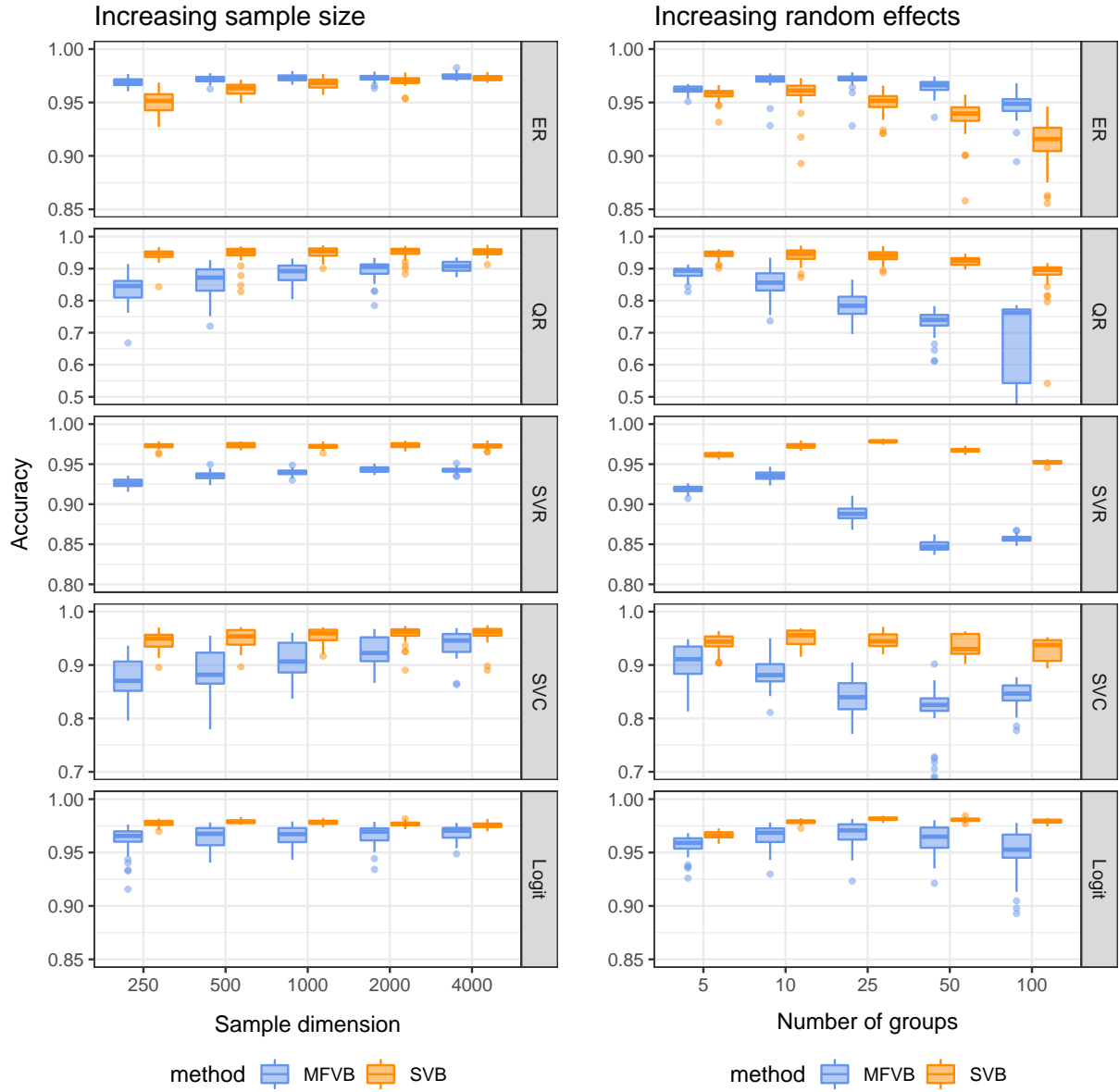


Figure 10: Sampling distribution of the marginal accuracy score defined in (24) for the simulation setup described in Section 8.3. Each row corresponds to a model, each column corresponds to a simulation setting. The left column is for setting A, the right column is for setting B.



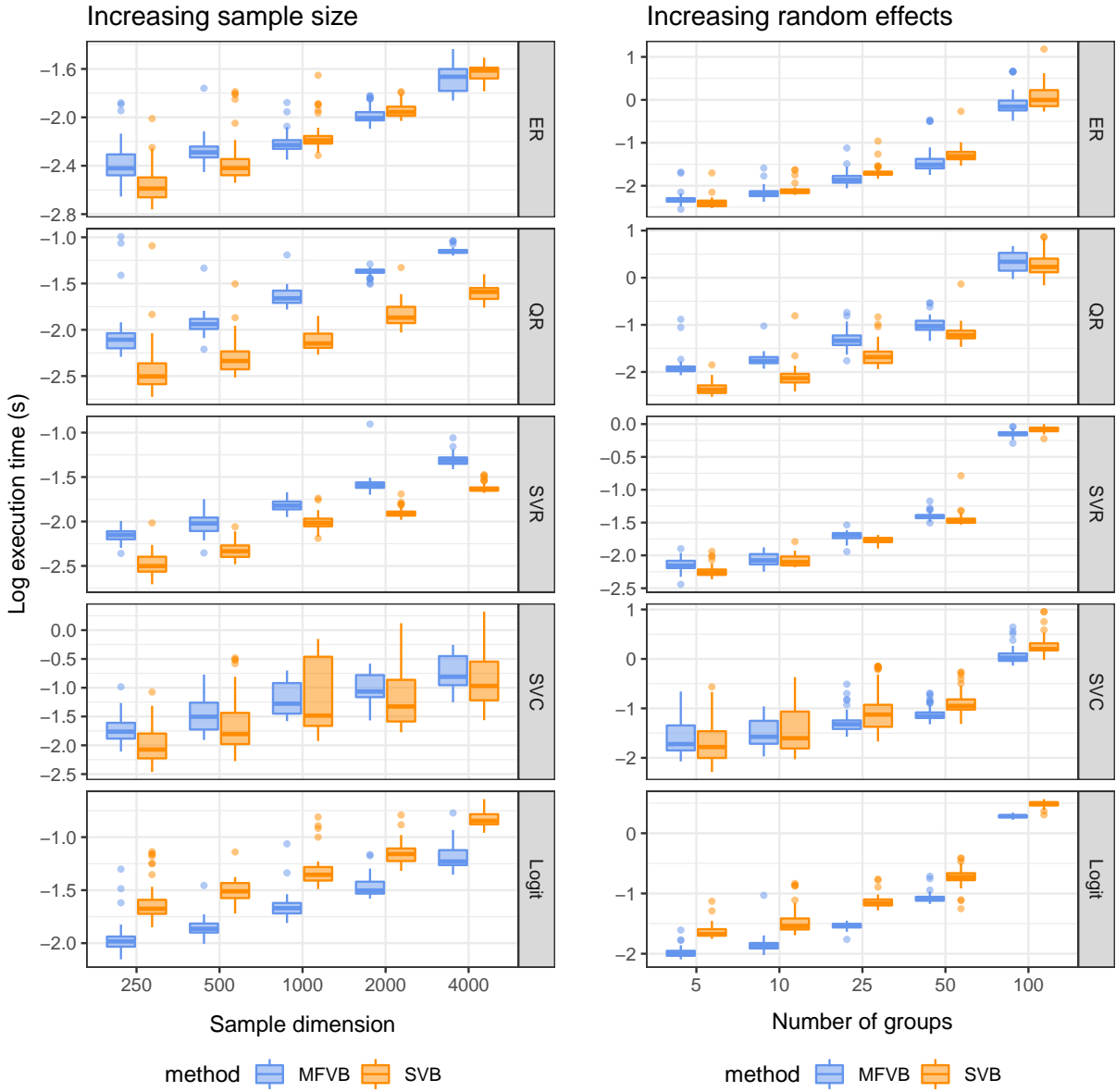


Figure 11: Sampling distribution of the  $\log_{10}$ -transformed execution time measured in seconds for the simulation setup described in Section 8.3. Each row corresponds to a model, each column corresponds to a simulation setting. The left column is for setting A, the right column is for setting B.

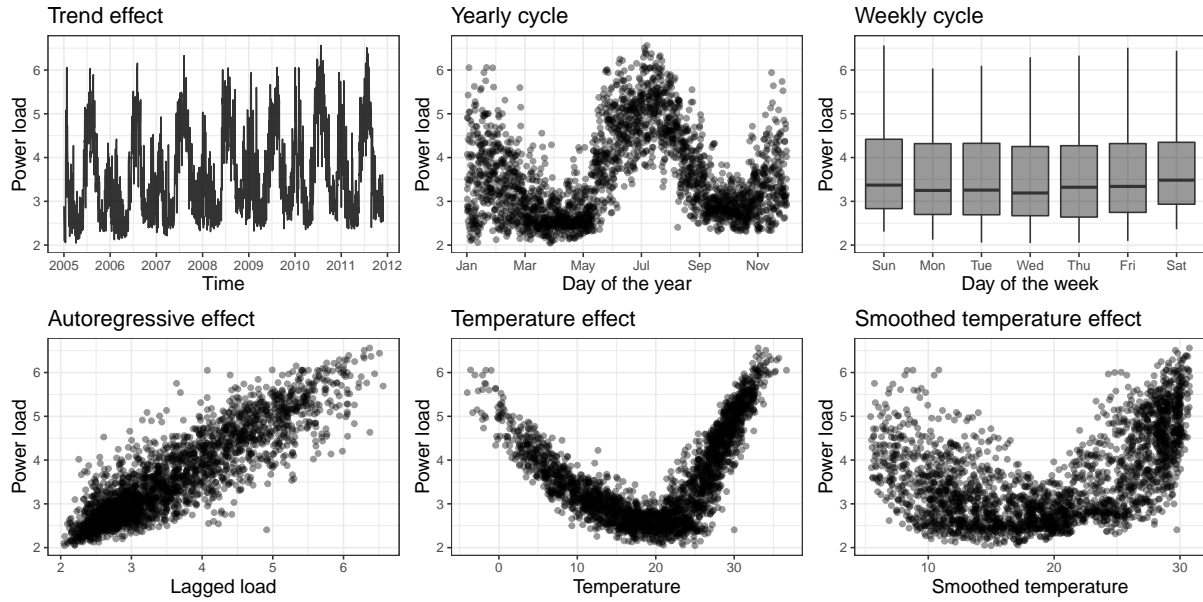


Figure 12: Pairwise scatter-plots of the power load consumption (in MWh) against the available covariates in the dataset. Top row: the time in days (left), the day of the year (middle) and the day of the week (right). Bottom row: the lagged power load (left), the temperature in Celsius scale (middle) and the smoothed temperature in Celsius scale (right).

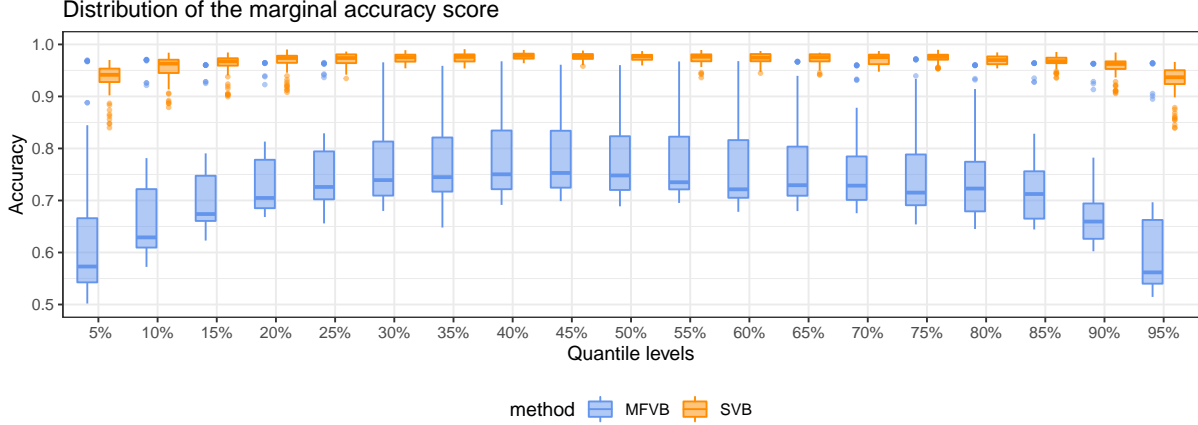


Figure 13: Distribution of the accuracy scores for the 19 estimated quantiles. For each quantile level, the boxplot is calculated over the individual accuracy scores of the 42 regression parameters in the model.

of the conditional distribution of the load consumption at each time without imposing any parametric assumption. As [Fasiolo et al. \(2021\)](#), we only consider the time interval between 11:30 and 12:00 a.m., but a similar analysis can be performed for all the remaining periods of the day, as it is common in literature. Figure 12 portrays how the observed power load is associated with some relevant covariates in the dataset.

The  $\tau$ -quantile of the power load, namely  $\text{Load}_t$ , is then modelled according with an additive specification, as described in Section 7.1. We only consider here the variables selected by [Gaillard et al. \(2016\)](#) and used also by [Fasiolo et al. \(2021\)](#), obtaining so the linear predictor:

$$\eta_t = \beta^\top \text{Day}_t + f_1^{15}(\text{Temp}_t) + f_2^{15}(\text{sTemp}_t) + f_3^{20}(\text{Cycle}_t) + f_4^{10}(\text{Load48}_t) + f_5^4(t),$$

where  $f_h^r(x) = \mathbf{u}_h^\top \mathbf{z}_h(x)$  is an orthogonal O’Sullivan spline basis expansion of rank  $r$  ([Wand and Ormerod, 2008](#)), having coefficients  $\mathbf{u}_h = (u_{h,1}, \dots, u_{h,r})^\top$  and basis functions  $\mathbf{z}_h(x) = (z_{h,1}(x), \dots, z_{h,r}(x))^\top$ ;  $\text{Day}_t$  is a factor variable indicating the day of the week;  $\text{Temp}_t$  is the hourly temperature;  $\text{sTemp}_t$  is the smoothed temperature, obtained as  $\text{sTemp}_t = 0.95 \cdot \text{Temp}_{t-1} + 0.05 \cdot \text{Temp}_t$ ;  $\text{Cycle}_t$  is a cyclic variable indicating the position within the year;  $\text{Load48}_t$  is the power load observed at the same time of the previous day; and  $t$  is a trend variable indicating the time point.

We set diffuse prior distributions for all the parameters in the model, that is:  $\sigma_\beta^2 = 10^6$ ,  $A_\varepsilon = 2.0001$ ,  $B_\varepsilon = 1.0001$ ,  $A_h = 2.0001$ ,  $B_h = 1.0001$ ,  $h = 1, \dots, 5$ . The parameters are then estimated using Markov chain Monte Carlo ([Kozumi and Kobayashi, 2011](#)), mean field variational Bayes ([Wand et al., 2011](#)) and semiparametric variational Bayes (Algorithm 1).

The outcome of our analysis confirms an excellent performance of the proposed semiparametric variational approach in approximating the Monte Carlo posterior, as shown in Figure 13. The accuracy scores for all the considered quantile levels are all very close to 1 and almost always exceeding 0.9 for semiparametric variational Bayes. On the other hand, mean field variational Bayes has a median accuracy centered around 0.7, with many values falling below 0.6, especially for the most extreme quantiles. Therefore, also in a real data example semiparametric variational Bayes strongly outperforms conjugate mean field approximation.

## 10 Discussion

We developed a new semiparametric variational method for estimating risk-based Bayesian regression models. Our approach is general and can be implemented for a wide class of mixed regression models far beyond the few examples we presented here. It can overcome issues related to non-regular loss functions and non-conjugate priors while maintaining the efficiency of a Newton algorithm. Such a method outperforms the accuracy of conjugate mean field variational Bayes in many examples, with good-to-excellent results in approximating the true target posterior distribution.

This work also introduces the first deterministic approximation alternative to the Laplace method for Bayesian expectile regression, which until now has been estimated only through onerous simulation-based algorithms (Waldmann et al., 2017).

Many extensions to the basic approach are allowed, including models for multiple and cross-random effects, spatio-temporal processes and inducing shrinkage priors alternative to those presented here. We argue that frequentist mixed regression models can be dealt as well with a careful combination of expectation-maximization algorithm and Gaussian variational approximation as in Ormerod and Wand (2010), Hall et al. (2011a), Hall et al. (2011b), Ormerod and Wand (2012), among others. This would be extremely useful for those models that do not enjoy the classical regularity conditions needed for implementing the Laplace approximation and would give an efficient alternative to cumbersome Monte Carlo integration (Geraci and Bottai, 2007) and multivariate quadrature methods (Geraci and Bottai, 2014). This generalization will be the topic of future works in the direction of exploring the use of variational methods for frequentist inferential purposes.

A final innovation concerns with the loss smoothing for non-regular minimization problems. This practice is often employed when it comes to optimizing non-smooth risk functions and consists of replacing an originally non-regular loss with a tilted one. The new objective function will be almost equal to the original one except for the fact that is uniformly differentiable all over its domain. This way, many efficient routines are made available for the optimization, like the Newton and quasi-Newton algorithms. Some examples in the quantile regression literature can be found, e.g., in the works of Hunter and Lange (2000), Yue and Rue (2011), Oh et al. (2011) and Fasiolo et al. (2021). Similar approaches have been considered also in the support vector machines literature (Lee and Mangasarian, 2001). As emerges from Proposition 1 and Figures 1 (support vector classification), 2 (support vector regression), 3 (quantile regression), the variational loss averaging defined in formula (12) actually provides a new recipe for constructing smooth majorizing objective functions starting from non-differentiable loss functions. However, differently from other existing smoothing methods based on geometric considerations, our strategy is based upon a statistical argument with a straightforward probabilistic interpretation, similarly to the expectation-maximization algorithm. Moreover, our proposal comes together with a practical rule for determining the local degree of smoothing induced by the approximation, which is in turn determined by the posterior variance of the  $i$ -th linear predictor. This leads to a different smoothing factor for each observation, allowing for adaptive calibration of the new loss.

## A Thecnical details and integration results

The calculation of non-standard expected values is the main challenge in variational Bayesian inference. Here, we face this issue with a careful combination of integral simplification, analytic solution and efficient univariate numerical quadrature. The results in this section are then introduced in order to characterize and simplify the most complex integration tasks encountered in this article, but may also provide useful insights for future works not necessarily restricted to the variational approach.

In the rest of this section, we will make use of the following notation:  $g : \mathbb{R} \rightarrow \mathbb{R}$  is a measurable function, having integrable  $n$ -th order weak derivative  $g_n$  up to the order  $N$ . We recall that  $g_n$  is defined as the measurable function satisfying the integral equation

$$\int_a^b \frac{d^n}{dx^n} \varphi(x) g(x) dx = (-1)^n \int_a^b \varphi(x) g_n(x) dx,$$

for any infinitely differentiable function  $\varphi : [a, b] \rightarrow \mathbb{R}$  such that  $\varphi(a) = \varphi(b) = 0$ . If  $g$  is  $n$  times differentiable, then  $g_n = d^n g / dx^n$ . We denote with  $H_n : \mathbb{R} \rightarrow \mathbb{R}$  the  $n$ -th order Hermite polynomial, which is the solution of the differential equation

$$\frac{d^n}{dz^n} \phi(z) = (-1)^n H_n(z) \phi(z), \quad z \in \mathbb{R}, \quad n \in \mathbb{N}.$$

In particular, we recall that  $H_0(z) = 1$ ,  $H_1(z) = z$  and  $H_2(z) = z^2 - 1$ . Finally, we introduce the notation  $(\mathbf{x})^n$  for  $n = 0, 1, 2$ , that is  $(\mathbf{x})^0 = 1$ ,  $(\mathbf{x})^1 = \mathbf{x}$  and  $(\mathbf{x})^2 = \mathbf{x} \mathbf{x}^\top$ .

Most of the non-analytic integral encountered in our work take the following functional form

$$\mathcal{F}_n(g, \mathbf{a}, \boldsymbol{\mu}, \boldsymbol{\Sigma}) = \int_{\mathbb{R}^d} g_n(\mathbf{a}^\top \mathbf{x}) \phi_d(\mathbf{x}; \boldsymbol{\mu}, \boldsymbol{\Sigma}) d\mathbf{x}, \quad (26)$$

$$\mathcal{G}_n(g, \mathbf{a}, \boldsymbol{\mu}, \boldsymbol{\Sigma}) = \int_{\mathbb{R}^d} g(\mathbf{a}^\top \mathbf{x}) (\mathbf{x})^n \phi_d(\mathbf{x}; \boldsymbol{\mu}, \boldsymbol{\Sigma}) d\mathbf{x}, \quad (27)$$

$$\mathcal{H}_n(g, \mathbf{a}, \boldsymbol{\mu}, \boldsymbol{\Sigma}) = \int_{-\infty}^{+\infty} g(\mathbf{a}^\top \boldsymbol{\mu} + \sqrt{\mathbf{a}^\top \boldsymbol{\Sigma} \mathbf{a}} z) H_n(z) \phi(z) dz, \quad (28)$$

where  $\mathbf{a} \in \mathbb{R}^d$ . Such integrals are assumed to be well-defined at least for  $n = 0, 1, 2$ . The main properties of functionals (26), (27), (28) are then provided in the following propositions.

**Proposition 5.** *Let  $g : \mathbb{R} \rightarrow \mathbb{R}$  be a function such that  $g_n$  and  $\mathcal{F}_n$  exist up to the order  $N$ . Then:*

- (1)  $\mathcal{F}_n$  has infinitely many continuous derivatives with respect to  $\boldsymbol{\mu}$  and  $\boldsymbol{\Sigma}$ ;
- (2) if  $g_n$  is continuous, then  $\mathcal{F}_n(g, \mathbf{a}, \boldsymbol{\mu}, \boldsymbol{\Sigma}) \rightarrow g_n(\mathbf{a}^\top \boldsymbol{\mu})$  as  $\mathbf{a}^\top \boldsymbol{\Sigma} \mathbf{a} \rightarrow 0$ ;
- (3) if  $g$  is convex in  $x$ , then  $\mathcal{F}_0$  is jointly convex with respect to  $\mathbf{a}^\top \boldsymbol{\mu}$  and  $\sqrt{\mathbf{a}^\top \boldsymbol{\Sigma} \mathbf{a}}$ ;
- (4) if  $g$  is convex in  $x$ , then  $g(\mathbf{a}^\top \boldsymbol{\mu}) \leq \mathcal{F}_0(g, \mathbf{a}, \boldsymbol{\mu}, \boldsymbol{\Sigma})$ .

**Proposition 6.** *Let  $\mathbf{n} = (n_1, \dots, n_d) \in \mathbb{N}^d$  be a multi-index vector with rank  $n = n_1 + \dots + n_d$ . Then, if  $\mathcal{F}_0, \dots, \mathcal{F}_n$  are well-defined, the  $\mathbf{n}$ -th order mixed derivative of  $\mathcal{F}_0$  with respect to  $\boldsymbol{\mu}$  is*

$$\frac{\partial^n \mathcal{F}_0}{\partial \mu_1^{n_1} \dots \partial \mu_d^{n_d}} = \left( \prod_{j=1}^d a_j^{n_j} \right) \mathcal{F}_n.$$

**Proposition 7.** *Assuming that  $\mathcal{F}_n$ ,  $\mathcal{G}_n$  and  $\mathcal{H}_n$  are well-defined for  $n = 0, 1, 2$ , then we have*

$$\begin{aligned} \mathcal{G}_0 &= \mathcal{F}_0 = \mathcal{H}_0, & \mathcal{G}_1 &= \boldsymbol{\mu} \mathcal{H}_0 + \frac{\boldsymbol{\Sigma} \mathbf{a}}{\sqrt{\mathbf{a}^\top \boldsymbol{\Sigma} \mathbf{a}}} \mathcal{H}_1, \\ \mathcal{G}_2 &= (\boldsymbol{\mu} \boldsymbol{\mu}^\top + \boldsymbol{\Sigma}) \mathcal{H}_0 + \frac{\boldsymbol{\Sigma} \mathbf{a} \boldsymbol{\mu}^\top + \boldsymbol{\mu} \mathbf{a}^\top \boldsymbol{\Sigma}}{\sqrt{\mathbf{a}^\top \boldsymbol{\Sigma} \mathbf{a}}} \mathcal{H}_1 + \frac{\boldsymbol{\Sigma} \mathbf{a} \mathbf{a}^\top \boldsymbol{\Sigma}}{\mathbf{a}^\top \boldsymbol{\Sigma} \mathbf{a}} \mathcal{H}_2. \end{aligned}$$

**Proposition 8.** Let  $\mathcal{H}_n = \mathcal{H}_n(\tilde{g}, \mathbf{a}, \boldsymbol{\mu}, \boldsymbol{\Sigma})$  with  $\tilde{g}(\cdot) = \mathbb{I}_{(b,c]}(\cdot)$ , where  $b, c \in \mathbb{R}$  such that  $b < c$ . Then,  $\mathcal{H}_n$  is well-defined and is equal to

$$\mathcal{H}_n = \begin{cases} \Phi(z^+) - \Phi(z^-) & \text{if } n = 0, \\ (-1)[H_{n-1}(z^+)\phi(z^+) - H_{n-1}(z^-)\phi(z^-)] & \text{if } n > 0, \end{cases}$$

$$\text{where } z^- = \frac{b - \mathbf{a}^\top \boldsymbol{\mu}}{\sqrt{\mathbf{a}^\top \boldsymbol{\Sigma} \mathbf{a}}} \text{ and } z^+ = \frac{c - \mathbf{a}^\top \boldsymbol{\mu}}{\sqrt{\mathbf{a}^\top \boldsymbol{\Sigma} \mathbf{a}}}.$$

Proposition 5 introduces some fundamental properties of the functional  $\mathcal{F}_n$  and provides mild regularity conditions for our variational problems to be well-defined. Those conditions essentially imply that  $g(\cdot)$  is a measurable, convex, sub-exponential loss function. Actually, such properties are satisfied by almost all the most popular loss functions used for classification and regression tasks, going from the Hinge loss for support vector machine to the exponential family negative log-likelihoods for generalized linear models.

Proposition 6 characterizes the recursive relation connecting the derivatives of  $\mathcal{F}_0$  with  $\mathcal{F}_n$ . This allows to simplify the formulation of the first and second order necessary conditions needed for optimizing  $\mathcal{F}_0$  with respect to  $\boldsymbol{\mu}$  and  $\boldsymbol{\Sigma}$ .

Proposition 7 permits to rephrase a wide class of complicate multidimensional integrals in terms of univariate expectations, that are way more feasible to solve than multivariate ones.

Finally, Proposition 8, together with Proposition 7, provides a closed form solution to the integrals  $\mathcal{H}_n$ ,  $n = 0, 1, 2$ , for a class of functions  $g(\cdot)$  that arises to be very useful when calculating the truncated moments of a multivariate Gaussian random vector subjected to linear constraints. Specifically, we use such results for deriving a variational approximation algorithm with closed form updating formulas for support vector machine, quantile and expectile regression. For more details refer to Section 5 and Appendix B.

A specialized version of Proposition 7 has been used by Hall et al. (2020) for developing an expectation-propagation algorithm in the context of binary mixed regression. Previously, the works of Ormerod and Wand (2012) and Tan and Nott (2013) helped to clarify the potential of similar integral transformation techniques for calculating the marginal likelihood of possibly complicated generalized linear mixed models. Indeed, due to the curse of dimensionality, any multidimensional-to-unidimensional integral collapsing has the double advantage to allow for a more accurate numerical evaluation with an exponentially lower computation cost. Here, we extend this approach in order to make inference on a larger class of models that includes, as remarkable cases, generalized linear mixed models.

**Remark 3.** The properties of the  $\Psi$ -functions described in Section 4 all derive from the observation that  $\Psi_n(y, \mathbf{a}^\top \boldsymbol{\mu}, \mathbf{a}^\top \boldsymbol{\Sigma} \mathbf{a}) = \mathcal{F}_n(\psi(y, \cdot), \mathbf{a}, \boldsymbol{\mu}, \boldsymbol{\Sigma})$ , for any  $y \in \mathcal{Y}$ . In particular, Theorem 1 directly follows from Proposition 5, that is proved in the following.

## Proof of Proposition 5

(1) The differentiability of  $\mathcal{F}_n$  with respect to  $\boldsymbol{\mu}$  and  $\boldsymbol{\Sigma}$  is guaranteed by the derivation under integral sign theorem and by the fact that  $\phi(\cdot; \mu, \sigma^2)$  is an analytic function having infinitely many continuous derivatives with respect to  $\mu$  and  $\sigma$ . In fact, defining the scalar variable  $x = \mathbf{a}^\top \mathbf{x} \sim \mathcal{N}(\mu, \sigma^2)$ , with  $\mu = \mathbf{a}^\top \boldsymbol{\mu}$  and  $\sigma^2 = \mathbf{a}^\top \boldsymbol{\Sigma} \mathbf{a}$ , we have

$$\mathcal{F}_n = \int_{\mathbb{R}^d} g_n(\mathbf{a}^\top \mathbf{x}) \phi_d(\mathbf{x}; \boldsymbol{\mu}, \boldsymbol{\Sigma}) d\mathbf{x} = \int_{-\infty}^{+\infty} g_n(x) \phi(x; \mu, \sigma^2) dx$$

and

$$\frac{\partial^r}{\partial \mu^r} \frac{\partial^s}{\partial \sigma^s} \int_{-\infty}^{+\infty} g_n(x) \phi(x; \mu, \sigma^2) dx = \int_{-\infty}^{+\infty} g_n(x) \frac{\partial^r}{\partial \mu^r} \frac{\partial^s}{\partial \sigma^s} \phi(x; \mu, \sigma^2) dx,$$

for any non-negative integer  $r$  and  $s$ .

(2) Let  $\mathbf{x}_k \sim N_d(\boldsymbol{\mu}, \boldsymbol{\Sigma}_k)$  be a sequence of random variables such that  $\mathbf{a}^\top \boldsymbol{\Sigma}_k \mathbf{a} \rightarrow 0$  as  $k \rightarrow \infty$ . Then, we have

$$\lim_{k \rightarrow \infty} \mathbb{E} |\mathbf{a}^\top \mathbf{x}_k - \mathbf{a}^\top \boldsymbol{\mu}|^2 = \lim_{k \rightarrow \infty} (\mathbf{a}^\top \boldsymbol{\Sigma}_k \mathbf{a}) = 0,$$

which leads to  $\mathbf{a}^\top \mathbf{x}_k \xrightarrow{L^2} \mathbf{a}^\top \boldsymbol{\mu}$  and  $\mathbf{a}^\top \mathbf{x}_k \xrightarrow{P} \mathbf{a}^\top \boldsymbol{\mu}$ . Since the convergence in probability is closed with respect to continuous transformations, if  $g_n$  is continuous, we get  $g_n(\mathbf{a}^\top \mathbf{x}_k) \xrightarrow{P} g_n(\mathbf{a}^\top \boldsymbol{\mu})$ . Hence,  $\mathbb{E}\{g_n(\mathbf{a}^\top \mathbf{x}_k)\} \rightarrow g_n(\mathbf{a}^\top \boldsymbol{\mu})$  as  $k \rightarrow \infty$ , which concludes the proof.

(3) For what regards the joint convexity of  $\mathcal{F}_0$ , we consider the transformation  $\mu = \mathbf{a}^\top \boldsymbol{\mu}$  and  $\sigma^2 = \mathbf{a}^\top \boldsymbol{\Sigma} \mathbf{a}$ . Recall that any smooth function is convex whenever its Hessian matrix is positive semidefinite, namely  $\mathcal{F}_0$  is jointly convex in  $\mu$  and  $\sigma$  if and only if

$$\nabla^2 \mathcal{F}_0 = \begin{bmatrix} \partial_{\mu\mu}^2 \mathcal{F}_0 & \partial_{\mu\sigma}^2 \mathcal{F}_0 \\ \partial_{\sigma\mu}^2 \mathcal{F}_0 & \partial_{\sigma\sigma}^2 \mathcal{F}_0 \end{bmatrix} \succeq 0.$$

Using the definition of weak derivatives of  $g$  together with a location-scale change of variable, we can write

$$\begin{aligned} \partial_{\mu\mu}^2 \mathcal{F}_0 &= \frac{\partial^2 \mathcal{F}_0}{\partial \mu \partial \mu} = \int_{-\infty}^{+\infty} g_2(\mu + \sigma z) \phi(z) dz, \\ \partial_{\mu\sigma}^2 \mathcal{F}_0 &= \frac{\partial^2 \mathcal{F}_0}{\partial \mu \partial \sigma} = \int_{-\infty}^{+\infty} g_2(\mu + \sigma z) z \phi(z) dz, \\ \partial_{\sigma\sigma}^2 \mathcal{F}_0 &= \frac{\partial^2 \mathcal{F}_0}{\partial \sigma \partial \sigma} = \int_{-\infty}^{+\infty} g_2(\mu + \sigma z) z^2 \phi(z) dz. \end{aligned}$$

Recall that  $g_2(x) \geq 0$  for any  $x \in \mathbb{R}$ , because of the convexity of  $g$ . Next, let us define  $f_1(z) = 1$ ,  $f_2(z) = z$  and  $h(z) = g_2(\mu + \sigma z) \phi(z)$ . In this way, the above derivatives may be written as

$$\frac{\partial^2 \mathcal{F}_0}{\partial \mu \partial \mu} = \langle f_1, f_1 \rangle_{\mathbb{H}}, \quad \frac{\partial^2 \mathcal{F}_0}{\partial \mu \partial \sigma} = \langle f_1, f_2 \rangle_{\mathbb{H}}, \quad \frac{\partial^2 \mathcal{F}_0}{\partial \sigma \partial \sigma} = \langle f_2, f_2 \rangle_{\mathbb{H}}$$

where  $\mathbb{H}$  is a positive measure having density function  $h(\cdot)$ , i.e.  $\mathbb{H}(dx) = h(x) dx$ , while  $\langle \cdot, \cdot \rangle_{\mathbb{H}}$  and  $\|\cdot\|_{\mathbb{H}}$  are, respectively, the inner product and the norm induced by  $\mathbb{H}$ :

$$\langle f_1, f_2 \rangle_{\mathbb{H}} = \int_{-\infty}^{+\infty} f_1(x) f_2(x) \mathbb{H}(dx), \quad \|f\|_{\mathbb{H}}^2 = \int_{-\infty}^{+\infty} |f(x)|^2 \mathbb{H}(dx).$$

Then, thanks to the Holder inequality, we get  $|\langle f_1, f_2 \rangle_{\mathbb{H}}| \leq \|f_1\|_{\mathbb{H}} \|f_2\|_{\mathbb{H}}$ , namely  $|\partial_{\mu\sigma}^2 \mathcal{F}_0|^2 \leq (\partial_{\mu\mu}^2 \mathcal{F}_0)(\partial_{\sigma\sigma}^2 \mathcal{F}_0)$ . Which implies that  $\nabla^2 \mathcal{F}_0$  is a proper covariance matrix with positive semidefinite signature and, thereby,  $\mathcal{F}_0$  is a convex function with respect to  $\mu$  and  $\sigma$ .

(4) The lower bound  $g(\mathbf{a}^\top \boldsymbol{\mu}) \leq \mathcal{F}_0(g, \mathbf{a}, \boldsymbol{\mu}, \boldsymbol{\Sigma})$  immediately follows from the Jensen inequality:  $g\{\mathbf{a}^\top \mathbb{E}(\mathbf{x})\} \leq \mathbb{E}\{g(\mathbf{a}^\top \mathbf{x})\}$ . This concludes the proof.  $\square$



## Proof of Proposition 6

Let consider the Gaussian random variable  $x = \mathbf{a}^\top \mathbf{x} \sim N(\mathbf{a}^\top \boldsymbol{\mu}, \mathbf{a}^\top \boldsymbol{\Sigma} \mathbf{a})$ , with  $\mathbf{x} \sim N_d(\boldsymbol{\mu}, \boldsymbol{\Sigma})$ , so that the following  $d$ -dimensional integral collapses into a univariate integral:

$$\begin{aligned} \mathcal{F}_0(g, \mathbf{a}, \boldsymbol{\mu}, \boldsymbol{\Sigma}) &= \int_{\mathbb{R}^d} g(\mathbf{a}^\top \mathbf{x}) \phi_d(\mathbf{x}; \boldsymbol{\mu}, \boldsymbol{\Sigma}) d\mathbf{x} \\ &= \int_{-\infty}^{+\infty} g(x) \phi(x; \mathbf{a}^\top \boldsymbol{\mu}, \mathbf{a}^\top \boldsymbol{\Sigma} \mathbf{a}) dx. \end{aligned}$$

In order to prove the statement in Proposition 6 we use an induction argument. Let us start from the initial step deriving under integral sign with respect to  $\mu_j$ :

$$\begin{aligned} \frac{\partial \mathcal{F}_0}{\partial \mu_j} &= \int_{-\infty}^{+\infty} \frac{g(x)}{\sqrt{\mathbf{a}^\top \boldsymbol{\Sigma} \mathbf{a}}} \frac{\partial}{\partial \mu_j} \phi\left(\frac{x - \mathbf{a}^\top \boldsymbol{\mu}}{\sqrt{\mathbf{a}^\top \boldsymbol{\Sigma} \mathbf{a}}}\right) dx \\ &= -\frac{a_j}{\sqrt{\mathbf{a}^\top \boldsymbol{\Sigma} \mathbf{a}}} \int_{-\infty}^{+\infty} \frac{g(x)}{\sqrt{\mathbf{a}^\top \boldsymbol{\Sigma} \mathbf{a}}} \phi'\left(\frac{x - \mathbf{a}^\top \boldsymbol{\mu}}{\sqrt{\mathbf{a}^\top \boldsymbol{\Sigma} \mathbf{a}}}\right) dx. \end{aligned}$$

Because of the location-scale representation of the Gaussian distribution, we can write  $x = \mathbf{a}^\top \boldsymbol{\mu} + \sqrt{\mathbf{a}^\top \boldsymbol{\Sigma} \mathbf{a}} z$ , where  $z \sim N(0, 1)$  and  $dy = \sqrt{\mathbf{a}^\top \boldsymbol{\Sigma} \mathbf{a}} dz$ ; in this way, we have

$$\frac{\partial \mathcal{F}_0}{\partial \mu_j} = -\frac{a_j}{\sqrt{\mathbf{a}^\top \boldsymbol{\Sigma} \mathbf{a}}} \int_{-\infty}^{+\infty} g(\mathbf{a}^\top \boldsymbol{\mu} + \sqrt{\mathbf{a}^\top \boldsymbol{\Sigma} \mathbf{a}} z) \phi'(z) dz.$$

Observing that  $\phi_n(z)$  vanishes in the limit as  $|z| \rightarrow \infty$  for any  $n \in \mathbb{N}$ , we are allowed to integrate by parts with respect to  $z$  and apply the definition of weak derivative of  $g$ , obtaining

$$\frac{\partial \mathcal{F}_0}{\partial \mu_j} = a_j \int_{-\infty}^{+\infty} g_1(\mathbf{a}^\top \boldsymbol{\mu} + \sqrt{\mathbf{a}^\top \boldsymbol{\Sigma} \mathbf{a}} z) \phi(z) dz,$$

where

$$dg(\mathbf{a}^\top \boldsymbol{\mu} + \sqrt{\mathbf{a}^\top \boldsymbol{\Sigma} \mathbf{a}} z) = \sqrt{\mathbf{a}^\top \boldsymbol{\Sigma} \mathbf{a}} g_1(\mathbf{a}^\top \boldsymbol{\mu} + \sqrt{\mathbf{a}^\top \boldsymbol{\Sigma} \mathbf{a}} z) dz.$$

For concluding the first step of the proof, we just need to back-transform  $z$  to  $x$ :

$$\frac{\partial \mathcal{F}_0}{\partial \mu_j} = a_j \int_{-\infty}^{+\infty} g_1(x) \phi(x; \mathbf{a}^\top \boldsymbol{\mu}, \mathbf{a}^\top \boldsymbol{\Sigma} \mathbf{a}) dx = a_j \mathbb{E}\{g_1(\mathbf{a}^\top \mathbf{x})\},$$

which satisfies the formula in Proposition 6 for  $\mathbf{n} = \mathbf{e}_j$ .

Let us move to the induction step. We consider the  $\mathbf{n}$ -th order mixed derivative of  $\mathcal{F}_0$  and we derive again under integral sign with respect to  $\mu_j$ :

$$\frac{\partial}{\partial \mu_j} \frac{\partial^n \mathcal{F}_0}{\partial \mu_1^{n_1} \dots \partial \mu_d^{n_d}} = \left( \prod_{j=1}^d a_j^{n_j} \right) \int_{-\infty}^{+\infty} g_n(x) \frac{\partial}{\partial \mu_j} \phi(x; \mathbf{a}^\top \boldsymbol{\mu}, \mathbf{a}^\top \boldsymbol{\Sigma} \mathbf{a}) dy.$$

Following the same arguments used for the initial step, sequentially applying derivation, transformation, integration by parts and back-transformation, we get that the right hand side integral becomes

$$\begin{aligned}
\int_{-\infty}^{+\infty} \frac{g_n(x)}{\sqrt{\mathbf{a}^\top \Sigma \mathbf{a}}} \frac{\partial}{\partial \mu_j} \phi\left(\frac{x - \mathbf{a}^\top \boldsymbol{\mu}}{\sqrt{\mathbf{a}^\top \Sigma \mathbf{a}}}\right) dx &= -\frac{a_j}{\sqrt{\mathbf{a}^\top \Sigma \mathbf{a}}} \int_{-\infty}^{+\infty} \frac{g_n(x)}{\sqrt{\mathbf{a}^\top \Sigma \mathbf{a}}} \phi'\left(\frac{x - \mathbf{a}^\top \boldsymbol{\mu}}{\sqrt{\mathbf{a}^\top \Sigma \mathbf{a}}}\right) dx \\
&= -\frac{a_j}{\sqrt{\mathbf{a}^\top \Sigma \mathbf{a}}} \int_{-\infty}^{+\infty} g_n(\mathbf{a}^\top \boldsymbol{\mu} + \sqrt{\mathbf{a}^\top \Sigma \mathbf{a}} z) \phi'(z) dz \\
&= a_j \int_{-\infty}^{+\infty} g_{n+1}(\mathbf{a}^\top \boldsymbol{\mu} + \sqrt{\mathbf{a}^\top \Sigma \mathbf{a}} z) \phi(z) dz \\
&= a_j \int_{-\infty}^{+\infty} \frac{g_{n+1}(x)}{\sqrt{\mathbf{a}^\top \Sigma \mathbf{a}}} \phi\left(\frac{x - \mathbf{a}^\top \boldsymbol{\mu}}{\sqrt{\mathbf{a}^\top \Sigma \mathbf{a}}}\right) dx.
\end{aligned}$$

This leads to

$$\begin{aligned}
\frac{\partial^{n+1} \mathcal{F}_0}{\partial \mu_1^{n_1} \dots \partial \mu_1^{n_j+1} \dots \partial \mu_d^{n_d}} &= \left( a_j^{n_j+1} \prod_{k \neq j} a_k^{n_k} \right) \int_{-\infty}^{+\infty} \frac{g_{n+1}(x)}{\sqrt{\mathbf{a}^\top \Sigma \mathbf{a}}} \phi\left(\frac{x - \mathbf{a}^\top \boldsymbol{\mu}}{\sqrt{\mathbf{a}^\top \Sigma \mathbf{a}}}\right) dy, \\
&= \left( a_j^{n_j+1} \prod_{k \neq j} a_k^{n_k} \right) \mathbb{E}\{g_{n+1}(\mathbf{a}^\top \mathbf{x})\}.
\end{aligned}$$

This concludes the induction step and thus the proof.  $\square$

## Proof of Proposition 7

In order to prove Proposition 7, we need to introduce some intermediate results.

**Lemma 1** (Lemma 1 from Hall et al. (2020)). *Let  $\mathbf{x} \sim \text{Nd}(\mathbf{0}_d, \mathbf{I}_d)$  and  $\mathbf{a}_1, \mathbf{a}_2, \mathbf{a}_3 \in \mathbb{R}^d$ , then*

$$\begin{aligned}
\int_{\mathbb{R}^d} g(\mathbf{a}_1^\top \mathbf{x}) \phi_d(\mathbf{x}) d\mathbf{x} &= \mathcal{H}_0, \\
\int_{\mathbb{R}^d} g(\mathbf{a}_1^\top \mathbf{x}) (\mathbf{a}_2^\top \mathbf{x}) \phi_d(\mathbf{x}) d\mathbf{x} &= \frac{(\mathbf{a}_1^\top \mathbf{a}_2)}{\|\mathbf{a}_1\|} \mathcal{H}_1, \\
\int_{\mathbb{R}^d} g(\mathbf{a}_1^\top \mathbf{x}) (\mathbf{a}_2^\top \mathbf{x}) (\mathbf{a}_3^\top \mathbf{x}) \phi_d(\mathbf{x}) d\mathbf{x} &= (\mathbf{a}_2^\top \mathbf{a}_3) \mathcal{H}_0 + \frac{(\mathbf{a}_1^\top \mathbf{a}_2)(\mathbf{a}_1^\top \mathbf{a}_3)}{\|\mathbf{a}_1\|^2} \mathcal{H}_2.
\end{aligned}$$

where  $\mathcal{H}_n = \mathcal{H}_n(g, \mathbf{a}_1, \mathbf{0}_d, \mathbf{I}_d)$ .

*Proof.* See the proof of Lemma 1 in the supplement material of Hall et al. (2020).  $\square$

**Lemma 2.** *Let  $\mathcal{G}_n = \mathcal{G}_n(g, \mathbf{a}, \mathbf{0}_d, \mathbf{I}_d)$  and  $\mathcal{H}_n = \mathcal{H}_n(g, \mathbf{a}, \mathbf{0}_d, \mathbf{I}_d)$  for  $n = 0, 1, 2$ , then*

$$\mathcal{G}_0 = \mathcal{H}_0, \quad \mathcal{G}_1 = \frac{\mathbf{a}}{\|\mathbf{a}\|} \mathcal{H}_1, \quad \mathcal{G}_2 = \mathbf{I}_d \mathcal{H}_0 + \frac{\mathbf{a} \mathbf{a}^\top}{\|\mathbf{a}\|^2} \mathcal{H}_2.$$

*Proof.* Let us consider a particular application of Lemma 1, assuming  $\mathbf{a}_1 = \mathbf{a}$ ,  $\mathbf{a}_2 = \mathbf{e}_i$ ,  $\mathbf{a}_3 = \mathbf{e}_j$ , where  $\mathbf{e}_i$  is the  $i$ -th column of an identity matrix. Then, for  $\mathcal{G}_n = \mathcal{G}_n(g, \mathbf{a}, \mathbf{0}_d, \mathbf{I}_d)$ , we have

$$\mathcal{G}_0 = \int_{\mathbb{R}^d} g(\mathbf{a}^\top \mathbf{x}) \phi_d(\mathbf{x}) d\mathbf{x} = \int_{-\infty}^{+\infty} g(\|\mathbf{a}\|z) \phi(z) dz = \mathcal{H}_0(g, \mathbf{a}, \mathbf{0}_d, \mathbf{I}_d).$$

The same result applies for the  $j$ -th component of the vector  $\mathcal{G}_1$ , being

$$[\mathcal{G}_1]_j = \int_{\mathbb{R}^d} g(\mathbf{a}^\top \mathbf{x}) (\mathbf{e}_j^\top \mathbf{x}) \phi_d(\mathbf{x}) d\mathbf{x} = \frac{\mathbf{a}^\top \mathbf{e}_j}{\|\mathbf{a}\|} \int_{-\infty}^{+\infty} g(\|\mathbf{a}\|z) z \phi(z) dz = \frac{\mathbf{a}^\top \mathbf{e}_j}{\|\mathbf{a}\|} \mathcal{H}_1(g, \mathbf{a}, \mathbf{0}_d, \mathbf{I}_d).$$

Finally, let us consider the  $(i, j)$ -th element of the matrix  $\mathcal{G}_2$ , that is

$$\begin{aligned} [\mathcal{G}_2]_{ij} &= \int_{\mathbb{R}^d} g(\mathbf{a}^\top \mathbf{x}) (\mathbf{e}_i^\top \mathbf{x}) (\mathbf{e}_j^\top \mathbf{x}) \phi_d(\mathbf{x}) d\mathbf{x} \\ &= (\mathbf{e}_i^\top \mathbf{e}_j) \int_{-\infty}^{+\infty} g(\|\mathbf{a}\|z) \phi(z) dz + \frac{(\mathbf{a}^\top \mathbf{e}_i)(\mathbf{a}^\top \mathbf{e}_j)}{\|\mathbf{a}\|^2} \int_{-\infty}^{+\infty} g(\|\mathbf{a}\|z) (z^2 - 1) \phi(z) dz \\ &= (\mathbf{e}_i^\top \mathbf{e}_j) \mathcal{H}_0(g, \mathbf{a}, \mathbf{0}_d, \mathbf{I}_d) + \frac{(\mathbf{a}^\top \mathbf{e}_i)(\mathbf{a}^\top \mathbf{e}_j)}{\|\mathbf{a}\|^2} \mathcal{H}_2(g, \mathbf{a}, \mathbf{0}_d, \mathbf{I}_d). \end{aligned}$$

Which concludes the proof of Lemma 2.  $\square$

Now, we have all the ingredients to complete the proof of Proposition 7. Firstly, let us consider the change of variable  $\mathbf{x} = \boldsymbol{\mu} + \mathbf{L}\mathbf{z}$  and its inverse map  $\mathbf{z} = \mathbf{L}^{-1}(\mathbf{x} - \boldsymbol{\mu})$ , where  $\mathbf{L}$  is the lower-triangular Cholesky factor of  $\boldsymbol{\Sigma}$ , i.e.  $\boldsymbol{\Sigma} = \mathbf{L}\mathbf{L}^\top$ , so that the volume element transforms as  $d\mathbf{x} = |\boldsymbol{\Sigma}|^{1/2} d\mathbf{z}$ . Therefore,

$$\mathcal{G}_n = \int_{\mathbb{R}^d} (\mathbf{x})^n g(\mathbf{a}^\top \mathbf{x}) \phi_d(\mathbf{x}; \boldsymbol{\mu}, \boldsymbol{\Sigma}) d\mathbf{x} = \int_{\mathbb{R}^d} (\boldsymbol{\mu} + \mathbf{L}\mathbf{z})^n g(\mathbf{a}^\top \boldsymbol{\mu} + \mathbf{a}^\top \mathbf{L}\mathbf{z}) \phi_d(\mathbf{z}) d\mathbf{z}.$$

In particular, we have

$$\begin{aligned} \mathcal{G}_0 &= \int_{\mathbb{R}^d} g(\mathbf{a}^\top \boldsymbol{\mu} + \mathbf{a}^\top \mathbf{L}\mathbf{z}) \phi_d(\mathbf{z}) d\mathbf{z} = \tilde{\mathcal{H}}_0, \\ \mathcal{G}_1 &= \int_{\mathbb{R}^d} (\boldsymbol{\mu} + \mathbf{L}\mathbf{z}) g(\mathbf{a}^\top \boldsymbol{\mu} + \mathbf{a}^\top \mathbf{L}\mathbf{z}) \phi_d(\mathbf{z}) d\mathbf{z} = \boldsymbol{\mu} \tilde{\mathcal{H}}_0 + \mathbf{L} \tilde{\mathcal{H}}_1, \\ \mathcal{G}_2 &= \int_{\mathbb{R}^d} (\boldsymbol{\mu} + \mathbf{L}\mathbf{z})(\boldsymbol{\mu} + \mathbf{L}\mathbf{z})^\top g(\mathbf{a}^\top \boldsymbol{\mu} + \mathbf{a}^\top \mathbf{L}\mathbf{z}) \phi_d(\mathbf{z}) d\mathbf{z} \\ &= \boldsymbol{\mu} \boldsymbol{\mu}^\top \tilde{\mathcal{H}}_0 + \boldsymbol{\mu} \tilde{\mathcal{H}}_1^\top \mathbf{L}^\top + \mathbf{L} \tilde{\mathcal{H}}_1 \boldsymbol{\mu}^\top + \mathbf{L} \tilde{\mathcal{H}}_2 \mathbf{L}^\top, \end{aligned}$$

where the functional  $\tilde{\mathcal{H}}_n = \int_{\mathbb{R}^d} (\mathbf{z})^n g(\mathbf{a}^\top \boldsymbol{\mu} + \mathbf{a}^\top \mathbf{L}\mathbf{z}) \phi_d(\mathbf{z}) d\mathbf{z}$  can be obtained by means of Lemma 2. Hence, due to the identity  $\|\mathbf{L}^\top \mathbf{a}\| = \sqrt{\mathbf{a}^\top \boldsymbol{\Sigma} \mathbf{a}}$ , we get

$$\begin{aligned} \tilde{\mathcal{H}}_0 &= \int_{-\infty}^{+\infty} g(\mathbf{a}^\top \boldsymbol{\mu} + \|\mathbf{L}^\top \mathbf{a}\| z) \phi(z) dz = \mathcal{H}_0, \\ \tilde{\mathcal{H}}_1 &= \frac{\mathbf{L}^\top \mathbf{a}}{\|\mathbf{L}^\top \mathbf{a}\|} \int_{-\infty}^{+\infty} g(\mathbf{a}^\top \boldsymbol{\mu} + \|\mathbf{L}^\top \mathbf{a}\| z) z \phi(z) dz = \frac{\mathbf{L}^\top \mathbf{a}}{\|\mathbf{L}^\top \mathbf{a}\|} \mathcal{H}_1, \\ \tilde{\mathcal{H}}_2 &= \mathbf{I}_d \int_{-\infty}^{+\infty} g(\mathbf{a}^\top \boldsymbol{\mu} + \|\mathbf{L}^\top \mathbf{a}\| z) H_2(z) \phi(z) dz \\ &\quad + \frac{\mathbf{L}^\top \mathbf{a} \mathbf{a}^\top \mathbf{L}}{\|\mathbf{L}^\top \mathbf{a}\|^2} \int_{-\infty}^{+\infty} g(\mathbf{a}^\top \boldsymbol{\mu} + \|\mathbf{L}^\top \mathbf{a}\| z) (z^2 - 1) \phi(z) dz = \mathbf{I}_d \mathcal{H}_0 + \frac{\mathbf{L}^\top \mathbf{a} \mathbf{a}^\top \mathbf{L}}{\|\mathbf{L}^\top \mathbf{a}\|^2} \mathcal{H}_2. \end{aligned}$$

Finally, we note that

$$\begin{aligned}\mathbf{L} \tilde{\mathcal{H}}_1 &= \frac{\mathbf{L} \mathbf{L}^\top \mathbf{a}}{\|\mathbf{L}^\top \mathbf{a}\|} \mathcal{H}_1 = \frac{\boldsymbol{\Sigma} \mathbf{a}}{\sqrt{\mathbf{a}^\top \boldsymbol{\Sigma} \mathbf{a}}} \mathcal{H}_1, \\ \mathbf{L} \tilde{\mathcal{H}}_2 \mathbf{L}^\top &= \mathbf{L} \mathbf{L}^\top \mathcal{H}_0 + \frac{\mathbf{L} \mathbf{L}^\top \mathbf{a} \mathbf{a}^\top \mathbf{L} \mathbf{L}^\top}{\|\mathbf{L}^\top \mathbf{a}\|^2} \mathcal{H}_2 = \boldsymbol{\Sigma} \mathcal{H}_0 + \frac{\boldsymbol{\Sigma} \mathbf{a} \mathbf{a}^\top \boldsymbol{\Sigma}}{\mathbf{a}^\top \boldsymbol{\Sigma} \mathbf{a}} \mathcal{H}_2.\end{aligned}$$

Which concludes the proof of Proposition 7.  $\square$

### Proof of Proposition 8

Assuming  $g(\cdot) = \mathbb{I}_{(b,c]}(\cdot)$ , the functional  $\mathcal{H}_n(g, \mathbf{a}, \boldsymbol{\mu}, \boldsymbol{\Sigma})$  simplifies as

$$\begin{aligned}\mathcal{H}_n(g, \mathbf{a}, \boldsymbol{\mu}, \boldsymbol{\Sigma}) &= \int_{-\infty}^{+\infty} g\left(\mathbf{a}^\top \boldsymbol{\mu} + \sqrt{\mathbf{a}^\top \boldsymbol{\Sigma} \mathbf{a}} z\right) H_n(z) \phi(z) dz \\ &= \int_{-\infty}^{+\infty} \mathbb{I}_{(b,c]}\left(\mathbf{a}^\top \boldsymbol{\mu} + \sqrt{\mathbf{a}^\top \boldsymbol{\Sigma} \mathbf{a}} z\right) H_n(z) \phi(z) dz \\ &= \int_{-\infty}^{+\infty} \mathbb{I}\left(\frac{b - \mathbf{a}^\top \boldsymbol{\mu}}{\sqrt{\mathbf{a}^\top \boldsymbol{\Sigma} \mathbf{a}}} < z < \frac{c - \mathbf{a}^\top \boldsymbol{\mu}}{\sqrt{\mathbf{a}^\top \boldsymbol{\Sigma} \mathbf{a}}}\right) H_n(z) \phi(z) dz,\end{aligned}$$

that is a univariate definite integral with lower and upper bounds  $z^-$  and  $z^+$ . Then, using the recurrent identity

$$H_0(z) = 1, \quad H_n(z) \phi(z) = -\frac{d}{dz} H_{n-1}(z) \phi(z), \quad n \geq 1,$$

and integrating with respect to  $z$ , we obtain

$$\int_{z^-}^{z^+} H_n(z) \phi(z) dz = \begin{cases} [\Phi(z)]_{z^-}^{z^+} & \text{if } n = 0, \\ (-1) [H_{n-1}(z) \phi(z)]_{z^-}^{z^+} & \text{if } n \geq 1, \end{cases}$$

which concludes the proof.  $\square$

## B Optimal distributions and evidence lower bound

In this section we derive the explicit solutions of the optimal variational distributions  $q^*(\sigma_\varepsilon^2)$ ,  $q^*(\sigma_u^2)$  and  $q^*(\boldsymbol{\beta}, \mathbf{u})$  presented in Section 4. Moreover, we prove the statements in Propositions 1-4, that are concerned with the calculation of the  $\Psi$ -functions for the model specifications considered in Section 5.

### Optimal distribution of $\sigma_\varepsilon^2$

We consider the pseudo-likelihood model for the  $i$ -th observation

$$\log p(y_i | \boldsymbol{\theta}) = -\frac{1}{\phi} \log \sigma_\varepsilon^2 - \frac{1}{\phi} \psi(y_i, \eta_i) / \sigma_\varepsilon^2,$$

and we recall the prior law  $\sigma_\varepsilon^2 \sim \text{IG}(A_\varepsilon, B_\varepsilon)$ . Then, the Gibbs full-conditional distribution of  $\sigma_\varepsilon^2$  can be easily obtained by standard calculations and corresponds to an Inverse-Gamma distribution  $\text{IG}(\tilde{\alpha}_\varepsilon, \tilde{\beta}_\varepsilon)$ ,

with parameters  $\tilde{\alpha}_\varepsilon = A_\varepsilon + n/\phi$  and  $\tilde{\beta}_\varepsilon = B_\varepsilon + \sum_{i=1}^n \psi(y_i, \eta_i)/\phi$ . Now, computing the partial expectation of the log-full-conditional distribution, we obtain the optimal density  $q^*(\sigma_\varepsilon^2) \propto \exp [\mathbb{E}_{-\sigma_\varepsilon^2} \{\log p(\sigma_\varepsilon^2 | \text{rest})\}]$ , that is

$$\begin{aligned} \log q^*(\sigma_\varepsilon^2) &= -(A_\varepsilon + n/\phi + 1) \log \sigma_\varepsilon^2 - \left\{ B_\varepsilon + \frac{1}{\phi} \sum_{i=1}^n \mathbb{E}_q(\psi(y_i, \eta_i)) \right\} / \sigma_\varepsilon^2 + \text{const} \\ &= -(A_\varepsilon + n/\phi + 1) \log \sigma_\varepsilon^2 - \left\{ B_\varepsilon + \frac{1}{\phi} \sum_{i=1}^n \Psi_{0,i} \right\} / \sigma_\varepsilon^2 + \text{const}. \end{aligned}$$

The latter is the kernel of an Inverse-Gamma distribution  $\text{IG}(\hat{\alpha}_\varepsilon, \hat{\beta}_\varepsilon)$  where  $\Psi_{0,i} = \mathbb{E}_q\{\psi(y_i, \eta_i)\}$ . Then, the proof is concluded.  $\square$

### Optimal distribution of $\sigma_u^2$

We consider the joint prior model for  $(\mathbf{u}, \sigma_u^2)$ , which is

$$\mathbf{u} | \sigma_u^2 \sim \text{Nd}(\mathbf{0}_d, \sigma_u^2 \mathbf{R}^{-1}), \quad \sigma_u^2 \sim \text{IG}(A_u, B_u).$$

Standard calculations leads to an Inverse-Gamma full-conditional distribution of  $\sigma_u^2$ , that is  $\text{IG}(\tilde{\alpha}_u, \tilde{\beta}_u)$  with parameters  $\tilde{\alpha}_u = A_u + d/2$  and  $\tilde{\beta}_u = B_u + (\mathbf{u}^\top \mathbf{R} \mathbf{u})/2$ . Compute then the partial variational expectation of the log-full-conditional density in order to find the optimal approximation  $q^*(\sigma_u^2) \propto \exp [\mathbb{E}_{-\sigma_u^2} \{\log p(\sigma_u^2 | \text{rest})\}]$ :

$$\log q(\sigma_u^2) = -(A_u + d/2 + 1) \log \sigma_u^2 - \left\{ B_u + \frac{1}{2} \mathbb{E}_q(\mathbf{u}^\top \mathbf{R} \mathbf{u}) \right\} / \sigma_u^2 + \text{const}$$

Notice that the latter is the kernel of an Inverse-Gamma random variable  $\text{IG}(\hat{\alpha}_u, \hat{\beta}_u)$  and  $\mathbb{E}_q(\mathbf{u}^\top \mathbf{R} \mathbf{u}) = \boldsymbol{\mu}_u^\top \mathbf{R} \boldsymbol{\mu}_u + \text{trace}(\mathbf{R} \boldsymbol{\Sigma}_{uu})$ . This concludes the proof.  $\square$

### Optimal distribution of $(\boldsymbol{\beta}, \mathbf{u})$

The evidence lower bound (13) as a function of  $\boldsymbol{\mu}$  and  $\boldsymbol{\Sigma}$  can be expressed as

$$\begin{aligned} \log \underline{p}(\mathbf{y}; q, \boldsymbol{\mu}, \boldsymbol{\Sigma}) &= \mathbb{E}_q\{\log p(\mathbf{y}, \boldsymbol{\theta})\} - \mathbb{E}_q\{\log q(\boldsymbol{\theta})\} \\ &= \ell(\boldsymbol{\mu}, \boldsymbol{\Sigma}) + \frac{1}{2} \log \det(\boldsymbol{\Sigma}) + \text{const}, \end{aligned}$$

where  $\ell(\boldsymbol{\mu}, \boldsymbol{\Sigma}) = \mathbb{E}_q\{\log p(\mathbf{y}, \boldsymbol{\theta})\} + \text{const}$  is a smooth, concave function (Proposition 1). Since also  $\log \det(\boldsymbol{\Sigma})$  is smooth and concave, the lower bound is a well-behaved function whose global maximum must satisfy the following first order equations:  $\nabla_{\boldsymbol{\mu}} \ell(\boldsymbol{\mu}, \boldsymbol{\Sigma}) = 0$  and  $\nabla_{\boldsymbol{\Sigma}} \ell(\boldsymbol{\mu}, \boldsymbol{\Sigma}) - \frac{1}{2} \boldsymbol{\Sigma}^{-1} = 0$ , where  $\nabla_{\boldsymbol{\Sigma}} \ell$  denotes the  $K \times K$  matrix having  $(i, j)$  entry equal to  $(\nabla_{\boldsymbol{\Sigma}} \ell)_{ij} = \partial \ell / \partial \Sigma_{ij}$ . By definition,  $\mathbf{g}(\boldsymbol{\mu}, \boldsymbol{\Sigma}) = \nabla_{\boldsymbol{\mu}} \ell(\boldsymbol{\mu}, \boldsymbol{\Sigma})$ , while  $\mathbf{H}(\boldsymbol{\mu}, \boldsymbol{\Sigma}) = \frac{1}{2} \nabla_{\boldsymbol{\Sigma}} \ell(\boldsymbol{\mu}, \boldsymbol{\Sigma})$ ; see, for instance, Rohde and Wand, 2016 for a detailed proof. Therefore, if a good starting value is provided, any contractive fixed-point algorithm climbing the lower bound surface has a limiting point corresponding with a global maximum.

Now, recall that  $\mathbf{g}(\boldsymbol{\mu}, \boldsymbol{\Sigma})$  and  $\mathbf{H}(\boldsymbol{\mu}, \boldsymbol{\Sigma})$  are the gradient and Hessian of  $\ell(\boldsymbol{\mu}, \boldsymbol{\Sigma})$  calculated with respect to  $\boldsymbol{\mu}$  and define  $\mathbf{Q} = \text{blockdiag}\{\sigma_\beta^{-2} \mathbf{I}_p, \hat{\gamma}_u \mathbf{R}\}$ , thus we have

$$\begin{aligned} \ell(\boldsymbol{\mu}, \boldsymbol{\Sigma}) &= -\hat{\gamma}_\varepsilon \{\mathbf{1}_n^\top \boldsymbol{\Psi}_0\} / \phi - \frac{1}{2} \boldsymbol{\mu}^\top \mathbf{Q} \boldsymbol{\mu} - \frac{1}{2} \text{trace}(\mathbf{Q} \boldsymbol{\Sigma}) + \text{const}, \\ \mathbf{g}(\boldsymbol{\mu}, \boldsymbol{\Sigma}) &= -\hat{\gamma}_\varepsilon \nabla_{\boldsymbol{\mu}} \{\mathbf{1}_n^\top \boldsymbol{\Psi}_0\} / \phi - \mathbf{Q} \boldsymbol{\mu}, \\ \mathbf{H}(\boldsymbol{\mu}, \boldsymbol{\Sigma}) &= -\hat{\gamma}_\varepsilon \nabla_{\boldsymbol{\mu}}^2 \{\mathbf{1}_n^\top \boldsymbol{\Psi}_0\} / \phi - \mathbf{Q}. \end{aligned}$$

Defining  $\Psi_r(y_i, m_i, \nu_i) = \mathcal{F}_r(\psi(y_i, \cdot), \mathbf{c}_i, \boldsymbol{\mu}, \boldsymbol{\Sigma})$  and applying Proposition 6 in Appendix A, we obtain the gradient and Hessian

$$\nabla_{\boldsymbol{\mu}}\{\mathbf{1}_n^\top \boldsymbol{\Psi}_0\} = \sum_{i=1}^n \mathbf{c}_i \Psi_{1,i} = \mathbf{C}^\top \boldsymbol{\Psi}_1, \quad \nabla_{\boldsymbol{\mu}}^2\{\mathbf{1}_n^\top \boldsymbol{\Psi}_0\} = \sum_{i=1}^n \mathbf{c}_i \mathbf{c}_i^\top \Psi_{2,i} = \mathbf{C}^\top \text{diag}[\boldsymbol{\Psi}_2] \mathbf{C}.$$

Which concludes the proof.  $\square$

## Derivation of the evidence lower bound

First, consider the definition of the evidence lower bound and notice that it can be written in terms of a sum of expected values calculated with respect to the  $q$ -density as:

$$\log p(\mathbf{y}; q) = \int_{\Theta} q(\boldsymbol{\theta}) \log \left\{ \frac{p(\mathbf{y}, \boldsymbol{\theta})}{q(\boldsymbol{\theta})} \right\} d\boldsymbol{\theta} = \mathbb{E}_q\{\log p(\mathbf{y}, \boldsymbol{\theta})\} - \mathbb{E}_q\{\log q(\boldsymbol{\theta})\}$$

where  $\log p(\mathbf{y}, \boldsymbol{\theta}) = \log p(\mathbf{y}|\boldsymbol{\theta}) + \log p(\boldsymbol{\theta})$ . From the model specification, we have

$$\log p(\mathbf{y}, \boldsymbol{\theta}) = \sum_{i=1}^n \log p(y_i|\boldsymbol{\theta}) + \log p(\boldsymbol{\beta}, \mathbf{u}|\sigma_u^2) + \log p(\sigma_u^2) + \log p(\sigma_\varepsilon^2).$$

Similarly, for the variational density we have:

$$\log q(\boldsymbol{\theta}) = \log q(\boldsymbol{\beta}, \mathbf{u}) + \log q(\sigma_u^2) + \log q(\sigma_\varepsilon^2).$$

Therefore, the lower bound can be decomposed as a sum of terms associated to different parameter blocks:

$$\log p(\mathbf{y}; q) = \underbrace{\sum_{i=1}^n \mathbb{E}_q[\log p(y_i|\boldsymbol{\theta})]}_{T_1} + \underbrace{\mathbb{E}_q\left[\log \frac{p(\boldsymbol{\beta}, \mathbf{u}|\sigma_u^2)}{q(\boldsymbol{\beta}, \mathbf{u})}\right]}_{T_2} + \underbrace{\mathbb{E}_q\left[\log \frac{p(\sigma_u^2)}{q(\sigma_u^2)}\right]}_{T_3} + \underbrace{\mathbb{E}_q\left[\log \frac{p(\sigma_\varepsilon^2)}{q(\sigma_\varepsilon^2)}\right]}_{T_4}.$$

We can thus evaluate each term separately and sum up the individual contributions  $T_k$ ,  $k = 1, \dots, 4$ . The first term of the lower bound is the variational expectation of the pseudo log-likelihood function:

$$T_1 = -\frac{n}{\phi} \mathbb{E}_q(\log \sigma_\varepsilon^2) - \frac{1}{\phi} \mathbb{E}_q(1/\sigma_\varepsilon^2) \sum_{i=1}^n \mathbb{E}_q\{\psi(y_i, \eta_i)\}.$$

The second term is the expected contribution of  $\boldsymbol{\vartheta} = (\boldsymbol{\beta}, \mathbf{u})$  to the lower bound:

$$\begin{aligned} T_2 &= \mathbb{E}_q \left[ -\frac{p}{2} \log(2\pi) - \frac{p}{2} \log \sigma_\beta^2 - \frac{1}{2} \boldsymbol{\beta}^\top \boldsymbol{\beta} / \sigma_\beta^2 - \frac{p}{2} \log(2\pi) - \frac{d}{2} \log \sigma_u^2 + \frac{1}{2} \log \det(\mathbf{R}) \right. \\ &\quad \left. - \frac{1}{2} \mathbf{u}^\top \mathbf{R} \mathbf{u} / \sigma_u^2 + \frac{1}{2} (p+d) \log(2\pi) + \frac{1}{2} \log \det(\boldsymbol{\Sigma}) + \frac{1}{2} (\boldsymbol{\vartheta} - \boldsymbol{\mu})^\top \boldsymbol{\Sigma}^{-1} (\boldsymbol{\vartheta} - \boldsymbol{\mu}) \right] \\ &= -\frac{p}{2} \log \sigma_\beta^2 - \frac{d}{2} \mathbb{E}_q(\log \sigma_u^2) + \frac{1}{2} \log \det(\mathbf{R}) + \frac{1}{2} \log \det(\boldsymbol{\Sigma}) - \frac{1}{2} C_1 + \frac{1}{2} C_2 \\ &= -\frac{p}{2} \log \sigma_\beta^2 - \frac{d}{2} \mathbb{E}_q(\log \sigma_u^2) + \frac{1}{2} \log \det(\mathbf{R}) + \frac{1}{2} \log \det(\boldsymbol{\Sigma}) - \frac{1}{2} \boldsymbol{\mu}^\top \mathbf{Q} \boldsymbol{\mu} - \frac{1}{2} \text{trace}(\mathbf{Q} \boldsymbol{\Sigma}) + \frac{1}{2} (p+d), \end{aligned}$$

where we used the following identities:

$$\begin{aligned} C_1 &= \mathbb{E}_q[\boldsymbol{\beta}^\top \boldsymbol{\beta} / \sigma_\beta^2 + \mathbf{u}^\top \mathbf{R} \mathbf{u} / \sigma_u^2] = \boldsymbol{\mu}^\top \mathbf{Q} \boldsymbol{\mu} + \text{trace}(\mathbf{Q} \boldsymbol{\Sigma}), \\ C_2 &= \mathbb{E}_q[(\boldsymbol{\vartheta} - \boldsymbol{\mu})^\top \boldsymbol{\Sigma}^{-1} (\boldsymbol{\vartheta} - \boldsymbol{\mu})] = p + d. \end{aligned}$$

The third term is the expected contribution of  $\sigma_u^2$  to the lower bound:

$$\begin{aligned} T_3 &= \mathbb{E}_q \left[ A_u \log B_u - \log \Gamma(A_u) - (A_u + 1) \log \sigma_u^2 - B_u / \sigma_u^2 \right. \\ &\quad \left. - (A_u + \frac{d}{2}) \log \hat{\beta}_u + \log \Gamma(\hat{\alpha}_u) + (A_u + \frac{d}{2} + 1) \log \sigma_u^2 + \hat{\beta}_u / \sigma_u^2 \right] \\ &= \mathbb{E}_q \left[ A_u \log(B_u / \hat{\beta}_u) - \log \{ \Gamma(A_u) / \Gamma(\hat{\alpha}_u) \} - \frac{d}{2} \log \hat{\beta}_u + \frac{d}{2} \log \sigma_u^2 - (B_u - \hat{\beta}_u) / \sigma_u^2 \right] \\ &= A_u \log(B_u / \hat{\beta}_u) - \log \{ \Gamma(A_u) / \Gamma(\hat{\alpha}_u) \} - \frac{d}{2} \{ \log \hat{\beta}_u - \mathbb{E}_q(\log \sigma_u^2) \} - (B_u - \hat{\beta}_u) \mathbb{E}_q(1 / \sigma_u^2). \end{aligned}$$

The fourth term is the expected contribution of  $\sigma_\varepsilon^2$  to the lower bound:

$$T_4 = A_\varepsilon \log(B_\varepsilon / \hat{\beta}_\varepsilon) - \log \{ \Gamma(A_\varepsilon) / \Gamma(\hat{\alpha}_\varepsilon) \} - (n/\phi) \{ \log \hat{\beta}_\varepsilon - \mathbb{E}_q(\log \sigma_\varepsilon^2) \} - (B_\varepsilon - \hat{\beta}_\varepsilon) \mathbb{E}_q(1 / \sigma_\varepsilon^2).$$

In the end, summing up the individual contributions  $T_1$ ,  $T_2$ ,  $T_3$ ,  $T_4$  and simplifying the redundant components we obtain the final result.  $\square$

## Proof of Proposition 1 (support vector classification)

By the definition of hinge loss function, we have that  $\psi^{\text{svc}}(y, \eta) = \tilde{\psi}^{\text{svc}}(1 - y\eta)$ , where the first three weak derivatives of  $\tilde{\psi}^{\text{svc}}(\cdot)$  are

$$\begin{aligned} \tilde{\psi}_0^{\text{svc}}(x) &= |x| + x = 2\{x - x \mathbb{I}_{<0}(x)\}, \\ \tilde{\psi}_1^{\text{svc}}(x) &= \text{sign}(x) + 1 = 2\{1 - \mathbb{I}_{<0}(x)\}, \\ \tilde{\psi}_2^{\text{svc}}(x) &= 2\delta_0(x). \end{aligned}$$

Here, we use the identities  $2\max(0, x) = |x| + x$ ,  $|x| = x - 2x\mathbb{I}_{<0}(x)$ ,  $\text{sign}(x) = 1 - 2\mathbb{I}_{<0}(x)$ . Let  $x \sim \mathcal{N}(\mu, \nu^2)$ , then, applying Propositions 7 and 8, we have

$$\begin{aligned} \mathbb{E}\{\tilde{\psi}_0^{\text{svc}}(x)\} &= 2\mathbb{E}(x) - 2\mathbb{E}\{x \mathbb{I}_{<0}(x)\} = 2\mu\{1 - \Phi(0; \mu, \nu^2)\} + 2\nu^2\phi(0; \mu, \nu^2), \\ \mathbb{E}\{\tilde{\psi}_1^{\text{svc}}(x)\} &= 2 - 2\mathbb{E}\{\mathbb{I}_{<0}(x)\} = 2\{1 - \Phi(0; \mu, \nu^2)\}, \\ \mathbb{E}\{\tilde{\psi}_2^{\text{svc}}(x)\} &= \mathbb{E}\{\delta_0(x)\} = 2\phi(0; \mu, \nu^2). \end{aligned}$$

Now, defining  $\mu = 1 - y\eta$ , we have

$$\Phi(0; \mu, \nu^2) = 1 - \Phi(1; y\eta, \nu^2), \quad \phi(0; \mu, \nu^2) = \phi(1; y\eta, \nu^2),$$

Simplifying the results, we obtain the closed form expressions for  $\Psi_r^{\text{svc}}$ ,  $r = 0, 1, 2$ , provided in Proposition 1. Which concludes the proof.  $\square$

## Proof of Proposition 2 (support vector regression)

By the definition of  $\epsilon$ -insensitive loss function, we have that  $\psi^{\text{SVR}}(y, \eta) = \tilde{\psi}^{\text{SVR}}(y - \eta)$ , where the first three weak derivatives of  $\tilde{\psi}^{\text{SVR}}(\cdot)$  are

$$\begin{aligned}\tilde{\psi}_0^{\text{SVR}}(x) &= |x - \epsilon| + (x - \epsilon) + |x + \epsilon| - (x + \epsilon), \\ \tilde{\psi}_1^{\text{SVR}}(x) &= \text{sign}(x - \epsilon) + \text{sign}(x + \epsilon), \\ \tilde{\psi}_2^{\text{SVR}}(x) &= 2\delta_0(x - \epsilon) + 2\delta_0(x + \epsilon).\end{aligned}$$

Let  $x \sim N(\mu, \nu^2)$  and use, again, Proposition 8 for calculating

$$\begin{aligned}\mathbb{E}|x - \epsilon| + \mathbb{E}(x - \epsilon) &= 2(\mu - \epsilon)\{1 - \Phi(-\epsilon; \mu, \nu^2)\} + 2\sigma^2\phi(-\epsilon; \mu, \nu^2), \\ \mathbb{E}|x + \epsilon| - \mathbb{E}(x + \epsilon) &= 2(\mu + \epsilon)\{1 - \Phi(+\epsilon; \mu, \nu^2)\} + 2\sigma^2\phi(+\epsilon; \mu, \nu^2).\end{aligned}$$

These lead to the expected value

$$\begin{aligned}\mathbb{E}\{\tilde{\psi}_0^{\text{SVR}}(x)\} &= 2[(\mu - \epsilon)\{1 - \Phi(-\epsilon; \mu, \nu^2)\} + \nu^2\phi(-\epsilon; \mu, \nu^2) \\ &\quad + (\mu + \epsilon)\{1 - \Phi(+\epsilon; \mu, \nu^2)\} + \nu^2\phi(+\epsilon; \mu, \nu^2)].\end{aligned}$$

Similarly, using  $\text{sign}(x) = 1 - 2\mathbb{I}_{<0}(x)$ , we have

$$\begin{aligned}\mathbb{E}\{\tilde{\psi}_1^{\text{SVR}}(x)\} &= 2 - 2\mathbb{E}\{\mathbb{I}_{<+\epsilon}(x)\} - 2\mathbb{E}\{\mathbb{I}_{<-\epsilon}(x)\} = 2 - 2\Phi(+\epsilon; \mu, \nu^2) - 2\Phi(-\epsilon; \mu, \nu^2), \\ \mathbb{E}\{\tilde{\psi}_2^{\text{SVR}}(x)\} &= 2\mathbb{E}\{\delta_{+\epsilon}(x)\} + 2\mathbb{E}\{\delta_{-\epsilon}(x)\} = 2\phi(+\epsilon; \mu, \nu^2) + 2\phi(-\epsilon; \mu, \nu^2).\end{aligned}$$

Substituting  $\mu = y - \eta$  and simplifying the results, we obtain the closed form expressions for  $\Psi_r^{\text{SVR}}$ ,  $r = 0, 1, 2$ , provided in Proposition 2.  $\square$

## Proof of Proposition 3 (quantile regression)

Consider the quantile check loss  $\psi^{\text{QR}}(y, \eta) = \tilde{\psi}^{\text{QR}}(y - \eta)$  along with its first and second weak derivatives:

$$\begin{aligned}\tilde{\psi}_0^{\text{QR}}(x) &= \frac{1}{2}|x| + (\tau - \frac{1}{2})x = x\{\tau - \mathbb{I}_{<0}(x)\}, \\ \tilde{\psi}_1^{\text{QR}}(x) &= \frac{1}{2}\text{sign}(x) + (\tau - \frac{1}{2}) = \tau - \mathbb{I}_{<0}(x), \\ \tilde{\psi}_2^{\text{QR}}(x) &= \delta_0(x).\end{aligned}$$

Then, taking the expectation with respect to  $x \sim N(\mu, \nu^2)$ , we get

$$\begin{aligned}\mathbb{E}\{\tilde{\psi}_0^{\text{QR}}(x)\} &= \tau\mathbb{E}(x) - \mathbb{E}\{x\mathbb{I}_{<0}(x)\} = \mu\{\tau - \Phi(0; \mu, \nu^2)\} + \nu^2\phi(0; \mu, \nu^2), \\ \mathbb{E}\{\tilde{\psi}_1^{\text{QR}}(x)\} &= \tau - \mathbb{E}\{\mathbb{I}_{<0}(x)\} = \tau - \Phi(0; \mu, \nu^2), \\ \mathbb{E}\{\tilde{\psi}_2^{\text{QR}}(x)\} &= \mathbb{E}\{\delta_0(x)\} = \phi(0; \mu, \nu^2).\end{aligned}$$

Substituting  $\mu = y - \eta$  and simplifying the results, we obtain the closed form expressions for  $\Psi_r^{\text{QR}}$ ,  $r = 0, 1, 2$ , provided in Proposition 3.  $\square$



## Proof of Proposition 4 (expectile regression)

Consider the expectile loss  $\psi^{\text{ER}}(y, \eta) = \tilde{\psi}^{\text{ER}}(y - \eta)$ , along with its first and second weak derivatives:

$$\begin{aligned}\tilde{\psi}_0^{\text{ER}}(x) &= \frac{1}{2} x^2 |\tau - \mathbb{I}_{<0}(x)| = \frac{1}{2} x^2 \{\tau + (1 - 2\tau) \mathbb{I}_{<0}(x)\}, \\ \tilde{\psi}_1^{\text{ER}}(x) &= x |\tau - \mathbb{I}_{<0}(x)| = x \{\tau + (1 - 2\tau) \mathbb{I}_{<0}(x)\}, \\ \tilde{\psi}_2^{\text{ER}}(x) &= |\tau - \mathbb{I}_{<0}(x)| = \tau + (1 - 2\tau) \mathbb{I}_{<0}(x).\end{aligned}$$

Here, we use the identity  $|\tau - \mathbb{I}_{<0}(x)| = \tau + (1 - 2\tau) \mathbb{I}_{<0}(x)$ , which permits to simplify the following calculations. Next, we marginalize out  $x$  by assuming the distribution  $x \sim \mathcal{N}(\mu, \nu^2)$ , leading to

$$\begin{aligned}\mathbb{E}\{\tilde{\psi}_0^{\text{ER}}(x)\} &= \frac{1}{2} \tau \mathbb{E}(x^2) + \frac{1}{2} (1 - 2\tau) \mathbb{E}\{x^2 \mathbb{I}_{<0}(x)\} \\ &= \frac{1}{2} \tau (\mu^2 + \nu^2) + \frac{1}{2} (1 - 2\tau) \{(\mu^2 + \nu^2) \Phi(0; \mu, \nu^2) - \mu \nu^2 \phi(0; \mu, \nu^2)\} \\ &= \frac{1}{2} (\mu^2 + \nu^2) \{\tau + (1 - 2\tau) \Phi(0; \mu, \nu^2)\} - \frac{1}{2} (1 - 2\tau) \mu \nu^2 \phi(0; \mu, \nu^2).\end{aligned}$$

In the same way, we get

$$\begin{aligned}\mathbb{E}\{\tilde{\psi}_1^{\text{ER}}(x)\} &= \tau \mathbb{E}(x) + (1 - 2\tau) \mathbb{E}\{x \mathbb{I}_{<0}(x)\} \\ &= \tau \mu + (1 - 2\tau) \{\mu \Phi(0; \mu, \nu^2) - \nu^2 \phi(0; \mu, \nu^2)\} \\ &= \mu \{\tau + (1 - 2\tau) \Phi(0; \mu, \nu^2)\} - (1 - 2\tau) \nu^2 \phi(0; \mu, \nu^2),\end{aligned}$$

and

$$\mathbb{E}\{\tilde{\psi}_2^{\text{ER}}(x)\} = \tau + (1 - 2\tau) \mathbb{E}\{\mathbb{I}_{<0}(x)\} = \tau + (1 - 2\tau) \Phi(0; \mu, \nu^2).$$

Substituting  $\mu = y - \eta$  and simplifying the results, we obtain the closed form expressions for  $\Psi_r^{\text{ER}}$ ,  $r = 0, 1, 2$ , provided in Proposition 4.  $\square$

## C Marginal and augmented variational inference

Let us start by considering the first inequality in Theorem 2. Let  $q_A^*(\omega, \theta) \in \mathcal{Q}_A$ ,  $q_A^*(\theta) \in \mathcal{Q}_M$  and  $q_M^*(\theta) \in \mathcal{Q}_M$  be the optimal variational approximations defined in (20). Since  $q_M^*(\theta)$  is the global minimum of the Kullback-Leibler divergence calculated with respect to the marginal space  $\mathcal{Q}_M$ , we have

$$\text{KL}\{q_M^*(\theta) \parallel p(\theta|\mathbf{y})\} \leq \text{KL}\{\tilde{q}_M(\theta) \parallel p(\theta|\mathbf{y})\},$$

for any density function  $\tilde{q}_M(\theta) \in \mathcal{Q}_M$  and, in particular, for  $\tilde{q}_M(\theta) = q_A^*(\theta) \in \mathcal{Q}_M$ . This proves the first inequality in Theorem 2.

Let us move to the second inequality. Let  $q_A(\omega|\theta) = q_A(\omega, \theta)/q_A(\theta)$  be the conditional density function of  $\omega$  given  $\theta$  with respect to the  $q_A$ -measure. Then, from the Jensen inequality follows that

$$\log p(\theta|\mathbf{y}) = \log \int_{\Omega} q_A(\omega|\theta) \left\{ \frac{p(\omega, \theta|\mathbf{y})}{q_A(\omega|\theta)} \right\} d\omega \geq \int_{\Omega} q_A(\omega|\theta) \log \left\{ \frac{p(\omega, \theta|\mathbf{y})}{q_A(\omega|\theta)} \right\} d\omega.$$

Thus, by substitution, we end up with

$$\begin{aligned}\int_{\Theta} q_A(\theta) \log \left\{ \frac{p(\theta|\mathbf{y})}{q_A(\theta)} \right\} d\theta &= \int_{\Theta} q_A(\theta) [\log p(\theta|\mathbf{y}) - \log q_A(\theta)] d\theta \\ &\geq \int_{\Theta} q_A(\theta) \left[ \int_{\Omega} q_A(\omega|\theta) \log \left\{ \frac{p(\omega, \theta|\mathbf{y})}{q_A(\omega|\theta)} \right\} d\omega - \log q_A(\theta) \right] d\theta.\end{aligned}\tag{29}$$

Now, because of the identity

$$\log q_A(\boldsymbol{\theta}) = \underbrace{\left[ \int_{\Omega} q_A(\boldsymbol{\omega}|\boldsymbol{\theta}) d\boldsymbol{\omega} \right]}_{=1} \log q_A(\boldsymbol{\theta}) = \int_{\Omega} q_A(\boldsymbol{\omega}|\boldsymbol{\theta}) \log q(\boldsymbol{\theta}) d\boldsymbol{\omega},$$

the last integral in (29) becomes

$$\begin{aligned} & \int_{\Theta} q_A(\boldsymbol{\theta}) \left[ \int_{\Omega} q_A(\boldsymbol{\omega}|\boldsymbol{\theta}) \log \left\{ \frac{p(\boldsymbol{\omega}, \boldsymbol{\theta}|\mathbf{y})}{q_A(\boldsymbol{\omega}|\boldsymbol{\theta})} \right\} d\boldsymbol{\omega} - \log q_A(\boldsymbol{\theta}) \right] d\boldsymbol{\theta} \\ &= \int_{\Theta} q_A(\boldsymbol{\theta}) \left[ \int_{\Omega} q_A(\boldsymbol{\omega}|\boldsymbol{\theta}) \log \left\{ \frac{p(\boldsymbol{\omega}, \boldsymbol{\theta}|\mathbf{y})}{q_A(\boldsymbol{\omega}|\boldsymbol{\theta})} \right\} d\boldsymbol{\omega} - \int_{\Omega} q(\boldsymbol{\omega}|\boldsymbol{\theta}) \log q_A(\boldsymbol{\theta}) d\boldsymbol{\omega} \right] d\boldsymbol{\theta} \\ &= \iint_{\Omega \times \Theta} q_A(\boldsymbol{\omega}|\boldsymbol{\theta}) q_A(\boldsymbol{\theta}) \left[ \log \left\{ \frac{p(\boldsymbol{\omega}, \boldsymbol{\theta}|\mathbf{y})}{q_A(\boldsymbol{\omega}|\boldsymbol{\theta})} \right\} - \log q_A(\boldsymbol{\theta}) \right] d\boldsymbol{\omega} d\boldsymbol{\theta} \\ &= \iint_{\Theta \times \Omega} q_A(\boldsymbol{\omega}|\boldsymbol{\theta}) q_A(\boldsymbol{\theta}) \log \left\{ \frac{p(\boldsymbol{\omega}, \boldsymbol{\theta}|\mathbf{y})}{q_A(\boldsymbol{\omega}|\boldsymbol{\theta}) q_A(\boldsymbol{\theta})} \right\} d\boldsymbol{\omega} d\boldsymbol{\theta} \\ &= \iint_{\Theta \times \Omega} q_A(\boldsymbol{\omega}, \boldsymbol{\theta}) \log \left\{ \frac{p(\boldsymbol{\omega}, \boldsymbol{\theta}|\mathbf{y})}{q_A(\boldsymbol{\omega}, \boldsymbol{\theta})} \right\} d\boldsymbol{\omega} d\boldsymbol{\theta}. \end{aligned} \tag{30}$$

Observing that the left integral in (29) corresponds to the negative Kullback-Leibler divergence  $-\text{KL}\{q_A(\boldsymbol{\theta}) \parallel p(\boldsymbol{\theta}|\mathbf{y})\}$ , while the last integral in (30) corresponds to  $-\text{KL}\{q_A(\boldsymbol{\omega}, \boldsymbol{\theta}) \parallel p(\boldsymbol{\omega}, \boldsymbol{\theta}|\mathbf{y})\}$ , we have

$$\text{KL}\{q_A(\boldsymbol{\theta}) \parallel p(\boldsymbol{\theta}|\mathbf{y})\} \leq \text{KL}\{q_A(\boldsymbol{\omega}, \boldsymbol{\theta}) \parallel p(\boldsymbol{\omega}, \boldsymbol{\theta}|\mathbf{y})\},$$

which concludes the proof of Theorem 2.  $\square$

**Remark 4.** Inequalities (29) and (30) hold only under the compatibility Assumption 1 made upon  $\mathcal{Q}_M$  and  $\mathcal{Q}_A$ , which permits to write  $q_A(\boldsymbol{\omega}|\boldsymbol{\theta})$  as a proper conditional distribution generated by  $q_A(\boldsymbol{\omega}, \boldsymbol{\theta})$  and  $q_A(\boldsymbol{\theta})$ . Whenever the compatibility is not satisfied there are no guaranties that Theorem 2 still holds.

In the following we show this fact by using a counterexample. Let us consider a generic augmented space  $\mathcal{Q}_A$  such that  $p(\boldsymbol{\omega}, \boldsymbol{\theta}|\mathbf{y}) \in \mathcal{Q}_A$ . On the opposite, we consider  $\mathcal{Q}_M$  such that  $p(\boldsymbol{\theta}|\mathbf{y}) \notin \mathcal{Q}_M$ . This way,  $\mathcal{Q}_A$  and  $\mathcal{Q}_M$  are not compatible by construction, since there exists at least one element of  $\mathcal{Q}_A$  whose marginal density does not belong to  $\mathcal{Q}_M$ , namely  $p(\boldsymbol{\theta}|\mathbf{y}) = \int_{\Omega} p(\boldsymbol{\omega}, \boldsymbol{\theta}) d\boldsymbol{\omega}$ . Recall that the Kullback-Leibler divergence is always non-negative, i.e.  $\text{KL}(q \parallel p) \geq 0$ , and reaches 0 if and only if  $q = p$  almost everywhere, namely  $\text{KL}(p \parallel p) = 0$ . Then, there exists at least one element of  $\mathcal{Q}_A$  such that  $\text{KL}\{q_A(\boldsymbol{\omega}, \boldsymbol{\theta}) \parallel p(\boldsymbol{\omega}, \boldsymbol{\theta}|\mathbf{y})\} = 0$ , which corresponds to  $q_A(\boldsymbol{\omega}, \boldsymbol{\theta}) = p(\boldsymbol{\omega}, \boldsymbol{\theta}|\mathbf{y})$ , whereas  $\text{KL}\{q_M(\boldsymbol{\theta}) \parallel p(\boldsymbol{\theta}|\mathbf{y})\} > 0$  for any  $q_M(\boldsymbol{\theta}) \in \mathcal{Q}_M$ , since  $p(\boldsymbol{\theta}|\mathbf{y}) \notin \mathcal{Q}_M$ . This means that

$$\underbrace{\text{KL}\{q_M(\boldsymbol{\theta}) \parallel p(\boldsymbol{\theta}|\mathbf{y})\}}_{>0} \not\leq \underbrace{\text{KL}\{p(\boldsymbol{\omega}, \boldsymbol{\theta}|\mathbf{y}) \parallel p(\boldsymbol{\omega}, \boldsymbol{\theta}|\mathbf{y})\}}_{=0}, \quad \forall q_M(\boldsymbol{\theta}) \in \mathcal{Q}_M.$$

Which contradicts the inequality in Theorem 2.

## References

Alquier, P. and Ridgway, J. (2020). Concentration of tempered posteriors and of their variational approximations. *Ann. Statist.*, 48(3):1475–1497.

- Alquier, P., Ridgway, J., and Chopin, N. (2016). On the properties of variational approximations of Gibbs posteriors. *J. Mach. Learn. Res.*, 17:8374–8414.
- Armagan, A., Dunson, D. B., and Lee, J. (2013). Generalized double Pareto shrinkage. *Statist. Sinica*, 23(1):119–143.
- Bellini, F. and Bignozzi, V. (2015). On elicitable risk measures. *Quant. Finance*, 15(5):725–733.
- Bhattacharya, A., Pati, D., Pillai, N. S., and Dunson, D. B. (2015). Dirichlet-Laplace priors for optimal shrinkage. *J. Amer. Statist. Assoc.*, 110(512):1479–1490.
- Bishop, C. M. (2006). *Pattern recognition and machine learning*. Information Science and Statistics. Springer, New York.
- Bissiri, P. G., Holmes, C. C., and Walker, S. G. (2016). A general framework for updating belief distributions. *J. R. Stat. Soc. Ser. B. Stat. Methodol.*, 78(5):1103–1130.
- Blei, D. M., Kucukelbir, A., and McAuliffe, J. D. (2017). Variational inference: A review for statisticians. *J. Amer. Statist. Assoc.*, 112(518):859–877.
- Carvalho, C. M., Polson, N. G., and Scott, J. G. (2010). The horseshoe estimator for sparse signals. *Biometrika*, 97(2):465–480.
- Chan, J. C. C. and Jeliazkov, I. (2009). Efficient simulation and integrated likelihood estimation in state space models. *Int. J. Math. Model. Numer. Optim.*, 1(1-2):101–120.
- Cressie, N. A. C. (2015). *Statistics for spatial data*. Wiley Classics Library. John Wiley & Sons, Inc., New York, revised edition. Paperback edition of the 1993 edition.
- Dempster, A. P., Laird, N. M., and Rubin, D. B. (1977). Maximum likelihood from incomplete data via the EM algorithm. *J. Roy. Statist. Soc. Ser. B*, 39(1):1–38.
- Durante, D. and Rigon, T. (2019). Conditionally conjugate mean-field variational Bayes for logistic models. *Statist. Sci.*, 34(3):472–485.
- Durbin, J. and Koopman, S. J. (2012). *Time series analysis by state space methods*, volume 38 of *Oxford Statistical Science Series*. Oxford University Press, Oxford, second edition.
- Efron, B. (1991). Regression percentiles using asymmetric squared error loss. *Statist. Sinica*, 1(1):93–125.
- Fasiolo, M., Wood, S. N., Zaffran, M., Nedellec, R., and Goude, Y. (2021). Fast calibrated additive quantile regression. *J. Amer. Statist. Assoc.*, 116(535):1402–1412.
- Gaillard, P., Goude, Y., and Nedellec, R. (2016). Additive models and robust aggregation for gefcom2014 probabilistic electric load and electricity price forecasting. *Int. J. Forecast.*, 32(3):1038–1050.
- Gelman, A. and Hill, J. (2006). *Data analysis using regression and multilevel/hierarchical models*. Cambridge university press.
- Geraci, M. and Bottai, M. (2007). Quantile regression for longitudinal data using the asymmetric Laplace distribution. *Biostatistics*, 8(1):140–154.
- Geraci, M. and Bottai, M. (2014). Linear quantile mixed models. *Stat. Comput.*, 24(3):461–479.

- Germain, P., Bach, F., Lacoste, A., and Lacoste-Julien, S. (2016). Pac-bayesian theory meets Bayesian inference. *Advances in Neural Information Processing Systems*, 29.
- Griffin, J. E. and Brown, P. J. (2011). Bayesian hyper-lassos with non-convex penalization. *Aust. N. Z. J. Stat.*, 53(4):423–442.
- Hall, P., Johnstone, I. M., Ormerod, J. T., Wand, M. P., and Yu, J. C. F. (2020). Fast and accurate binary response mixed model analysis via expectation propagation. *J. Amer. Statist. Assoc.*, 115(532):1902–1916.
- Hall, P., Ormerod, J. T., and Wand, M. P. (2011a). Theory of Gaussian variational approximation for a Poisson mixed model. *Statist. Sinica*, 21(1):369–389.
- Hall, P., Pham, T., Wand, M. P., and Wang, S. S. J. (2011b). Asymptotic normality and valid inference for Gaussian variational approximation. *Ann. Statist.*, 39(5):2502–2532.
- Hastie, T., Tibshirani, R., and Friedman, J. (2009). *The elements of statistical learning. Data mining, inference, and prediction*. Springer Series in Statistics. Springer, New York, second edition.
- Hodges, J. S. (2014). *Richly parameterized linear models: Additive, time series, and spatial models using random effects*. Chapman & Hall/CRC Texts in Statistical Science Series. CRC Press, Boca Raton, FL.
- Hoffman, M. D., Blei, D. M., Wang, C., and Paisley, J. (2013). Stochastic variational inference. *J. Mach. Learn. Res.*, 14:1303–1347.
- Hong, T., Pinson, P., Fan, S., Zareipour, H., Troccoli, A., and Hyndman, R. J. (2016). Probabilistic energy forecasting: Global energy forecasting competition 2014 and beyond. *Int. J. Forecast.*, 32(3):896–913.
- Hunter, D. R. and Lange, K. (2000). Quantile regression via an MM algorithm. *J. Comput. Graph. Statist.*, 9(1):60–77.
- Jaakkola, T. S. and Jordan, M. I. (2000). Bayesian parameter estimation via variational methods. *Stat. Comput.*, 10(1):25–37.
- Johndrow, J. E., Smith, A., Pillai, N., and Dunson, D. B. (2019). Mcmc for imbalanced categorical data. *J. Amer. Statist. Assoc.*, 114(527):1394–1403.
- Knowles, D. and Minka, T. (2011). Non-conjugate variational message passing for multinomial and binary regression. *Advances in Neural Information Processing Systems*, 24:1701–1709.
- Koenker, R. (2005). *Quantile regression*, volume 38 of *Econometric Society Monographs*. Cambridge University Press, Cambridge.
- Koenker, R. and Bassett, Jr., G. (1978). Regression quantiles. *Econometrica*, 46(1):33–50.
- Kozumi, H. and Kobayashi, G. (2011). Gibbs sampling methods for Bayesian quantile regression. *J. Stat. Comput. Simul.*, 81(11):1565–1578.
- Kucukelbir, A., Tran, D., Ranganath, R., Gelman, A., and Blei, D. M. (2017). Automatic differentiation variational inference. *J. Mach. Learn. Res.*, 18:Paper No. 14, 45.

- Lange, K. (2010). *Numerical analysis for statisticians*. Statistics and Computing. Springer, New York, second edition.
- Lee, Y.-J. and Mangasarian, O. L. (2001). SSVM: a smooth support vector machine for classification. *Comput. Optim. Appl.*, 20(1):5–22.
- Leng, C., Tran, M.-N., and Nott, D. (2014). Bayesian adaptive Lasso. *Ann. Inst. Statist. Math.*, 66(2):221–244.
- Lindgren, F., Bolin, D., and Rue, H. (2022). The SPDE approach for Gaussian and non-Gaussian fields: 10 years and still running. *Spat. Stat.*, 50:100599.
- Lindgren, F., Rue, H., and Lindström, J. (2011). An explicit link between Gaussian fields and Gaussian Markov random fields: the stochastic partial differential equation approach. *J. R. Stat. Soc. Ser. B Stat. Methodol.*, 73(4):423–498.
- Liu, Q. and Pierce, D. A. (1994). A note on Gauss-Hermite quadrature. *Biometrika*, 81(3):624–629.
- Luts, J. and Ormerod, J. T. (2014). Mean field variational Bayesian inference for support vector machine classification. *Comput. Statist. Data Anal.*, 73:163–176.
- Luts, J. and Wand, M. P. (2015). Variational inference for count response semiparametric regression. *Bayesian Anal.*, 10(4):991–1023.
- McCullagh, P. and Nelder, J. A. (1989). *Generalized linear models. Second edition*. Chapman & Hall, London.
- McLean, M. W. and Wand, M. P. (2019). Variational message passing for elaborate response regression models. *Bayesian Anal.*, 14(2):371–398.
- Menictas, M. and Wand, M. P. (2015). Variational inference for heteroscedastic semiparametric regression. *Aust. N. Z. J. Stat.*, 57(1):119–138.
- Minka, T. P. (2013). Expectation propagation for approximate bayesian inference. *arXiv preprint arXiv:1301.2294*.
- Neville, S. E., Ormerod, J. T., and Wand, M. P. (2014). Mean field variational Bayes for continuous sparse signal shrinkage: pitfalls and remedies. *Electron. J. Stat.*, 8(1):1113–1151.
- Newey, W. K. and Powell, J. L. (1987). Asymmetric least squares estimation and testing. *Econometrica*, 55(4):819–847.
- Nocedal, J. and Wright, S. J. (2006). *Numerical optimization*. Springer Series in Operations Research and Financial Engineering. Springer, New York, second edition.
- Oh, H.-S., Lee, T. C. M., and Nychka, D. W. (2011). Fast nonparametric quantile regression with arbitrary smoothing methods. *J. Comput. Graph. Statist.*, 20(2):510–526.
- Ong, V. M.-H., Nott, D. J., and Smith, M. S. (2018). Gaussian variational approximation with a factor covariance structure. *J. Comput. Graph. Statist.*, 27(3):465–478.
- Ormerod, J. T. (2011). Skew-normal variational approximations for bayesian inference. *Unpublished article*.

- Ormerod, J. T. and Wand, M. P. (2010). Explaining variational approximations. *Amer. Statist.*, 64(2):140–153.
- Ormerod, J. T. and Wand, M. P. (2012). Gaussian variational approximate inference for generalized linear mixed models. *J. Comput. Graph. Statist.*, 21(1):2–17.
- Park, T. and Casella, G. (2008). The Bayesian lasso. *J. Amer. Statist. Assoc.*, 103(482):681–686.
- Polson, N. G., Scott, J. G., and Windle, J. (2013). Bayesian inference for logistic models using Pólya-Gamma latent variables. *J. Amer. Statist. Assoc.*, 108(504):1339–1349.
- Polson, N. G. and Scott, S. L. (2011). Data augmentation for support vector machines. *Bayesian Anal.*, 6(1):1–23.
- Rohde, D. and Wand, M. P. (2016). Semiparametric mean field variational Bayes: general principles and numerical issues. *J. Mach. Learn. Res.*, 17:Paper No. 172, 47.
- Rue, H. and Held, L. (2005). *Gaussian Markov random fields. Theory and applications*, volume 104. Chapman & Hall/CRC, Boca Raton, FL.
- Rue, H., Martino, S., and Chopin, N. (2009). Approximate Bayesian inference for latent Gaussian models by using integrated nested Laplace approximations. *J. R. Stat. Soc. Ser. B. Stat. Methodol.*, 71(2):319–392.
- Ruppert, D., Wand, M. P., and Carroll, R. J. (2003). *Semiparametric regression*. Cambridge University Press, Cambridge.
- Sobotka, F. and Kneib, T. (2012). Geoadditive expectile regression. *Comput. Statist. Data Anal.*, 56(4):755–767.
- Tan, L. S. L. and Nott, D. J. (2013). Variational inference for generalized linear mixed models using partially noncentered parametrizations. *Statist. Sci.*, 28(2):168–188.
- Triantafyllopoulos, K. (2021). *Bayesian inference of state space models: Kalman filtering and beyond*. Springer Series in Statistics. Springer, Cham.
- Vapnik, V. N. (1998). *Statistical learning theory*. John Wiley & Sons, Inc., New York.
- Waldmann, E., Sobotka, F., and Kneib, T. (2017). Bayesian regularisation in geoadditive expectile regression. *Stat. Comput.*, 27(6):1539–1553.
- Wand, M. P. (2014). Fully simplified multivariate normal updates in non-conjugate variational message passing. *J. Mach. Learn. Res.*, 15:1351–1369.
- Wand, M. P. and Ormerod, J. T. (2008). On semiparametric regression with O’Sullivan penalized splines. *Aust. N. Z. J. Stat.*, 50(2):179–198.
- Wand, M. P., Ormerod, J. T., Padoan, S. A., and Frühwirth, R. (2011). Mean field variational Bayes for elaborate distributions. *Bayesian Anal.*, 6(4):847–900.
- Wang, Y. and Blei, D. (2019). Variational bayes under model misspecification. *Advances in Neural Information Processing Systems*, 32.

- Wood, S. N. (2017). *Generalized additive models. An introduction with R, Second edition*. CRC Press, Boca Raton, FL.
- Xing, J.-J. and Qian, X.-Y. (2017). Bayesian expectile regression with asymmetric normal distribution. *Comm. Statist. Theory Methods*, 46(9):4545–4555.
- Yu, K. and Moyeed, R. A. (2001). Bayesian quantile regression. *Statist. Probab. Lett.*, 54(4):437–447.
- Yue, Y. R. and Rue, H. (2011). Bayesian inference for additive mixed quantile regression models. *Comput. Statist. Data Anal.*, 55(1):84–96.
- Zhu, J., Ahmed, A., and Xing, E. P. (2012). MedLDA: maximum margin supervised topic models. *J. Mach. Learn. Res.*, 13:2237–2278.
- Zhu, J., Chen, N., Perkins, H., and Zhang, B. (2014). Gibbs max-margin topic models with data augmentation. *J. Mach. Learn. Res.*, 15:1073–1110.
- Ziegel, J. F. (2016). Coherence and elicibility. *Math. Finance*, 26(4):901–918.